Characterizing variable renewable energy generation uncertainty towards improved forecasting and operational decision making

Ndamulelo Mararakanye

Dissertation presented for the degree Doctor of Philosophy in the

Faculty of Engineering at Stellenbosch University

Supervisor: Dr. Bernard Bekker

December 2022

Plagiarism declaration

By submitting this dissertation electronically, I declare that the entirety of the work contained therein is my own, original work, that I am the sole author thereof (save to the extent explicitly otherwise stated), and that reproduction and publication thereof by Stellenbosch University will not infringe any third-party rights and that I have not previously in its entirety or in part submitted it for obtaining any qualification.

Ndamulelo Mararakanye

Date: December 2022

Abstract

As its first novel contribution, this dissertation investigates the broad challenge of understanding the impacts of integrating a high share of variable renewable energy (VRE) generators into power systems. These generators are variable, uncertain, non-synchronous and location constrained, introducing a wide range of impacts that are unique to a specific region and require different input data, models, and simulation tools to study. It is resource intensive to study all these impacts and therefore important to effectively identify and study only those impacts that are most relevant to the region under consideration. In addressing this challenge, this dissertation firstly identifies three main factors that influence the VRE integration impacts in different regions: available resources, penetration level, and grid characteristics. Thereafter, the international experience is used to understand how these three factors contributed to the issues that were experienced in different regions. The outcome of this investigation is a framework for comprehending VRE integration issues based on available renewable resources, penetration level, and grid characteristics of a region under consideration. This framework can be used by network planners, policymakers, and grid operators to prioritize VRE integration issues of concern to their region prior to conducting detailed studies, thereby reducing the resources required.

This dissertation identifies wind power forecasting as key in mitigating some of the impacts introduced by high share of VREs. Within the context of wind power forecasting, this dissertation investigates the challenge of aggregating decentralized forecasts. These forecasts are typically optimized for local conditions because the individual wind farms do not have access to power data from other wind farms. Simply adding these decentralized forecasts together at the point where these forecasts are received (typically the system operator) may not capture some of the common spatial and temporal correlations of wind power, thereby lowering the potential accuracy of the aggregated wind power forecast. In response to this challenge, this dissertation proposes explanatory variables that are used to train the machine learning models to derive aggregated point and probabilistic wind power forecasts from decentralized forecasts. The proposed explanatory variables include clusters of point forecasts (to account for spatial correlations between wind farms), hour of day (to account for diurnal cycles), month of year (to account for seasonal cycles) and, atmospheric states (to account for correlations due to large-scale atmospheric circulations). Training machine learning models using these explanatory variables results in a significant improvement in the accuracy of aggregated forecasts, becoming the second novel contribution of this dissertation. This is particularly important in regions where individual wind farms generate their own forecasts.

This dissertation also acknowledges the fact that wind power forecasts are not always perfect, giving rise to the need to understand and estimate wind power forecasting uncertainty. One of the challenges concerning the characterization of forecasting uncertainty is that some of the parametric distributions (normal, beta, Weibull, etc.) commonly used for modeling forecast errors may be inappropriate in representing extreme errors. While non-parametric approaches can be accurate, extreme errors often do not occur frequently enough to make accurate non-parametric inferences. There remains a need to find a parametric model that best represents the extreme errors. To address these challenges, this dissertation identifies a suitable parametric distribution for representing extreme errors, investigates some of the factors that may influence extreme errors, and proposes a suitable model for representing spatial correlations of extreme errors between wind farms. Therefore, the third novel contribution of this dissertation is to propose modeling approaches for improving the estimation and understanding of extreme errors. This is an important step toward better allocation of operating reserves to account for forecasting uncertainty.

Continuing within the context of forecasting uncertainty, it is known that the conditional forecast error distributions change with the wind power forecast mostly due to the slope of wind to power conversion curves. The variance is often small at low and high power forecasts but large at mid-range power forecasts. The forecast error distribution is skewed right at low power forecasts, symmetric at mid-range power forecasts, and skewed left at high power forecasts. As a result, some of the commonly used distributions for modeling forecast errors may lack the flexibility required to represent conditional forecast error distributions at different wind power forecasts. As a fourth novel contribution, this dissertation proposed and evaluated an approach for deriving the conditional forecast error distribution for a given wind power forecast. These conditional distributions typically contain more probabilistic information (as compared to unconditional distribution), which can be used to improve reserve allocation in grids with high share of wind generators.

Opsomming

Die eerste oorspronklike bydrae vervat in hierdie proefskrif, is die resultaat van ‘n breë ondersoek na die impak van integrasie van 'n hoë aandeel wisselvallige hernubare energie (VRE) kragopwekkers in die kragstelsel. Hierdie kragopwekkers is nie-sinchronies, en die krag wat opegewek word is wisselend, kom met lae vlakke van sekerheid en is uniek aan ‘n spesifieke streek. Dit bring ‘n wye reeks impakte ter tafel wat eie is aan die ter saaklike geografiese area en vereis verskillende data stelle, modelle en simulasie-instrumente om te bestudeer. Die bestudering van al hierdie verskillende moontlike impakte vereis intensiewe hulpbron verbruik en dit is daarom belangrik om effektiewelik net die mees relevant impakte per streek te identifiseer en te bestudeer. Om hierdie uitdaging aan te spreek, word daar in hierdie proefskrif eerstens drie hooffaktore geïdentifiseer wat die VRE-integrasie-impakte in verskillende streke beïnvloed: beskikbare energiebronne, vlak van penetrasie en die kenmerke van die kragnetwerk. Hierna word internasionale voorbeelde gebruik om te verstaan hoe hierdie drie faktore bygedra het tot die uitdagings wat in die verskillende wêrelddele ondervind is. Die uitset van hierdie studie is 'n raamwerk wat sin gee aan die VRE-integrasie-impakte gebaseer op beskikbare hernubare energiebronne, penetrasievlakke en kenmerke van die kragnetwerk in die geografiese area wat ondersoek word. Hierdie raamwerk kan deur netwerkbeplanners, beleidmakers en netwerkoperateurs gebruik word om tyd en moeite te spaar deur eers die VRE-integrasie-uitdagings wat vir hulle streek van belang is te prioritiseer voordat gedetailleerde studies gedoen word.

Hierdie proefskrif identifiseer verder die vooruitskatting van windkrag opwekking as die sleutel om sommige van die impakte wat deur 'n groot aandeel VRE's veroorsaak word teen te werk. Binne die konteks van die vooruitskatting van windkrag opwekking ondersoek hierdie proefskrif die uitdagings van die samevoeging van gedesentraliseerde voorspellings. Hierdie voorspellings is tipies geoptimaliseer vir plaaslike toestande omdat individuele windplase nie toegang tot kragdata van ander windplase het nie. Deur die gedesentraliseerde voorspellings eenvoudig bymekaar te tel by die punt waar die voorspellings ontvang word (tipies by die stelseloperateur) veroorsaak dat die potensiële akkuraatheid van die saamgevoegde vooruitskatting verlaag word omdat die gedetaileerde ruimtelike-temporale korrelasies nie in ag geneem word nie. In antwoord op hierdie uitdaging, stel hierdie proefskrif verklarende veranderlikes voor wat gebruik word om die masjienleermodelle op te lei om groepe punt- en waarskynlikheids windkragvoorspellings van gedesentraliseerde voorspellings af te lei. Die voorgestelde verduidelikende veranderlikes sluit groepe van puntvoorspellings in (om rekening

te hou met ruimtelike korrelasies tussen windplase), uur van die dag (om rekening te hou met daaglikse siklusse), maand van die jaar (om rekening te hou met seisoenale siklusse) en atmosferiese toestande (om korrelasies as gevolg van grootskaalse atmosferiese sirkulasies in ag te neem). Die opleiding van masjienleermodelle wat hierdie verduidelikende veranderlikes gebruik, lei tot 'n beduidende verbetering in die akkuraatheid van saamgestelde voorspellings, die tweede oorspronklike bydrae van hierdie proefskrif. Dit is veral belangrik in streke waar individuele windplase hul eie voorspellings maak.

Hierdie proefskrif erken ook die feit dat die vooruitskatting van windkrag opwekking nie altyd perfek is nie, wat aanleiding gee tot die behoefte om hierdie onsekerheid te verstaan en te kan skat. Een van die uitdagings rakende die karakterisering van voorspellingsonsekerheid is dat sommige van die parametriese verdelings (normaal, beta, Weibull, ens.) wat algemeen gebruik word vir die modellering van voorspellingsfoute, onvanpas kan wees vir die voorstelling van uiterste foute. Terwyl nie-parametriese benaderings akkuraat kan wees, kom uiterste foute dikwels nie gereeld genoeg voor om akkurate nie-parametriese afleidings te maak nie. Daar is steeds 'n behoefte om 'n parametriese model te vind wat die uiterste foute die beste verteenwoordig.

Hierdie uitdagings word aangespreek, in die navorsing vervat in hierdie proefskrif deurdat, 'n geskikte parametriese verspreiding geïdentifiseer is om uiterste foute voor te stel, sommige van die faktore wat uiterste foute kan beïnvloed is ondersoek, en ‘n geskikte model word voorgestel om ruimtelike korrelasies van uiterste foute tussen windplase te verteenwoordig. Daarom is die derde oorspronklike bydrae vervat in hierdie proefskrif die voorstel van verbeterde modelleringsbenaderings wat lei tot verbetering van die skatting en begrip van uiterste foute. Die grootste bydrae wat hier gemaak word, is om die skatting en begrip van uiterste foute te verbeter. Dit is 'n belangrike stap in die rigting van 'n beter toewysing van bedryfsreserwes om rekening te hou met voorspellingsonsekerheid.

Om voort te gaan binne die konteks van voorspellingsonsekerheid, is dit bekend dat die voorwaardelike voorspellingsfoutverspreidings met die windkragvoorspelling verander, hoofsaaklik as gevolg van die helling van wind-na-krag-omskakelingskrommes. Die afwyking is dikwels klein by lae- en hoëkragvoorspellings, maar groot by middelslagkragvoorspellings. Die voorspellingsfoutverspreiding is skeef regs by laekragvoorspellings, simmetries by middelafstandkragvoorspellings, en skeef links by hoëkragvoorspellings. As gevolg hiervan, kan sommige van die algemeen gebruikte verspreidings vir die modellering van voorspellingsfoute nie die buigsaamheid hê wat nodig is om voorwaardelike voorspellingsfoutverspreidings by verskillende windkragvoorspellings voor te stel nie. As 'n

vierde nuwe bydrae stel hierdie proefskrif 'n benadering voor vir die afleiding van die voorwaardelike voorspellingsfoutverspreiding vir 'n gegewe windkragvoorspelling en evalueer die resultate. Hierdie voorwaardelike verspreidings bevat tipies meer waarskynlike inligting (in vergelyking met onvoorwaardelike verspreiding), wat ook gebruik kan word om reserwetoewysing in kragnetwerke met 'n groot aandeel windopwekkers te verbeter.

Acknowledgments

Thank you, Dr. Bernard Bekker, for your continued support on this journey. The lessons have been both philosophical and technical. The future seems indeed exciting. I am forever grateful.

Collaborating with you Dr. Amaris Dalton made me appreciate the effectiveness of a multi-disciplinary approach to research. Thank you for your contributions.

Thank you to Eskom for entrusting me with the data that informed this study. Without the data, the study would not have been possible.

Thank you to CRSES for the financial support as well as all the time allowed to attend technical conferences and platforms to present my research.

Thank you to EPPEI for funding assistance.

To my family, friends, and colleagues, thank you for your unwavering support.

Contents

1. Background and problem statement

1.1. The rise of global variable renewable energy capacity

Electricity generation from variable renewable energy (VRE) sources such as wind and solar photovoltaic (PV) is increasing worldwide. Over the past decade, the global wind power capacity has increased more than three times from 238 GW in 2011 to 845 GW in 2021 [9]. During the same period, the global solar PV capacity has increased more than 13 times from 70 GW to 942 GW [9]. The VRE installed capacity is expected to grow further in the near future as different regions strive to strengthen their response to the threat of climate change by meeting their nationally determined contributions of the United Nations Framework Convention on Climate Change (UNFCCC) Paris Agreement. The agreement was adopted by 196 parties at COP 21 in Paris on 12 December 2015 [10]. The European Commission wants renewable energy to account for at least 40% of the total energy generation by 2030 [11]. China intends to have 1200 GW of wind solar PV capacity by 2030, up from 650 GW in 2021 [9], [12]. India intends to triple its renewable energy capacity to 500 GW by 2030, up from 157 GW in March 2022, equating to 40% of its electricity from renewable sources [13]. The United States of America intends to decarbonize its electricity grid completely by 2035, which will necessitate the addition of 70 to 100 GW of solar PV and wind capacity per year [14].

South Africa, as a signatory to the Paris Agreement, is expected to significantly increase its wind and solar PV capacity in the medium to long term. By the end of 2021, the operational wind and solar PV capacity in South Africa was 2.4 GW and 2.2 GW, respectively, accounting for 8% of the country's total installed capacity [15]. The Integrated Resource Plan (IRP) 2010-2030 (released in 2011) is one of South Africa's key energy policies that indicates how and at what cost the country's forecasted electricity demand will be met [16]. This document was intended to be a "living plan" that would be revised on a regular basis [16]. The IRP 2019 (the most recent version) proposes a shift from a coal dominated to an increasingly diverse energy mix. The plan is to increase the capacity of wind and solar PV generation to 22.5 GW and 10.5 GW, respectively, by 2030, representing a contribution of 33% of the planned total installed capacity in the country [17].

Outside climate change mitigation, VREs contribute positively to other areas of economic development and human well-being. The cost of VREs has also fallen significantly over the past decade due to improving technologies, economies of scale, competitive supply chains, and improving developer experience [18]. The global weighted-average cost of electricity from

utility scale solar PV has dropped by 85% between 2010 and 2020, whereas the same cost from onshore and offshore wind has dropped by 56% and 48%, respectively, during the same period [18]. This is an indication that VREs are becoming cost competitive with nuclear and fossil fuel sources (at least from a cost of energy perspective). In addition, the VRE sector contributes to the economic development of a region by creating both upstream and downstream jobs in manufacturing, installation, maintenance, etc. The report in [19] estimates that in 2020 about 12 million people were directly and indirectly employed in the sector. Furthermore, the VRE infrastructure is decentralized according to the availability of resources in a region, which gives opportunity to much wider participation by communities compared to centralized nuclear- and fossil fuel-based infrastructure.

Problem 1: Understanding the impacts of integrating VREs into power systems

Despite the benefits mentioned above, the output power from VRE sources is variable and uncertain in all time scales, which can complicate balancing generation with varying load demand [20]. Experience has shown that as the share of VREs becomes relatively high, conventional sources may be required to increase or decrease their power output quickly to compensate for the additional variability and uncertainty introduced by VREs [2], [21]–[25]. In addition, the latest technologies of wind and PV generators are connected to the grid through power electronic based converters, which ultimately reduce the rotating mass (inertia) in the system, potentially causing frequency stability issues [24]–[26]. Furthermore, VREs are deployed in different sizes ranging from a few kWp to several MWp, often connected to distribution networks. However, distribution networks are typically not planned nor designed for large uptake of generators and can easily experience over-voltages and other power quality problems because of VREs [24]. Another related challenge is that VREs are usually located where the renewable resource is high, which may be far away from the load , resulting in weak interconnection between the central grid and the VRE generator [20], [27], [28]. This may lead to voltage fluctuations exceeding the stipulated limits in the grid code, which if not properly accounted for, may result in equipment damage and trigger instability or cascading blackouts [20], [29].

In general, studying each of the issues identified above requires different input data, models and simulation tools [1]. It is resource intensive to study all these issues and therefore important to effectively identify and study only those issues that are most relevant to the region under consideration. However, each region is different in terms of available resources, VREs targets (or penetration level) and grid characteristics. International experience shows that these are the

three main factors that influenced the VRE integration issues experienced in different regions [2]–[8]. Therefore, there is a need to understand how these factors contributed to the issues that were experienced in different regions. It is anticipated that this can be the first step in prioritizing VREs integration issues for detailed VRE grid integration studies.

1.2. The value of wind power forecasting

Wind power forecasting is one of the most effective ways to mitigate the impacts of wind power variability and uncertainty discussed in Section 1.1 above. Forecasting provides an estimate of wind power generation that is expected at a specific point time in the future. This can improve a variety of power system decision-making processes, including scheduling operating reserves, allocation of balancing power, unit commitment, trading of electricity spot market, efficient project construction, and maintenance planning [30]–[32].

Wind power forecasts can be classified by prediction horizon as follows: very short-term (few minutes to 1 hour), short-term (1 hour to 6 hours), medium-term (6 hours to 24 hours), long-term (24 hours to 72 hours), and very long-term (72 hours and longer) [30], [31]. This classification assists in determining the best forecasting approach based on the intended application [31].

Wind power forecasting approaches can be divided into two main categories: physical and statistical. Physical approaches typically use numerical weather prediction (NWP) models and current weather conditions to predict wind speed [33]–[35]. Some recent contributions of physical approaches applied in wind forecasting are found in [33], [36]–[40]. NWP models formulate the problem of wind speed prediction as a set of mathematical equations describing the atmosphere and oceans. Statistical approaches, on the other hand, take historical wind power data and/or NWP as inputs and use machine learning algorithms to generate wind power forecasts [33]–[35]. Some recent contributions of statistical approaches applied in wind forecasting are found in [41]–[44].

One of the key considerations in wind power forecasting is spatial-temporal correlations between wind farms that are geographically distributed. Power from geographically distributed wind farms exhibit spatial and temporal correlations, the degree of which varies based on numerous factors such as separation distance and direction, timescale, diurnal weather variations and movement of synoptic weather systems [41], [42], [45]. Recent research has shown the potential benefit of incorporating spatial and temporal correlations in wind forecasting, especially in terms of improving forecasting accuracy [33], [34], [36], [41]–[43].

Problem 2: Aggregating decentralized wind power forecasts

An observation made from the literature is that the majority of proposed forecasting methodologies assume that the problem of wind power forecasting of geographically distributed wind farms is solved in a centralized manner i.e. forecasts of all wind farms in a region are derived centrally by one forecasting company (facilitated by the system operator). Centralized forecasts typically employ a consistent forecasting approach across all wind farms, leading to consistent results [46]. In addition, the centralized forecaster will often have access to wind power data from all wind farms, making it easier to incorporate spatial-temporal correlations between wind farms into their forecasting methodologies. In other markets (e.g., South Africa), however, individual wind farms are required to provide forecasts to the power purchaser or system operator who will aggregate these forecasts [47]. These are called decentralized forecasts and they are typically optimized for local conditions because the individual wind farms do not have access to power data from other wind farms. Simply adding these decentralized point forecasts may not capture some of the well-known spatial and temporal correlations, thereby lowering the potential accuracy of the aggregated wind power forecast. Therefore, there is a need for a model that aggregates decentralized point forecasts while considering these correlations.

Another observation made from the literature is that most forecasting methodologies are based on the microscale and/or mesoscale NWP models. However, it was illustrated in [48]–[50] that the probabilistic properties of wind power generators' output, along with the level of correlation between wind generators' output, are dependent on the dominant large-scale atmospheric circulation archetypes. Thus, the information contained in large-scale atmospheric circulations can be useful in improving wind power forecasting. Large-scale atmospheric circulations have been incorporated in medium- to long-term wind forecasting [37], [51], [52], but have only been alluded to in short-term wind forecasting [33], [37], [53]. There is a need for more applied research on the potential benefits of incorporating large-scale atmospheric circulations in short-term wind power forecasting.

1.3. Uncertainty of wind power forecasts

Wind power forecasts have traditionally consisted of a single value, also known as point or deterministic forecasts [36], [41], [42]. However, these point forecasts do not account for unavoidable uncertainty in wind power forecasting caused by time-varying meteorological conditions, weather-to-power conversion process, and dynamic behavior of wind turbines [33]. Based on this realization, researchers and utilities are shifting away from only focusing on

increasing the accuracy of wind power forecasts towards also quantifying the uncertainty inherent in the forecast and incorporating this into their decisions [33], [41], [42], [44], [54], i.e., attaching a risk metric to the forecast.

Wind power forecasting uncertainty can be estimated using two methods: parametric and nonparametric[55]. Parametric approaches assume that wind power forecast errors follows a pre-defined distribution function that can be described by a set of parameters. Most studies in the literature assume normal distribution for modeling forecasting errors [56]–[61]. Other distributions that have been considered include beta [62], Weibull [63], Cauchy [64], and hyperbolic [65]. Parametric inference does not require many observations, resulting in low computational costs. However, parametric inference tends to be less flexible and thus the assumed distribution function may be incorrect [55]. Nonparametric approaches, on the other hand, make no assumptions about the distribution function to be estimated [55]. Some of the most common nonparametric approaches include quantile regression, kernel density estimation, ensemble forecasting, and artificial intelligence [55]. Nonparametric approaches tend to be highly flexible and more accurate compared to parametric approaches. However, this requires a very large number of observations, resulting in high computational costs [55].

Problem 3: Understanding and estimating extreme forecast errors

While the parametric distributions mentioned above are relatively suitable for representing the body of the forecast error distribution, the same assertion is not valid for the tails of the forecast error distribution. According to the findings in [61], [62], [66]–[68], normal, beta, and Weibull distributions are not fat-tailed enough, and therefore often underestimate the frequency of extreme forecast errors. On the other hand, the study in [65] demonstrated that the Cauchy distribution is overly fat-tailed and over-represents the frequency of extreme forecast errors. According to the findings in [65], [69], the hyperbolic distribution seems to perform better compared to normal, beta, Weibull, and Cauchy distributions in modeling extreme forecast errors. Other studies in the literature have considered non-parametric approaches for modeling forecast errors [70], [71]. While non-parametric approaches can be accurate, extreme forecast errors often do not occur frequently enough to make accurate non-parametric inferences [65], [72]. There therefore remains a need to find a parametric model that best represent the extreme forecast errors.

In addition, the importance of diurnal and seasonal cycles as well as large-scale atmospheric circulations on understanding wind power variation (and hence improving forecasting accuracy) has been described in Section 1.2 above. However, there is little to no investigation

in the literature on how these variables affect forecast errors – towards improved estimation of extreme forecast errors. There is a need to understand how these variables influence the occurrence of extreme forecast errors.

Furthermore, while univariate analysis can be useful in certain applications (e.g. congestion management), other operational decisions such as operating reserve allocation need to consider all wind farms within a region. It is thus important to evaluate the dependence structure of extreme forecast errors from geographically distributed wind farms.

Problem 4: Estimating wind power uncertainty at different penetration level

The forecast error distribution changes with the wind power forecast [62], [73]–[76][17]. The variance of forecast error also varies with the wind power forecast (heteroscedasticity) [73], [77]–[81]. The variance is often small at low and high-power forecasts but large at mid-range power forecasts. This is commonly linked to the slope of wind to power conversion curves – the steeper the slope, the larger the variance [81]. The forecast error is also bounded at each wind power forecast. For example, if the wind power forecast is 10% of installed wind capacity, the forecast error will range between -10% and 90% of installed wind capacity. This often implies skewness in forecast error distribution at different power forecasts - skewed right at low power forecasts, symmetric at mid-range power forecasts, and skewed left at high power forecasts [74]–[76]. As a result, the commonly used normal distribution may lack the flexibility required to represent conditional forecast error distributions at different wind power forecasts.

In [62], [76], [82], the beta distribution is used to model forecast errors at different wind power forecast bins. This methodology is extended in [83] to include additional distribution for modeling extreme forecast errors. In [74], the gamma-like (gamma plus flipped gamma) distributions are used to estimate forecast error distributions at different forecast bins. While the parametric models above have the required flexibility, they require separate distribution parameters for each bin, which can be challenging during practical application. To mitigate against this challenge, [73] proposes using logit transformation to ensure that the wind forecast and actual data are jointly close to normally distributed. The confidence intervals of forecast errors are estimated using this close to normally distributed data and are then compared with the intervals achieved by fitting beta distributions in different forecast bins. While some computed intervals are close to those from beta distributions, others are far apart, demonstrating a lack of flexibility in the logit transformation-based approach. There is, therefore, still a need for a better model that can easily be implemented to accurately estimate the conditional quantiles of wind power forecast error for a given wind power forecast.

2. Study hypotheses

In response to the problems raised in the previous section, the following hypotheses are formulated.

Hypothesis 1

Mapping out the impacts of VRE generation according to resource type, penetration level, and grid characteristics can assist network planners, policymakers, and grid operators to prioritize VRE integration issues of concern to their region prior to conducting detailed studies.

Hypothesis 2

Decentralized wind power point forecasts are optimized for local conditions, and this reduces the accuracy of aggregated forecasts when these forecasts are simply added together. The accuracy of aggregated forecasts can be improved by training machine learning models with features that account for some of the common spatial and temporal correlations of wind power, including those correlations caused by large-scale atmospheric circulations.

Hypothesis 3

a) Some of the commonly used distributions for modeling wind power forecast errors, such as normal, hyperbolic, Weibull and beta, may be inappropriate for representing extreme wind power forecast errors. The Generalized Pareto distribution (GPD) from Extreme Value Theory (EVT) can be used to better model extreme error distribution.
b) It can be demonstrated through a case study that diurnal and seasonal weather cycles as well as larger atmospheric circulations influence the occurrence of extreme forecast errors.
c) A region-wide view of extreme forecast errors can be obtained by modelling multivariate forecast error distributions using copula functions.

Hypothesis 4

Compared to the current state of the art models in literature, such as linear regression (assuming normality) and fitting beta distributions in different forecast bins, quantile smoothing splines regression can be used to better estimate the conditional quantiles of wind power forecast error for a given wind power forecast.

3. Hypothesis testing: Overview of papers and findings

Four articles are presented in this dissertation to test the four main hypotheses mentioned above – see the overview of this dissertation in Figure 1.

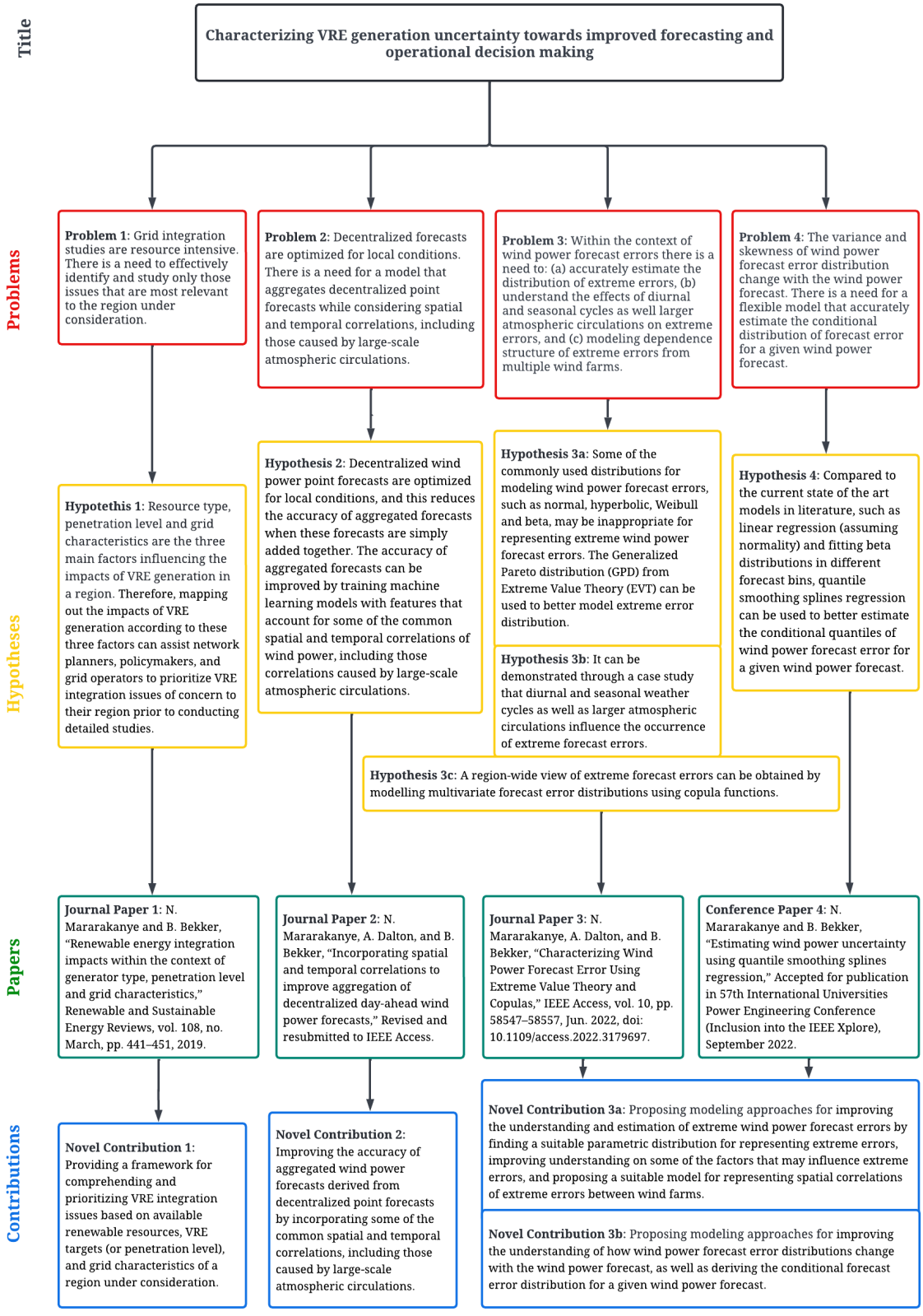

Figure 1: Dissertation overview.

3.1. N. Mararakanye and B. Bekker, "Renewable energy integration impacts within the context of generator type, penetration level and grid characteristics," Renewable and Sustainable Energy Reviews, vol. 108, no. March, pp. 441–451, 2019.

Overview

This paper presents a comprehensive literature review on how generator type, penetration level and grid characteristics contributed to VRE grid integration issues that were experienced in different regions across the world. It is anticipated that this review will enable network planners and policymakers with a framework within which to understand VRE integration issues of concern to their region, before conducting detailed studies. This framework can be seen as the first and important step towards characterizing the uncertainty of VRE generation.

Findings towards hypothesis validation

The following are the main findings regarding the **generator type**:

- The long-term (inter-annual) variability of wind is largely uncorrelated as compared to solar variability that is well correlated. This affects the long-term generation adequacy of the grid and thus the potential inter-annual wind energy deficits that should be taken into account on capacity expansion studies of regions that are planning to integrate high shares of wind generators. On a short time frame, the maximum wind and PV power output variations recorded in the literature increase with the increase in the time interval under consideration. This implies that the minute-minute power variations of wind and PV plants are small, while the hourly and eight-hourly power variations of wind and PV plants can be significantly high.
- The maximum wind power output variations are significantly reduced when installations across large area are considered. In addition, wind and solar have a complimentary behaviour, which can further reduce the need for reserve requirements at different time scales.
- Wind resource is location dependent, while solar resource is usually distributed more evenly across the country. Thus, there is a higher chance of weakly interconnected wind plants as compared to solar, which can increase the likelihood of violation of power quality parameters as well as transmission congestion.
- Finally, both wind and PV generators do not contribute natural inertia to the system. However, by operating both these generators at de-loading curve instead of following the MPP, the reserve power can be used to emulate system inertia. Wind generators also

have stored kinetic energy contained in their rotating mass that can be extracted through controllers. This provide additional options for frequency control that is not available in solar generators.

The following are the main findings regarding the **penetration level and grid characteristics**:

- Local and regional VRE integration issues can affect the power system at any penetration level depending on the strength of the transmission network and its capacity to dispatch the VRE power whenever required. To achieve high shares of VRE, there is a need to continuously investigate local and regional characteristics of the power system and make necessary transmission upgrades. In addition, adequate grid code procedures are also important in mitigating some of these issues.
- Variability and uncertainty of VRE plants start affecting the balancing operation of the power system when the instantaneous penetration level is above 20%. At this level, there is a need for power system flexibility. It was found that countries with high share of VRE have some strategy to maintain flexibility in the power system. Some countries are combined-cycle gas turbine-oriented while others are hydro-oriented or interconnection-oriented.
- Transient and frequency stability issues are expected to start affecting the power system when the instantaneous penetration level is 50%. This is because there will not be adequate inertia on the power system. Currently, incidents attributed to system inertia are rare because most regions do not have enough shares of power electronic-based sources. However, from the studies conducted in different regions there is a general agreement that a level of system inertia must be maintained to safely operate the grid during potential contingency events. Studies also foresee a major role that can be played by VRE control strategies as well as grid code procedures in maintaining the stability of power system.

The findings above confirm that VRE impacts are region specific and understanding the VRE impacts within the context of generator type, penetration level, and grid characteristics can assist network planners, policy makers, and operators in prioritizing VRE integration issues of concern to their region prior to conducting detailed studies. This is a validation of **Hypothesis 1**.

3.2. N. Mararakanye, A. Dalton, and B. Bekker, "Incorporating spatial and temporal correlations to improve aggregation of decentralized day-ahead wind power forecasts," Revised and resubmitted to IEEE Access.

Overview

A methodology is proposed that trains machine learning models using the explanatory variables listed below to derive aggregated point and probabilistic wind power forecasts:

- Decentralized point forecasts: To eliminate duplicate features and reduce the high dimension matrices required to model a high number of wind farms in a region (without losing important spatial information), the correlated point forecasts are first clustered into k clusters using the clustering large applications algorithm (CLARA).
- The hour of day and month of year: These are included to model the well-known statistical regularity of wind profiles along diurnal and seasonal timescales.
- Atmospheric states: These are derived from self-organizing maps (SOMs) to represent large-scale synoptic circulation climatology for a study area.

The machine learning models proposed to test the hypothesis are:

(a) the k-nearest neighbor (k-NN) to derive the aggregated wind power point forecast, and

(b) conditional KDE to derive aggregated wind power predictive densities.

The proposed methodology is demonstrated using the day-ahead point forecast data obtained from 29 wind farms in South Africa. The point forecasts are evaluated using mean absolute error (MAE), root mean squared error (RMSE), and coefficient of determination (R^2), while the probabilistic forecasts are evaluated using reliability, sharpness, and skill score.

Findings towards hypothesis validation

The forecasting results from the proposed approach are superior (55% less MAE, 47% less RMSE, and 22% more R^2) as compared to simply adding the decentralized point forecasts. In addition, the sharpness and skill score results showed a significant improvement when the proposed explanatory variables were considered as compared to simply adding decentralized forecasts. These results are a confirmation that training the considered machine learning models using the proposed explanatory variables improves the accuracy of aggregated wind power forecasts as compared to simply adding decentralized forecasts, thereby validating **Hypothesis 2**.

In addition to hypothesis validation above, the following findings relating to the proposed approach are made:

- In the case study, the proposed approach performs better between morning and mid-day, during autumn and winter seasons, and during large-scale atmospheric circulations dominated by high pressure conditions.

- The predictive densities obtained from the proposed approach are shown to be non-Gaussian and time-varying as expected given the time-varying nature of wind uncertainty.

3.3. N. Mararakanye, A. Dalton, and B. Bekker, "Characterizing Wind Power Forecast Error Using Extreme Value Theory and Copulas," IEEE Access, vol. 10, pp. 58547–58557, Jun. 2022, doi: 10.1109/access.2022.3179697.

Overview

This paper focuses on three key aspects associated with the extreme forecast errors of geographically distributed wind farms: suitable parametric distribution representation, effects of diurnality, seasonality and larger atmospheric circulations, and modeling multivariate distribution. Firstly, this paper proposes fitting a Generalized Pareto distribution (GPD) from extreme value theory to achieve a better estimation of extreme errors. Secondly, this paper splits extreme errors by hour, month, and atmospheric states to investigate the statistical regularities of GPD parameters along diurnal and seasonal timescales and larger atmospheric circulations. Thirdly, this paper uses copula functions to model multivariate extreme error distribution and investigates their effectiveness in providing a regional view of extreme errors. This paper tests the proposed methodology using the forecast error data obtained from 29 wind farms in South Africa.

Findings towards hypothesis validation

The main findings of this paper are:

- Some of the common distributions (normal, hyperbolic, Weibull, and beta) currently used for modeling wind power forecast errors can be inappropriate in representing extreme forecast errors. The extreme forecast errors can be modeled with better accuracy using the extreme value theory by fitting the GPD, which confirms **Hypothesis 3(a)**.
- Extreme forecast errors can have strong diurnal and seasonal components depending on the location of wind farms under consideration. Therefore, diurnal and seasonal cycles

play an important role in the occurrence of extreme forecast errors and can improve estimation thereof.

- Extreme forecast errors can also change significantly from one atmospheric state to the other. The dominant high-pressure circulation, particularly the ridging of the Indian Ocean High-Pressure System is associated with reduced extreme forecast errors. This not only improves the estimation of extreme forecast errors but also allows for the estimation of extreme forecast errors based on physical meteorological phenomena. In addition, this finding, along with the previous one, confirm **Hypothesis 3(b)**.
- Copulas can be effective in providing a wide range of probabilistic analyses, giving more insight into the characteristics of region-wide extreme forecast errors, thereby confirming **Hypothesis 3(c)**.

3.4. N. Mararakanye and B. Bekker, "Estimating wind power uncertainty using quantile smoothing splines regression," Accepted for publication in 57th International Universities Power Engineering Conference (Inclusion into the IEEE Xplore), September 2022.

Overview

This paper uses the quantile smoothing splines (QSS) regression to derive the conditional quantiles of wind power forecast error for a given wind power forecast. The proposed approach is tested using the day-ahead aggregated wind power data from eight wind farms in South Africa. The performance of the proposed approach is compared to that of a linear regression model (assuming normality), and fitting beta distributions in different forecast bins. This paper uses four common metrics for evaluating quantile estimations: reliability, sharpness, resolution, and skill score [84], [85].

Findings towards hypothesis validation

The main finding of this paper is that the reliability, sharpness, resolution, and skill score results of the QSS regression are superior compared to linear regression and fitting beta distributions in different bins, thereby confirming **Hypothesis 4**. In addition, this paper finds that the prediction intervals' resolution reveals that both QSS regression and fitting beta distributions in different bins can provide a wind power forecast-dependent assessment of uncertainty, whereas linear regression intervals, as expected, has no resolution.

.

4. Summary of novel contributions and their applications

The following three points are regarded as the dissertation's main novel contributions:

4.1. Providing a framework for comprehending VRE integration issues of a region under consideration

The first novel contribution of this dissertation is to provide a framework for comprehending VRE integration issues based on available renewable resources, VRE targets (or penetration level), and grid characteristics of a region under consideration. This is significant because different VRE integration issues require different input data, models, and simulation tools to study. It is thus resource intensive to study all VRE integration issues. The framework presented in this dissertation can be used by network planners, policymakers, and grid operators to understand VRE integration issues of concern to their region prior conducting detailed studies, thereby reducing the resources required.

4.2. Improving the accuracy of aggregated forecasts derived from decentralized point forecasts

The second novel contribution of this dissertation is to improve the accuracy of aggregated point and probabilistic forecasts derived from decentralized point forecasts by incorporating some of the common spatial and temporal correlations, including those caused by large-scale atmospheric circulations. The aggregated point forecasts of the considered case study have 55% less MAE, 47% less RMSE, and 22% more R^2 as compared to simply adding the decentralized point forecasts. This is particularly important in regions where individual wind farms generate their own forecasts and do not necessarily have access to the measurements from other wind farms. The proposed approach provides system operators with a way of aggregating these forecasts while considering some of the common spatial and temporal correlations. In addition, the derived predictive densities can be used to improve operational decisions such as dynamic operating reserve allocation and stochastic unit commitment. An additional contribution here is contained in the proposed approach towards atmospheric states, which demonstrates another way in which large-scale atmospheric circulation patterns can be incorporated into short-term wind power forecasting.

4.3. Improving the understanding and estimation of wind power forecasting uncertainty

The third and fourth novel contributions of this dissertation are to propose modeling approaches for improving the understanding and estimation of wind power forecasting uncertainty, by:

(a) Finding a suitable parametric distribution for representing extreme wind power forecast errors, improving understanding on some of the factors that may influence extreme errors, and proposing a suitable model for representing spatial correlations of extreme errors between wind farms.
(b) Investigating how wind power forecast error distribution changes with the wind power forecast, as well as deriving the conditional forecast error distribution for a given wind power forecast.

These contributions can assist system operators with a method of deriving conditional forecast error distributions that changes based on various states (i.e., hour, month, atmospheric and spatial configuration of wind farms), as well as wind power forecast. These conditional distributions typically contain more probabilistic information (as compared to unconditional distribution), which can improve operating reserve allocation to account for wind power uncertainty.

5. Limitations

The following limitations related to this dissertation have been identified:

- The proposed methodologies (in papers 2 – 4) were tested using the data obtained from 29 wind farms in South Africa. Since the individual wind power data is sensitive and confidential, Eskom (the utility company in South Africa) was only able to send the data in groups of three nearest wind farms (summed together). This implies a drop in resolution of the data, which may have impacted the performance of the proposed methodologies in this dissertation. It is anticipated that a higher resolution data will increase the accuracy of aggregated forecasts. Therefore, one can test the proposed methodologies using individual wind farms' data if this can be obtained. There is no reason identified why the proposed methodologies would not work if individual wind farms' data is used.
- The proposed methodologies (in papers 2 – 4) were tested using day-ahead hourly wind power forecast data. The effectiveness of the proposed methodologies can be tested for different time resolution and forecast horizon data. There is no reason identified why the proposed methodologies would not work for other time resolutions and forecast horizon data.
- Regarding Paper 2, there are numerous machine learning models that have been applied for wind power forecasting as shown in the literature review conducted in the paper. However, the *k*-NN- and KDE-based approaches are proposed to test this hypothesis because they are common and easy to implement. The other models are not tested in this dissertation because the two approaches are adequate in validating the formulated hypothesis. Other models can be implemented while monitoring the improvement in aggregated forecasting accuracy.

6. Future work

The following prospective future study areas have been identified:

- The power grid is often made up of a mix of VRE sources. The hypotheses in Paper 2-4 are formulated specifically around wind power application. However, the applicability of the proposed methodologies for aggregating wind power decentralized forecasts (Paper 2) and estimating wind power uncertainty (Paper 2 – 4) can be tested for other VRE sources such as solar PV. There is no identified reason why the proposed methodologies would not work for other VRE sources.
- The main drawback of the proposed conditional KDE approach (used in Paper 2) for deriving conditional aggregated wind power predictive densities is the difficulty in selecting good bandwidths, especially in the presence of large datasets and high dimensionality. Therefore, more work needs to be done in terms of bandwidths selection of high dimensional dataset in KDE-based approaches.
- Regarding papers 2 – 4, different approaches of estimating wind power forecasting uncertainty are proposed. This uncertainty is also shown to change under different conditions, such as time of day, season, atmospheric state, and wind power forecast. There is a need for more work on how the estimated conditional uncertainty can be incorporated into operational decisions such as dynamic operating reserve allocation and stochastic unit commitment.

7. References

[1] REN21, “Global status report,” Paris, France, 2022.

[2] UNFCCC, “The Paris Agreement.” https://unfccc.int/process-and-meetings/the-paris-agreement/the-paris-agreement (accessed Jul. 20, 2022).

[3] EU, “Renewable energy targets.” https://energy.ec.europa.eu/topics/renewable-energy/renewable-energy-directive-targets-and-rules/renewable-energy-targets_en (accessed Jul. 20, 2022).

[4] L. Myllyvirta and X. Zhang, “Analysis: What do China’s gigantic wind and solar bases mean for its climate goals?,” *CarbonBrief*, 2022. https://www.carbonbrief.org/analysis-what-do-chinas-gigantic-wind-and-solar-bases-mean-for-its-climate-goals/#:~:text=The%20planned%20installation%20of%20wind,generation%20by%20the%20same%20year. (accessed Jul. 28, 2022).

[5] ET Online, “India needs $225-250 bn investment to meet its 2030 renewable energy target:Moody’s,”*TheEconomicTimes*,2022.https://economictimes.indiatimes.com/industry/renewables/india-needs-225-250-bn-investment-to-meet-its-2030-renewable-energy-target-moodys/articleshow/92173747.cms?from=mdr (accessed Jul. 20, 2022).

[6] M. Motyka, J. Thomson, M. Piechowski, C. Rizzo, and S. Sanborn, “Renewable transition: Separating perception from reality,” *Delloitte*, 2021. https://www2.deloitte.com/us/en/insights/industry/power-and-utilities/us-renewable-energy-transition.html (accessed Jul. 20, 2022).

[7] Eskom, “Integrated Report,” Sandton, South Africa, 2021.

[8] Department of Energy, “Integrated Resource Plan for Electricity 2010-2030,” Pretoria, South Africa, 2011.

[9] Department of Energy, “Integrated Resource Plan,” Pretoria, South Africa, 2019.

[10] IRENA, “Renewable power generation costs in 2020,” Abu Dhabi, United Arab Emirates, 2021.

[11] IRENA and ILO, “Renewable energy and jobs - Annual review 2021,” Abu Dhabi, Geneva, 2021.

[12] P. Jain and P. Wijayatunga, “Grid integration of wind power: Best practices for emerging wind markets,” Asian Development Bank, Mandaluyong City, Philippines, 2016.

[13] J. Cochran *et al.*, "Flexibility in 21st century power systems," National Renewable Energy Laboratory, Golden, CO (United States), May 2014. doi: 10.2172/1130630.

[14] P. Denholm and M. Hand, "Grid flexibility and storage required to achieve very high penetration of variable renewable electricity," *Energy Policy*, vol. 39, no. 3, pp. 1817–1830, Mar. 2011, doi: 10.1016/j.enpol.2011.01.019.

[15] J. Cochran, M. Milligan, and J. Katz, *Sources of operational flexibility*. Golden, Colorado, USA: National Renewable Energy Laboratory, 2015. Accessed: Mar. 16, 2018. [Online]. Available: http://greeningthegrid.org/resources/factsheets/sources-of-operational-flexibility

[16] International Energy Agency, "System Integration of Renewables: Implications for Electricity Security," International Energy Agency, Paris, France, 2016. Accessed: Apr. 09,2018.[Online].Available:https://www.iea.org/media/topics/engagementworldwide/g7/IEAIRENAReporttotheG7onSystemIntegrationofRenewables.pdf

[17] N. E. Koltsaklis, A. S. Dagoumas, and I. P. Panapakidis, "Impact of the penetration of renewables on flexibility needs," *Energy Policy*, vol. 109, no. October 2016, pp. 360–369, 2017, doi: 10.1016/j.enpol.2017.07.026.

[18] P. Vithayasrichareon, J. Riesz, and I. MacGill, "Operational flexibility of future generation portfolios with high renewables," *Applied Energy*, vol. 206, no. August, pp. 32–41, 2017, doi: 10.1016/j.apenergy.2017.08.164.

[19] M. Dreidy, H. Mokhlis, and S. Mekhilef, "Inertia response and frequency control techniques for renewable energy sources: A review," *Renewable and Sustainable Energy Reviews*, vol. 69, pp. 144–155, 2017, doi: 10.1016/j.rser.2016.11.170.

[20] P. de Mello and C. P. van Dam, "Summary of recent wind integration studies: Experience from 2007-2010," California Energy Commision, California, USA, 2012.

[21] I. Dudurych, M. Burke, L. Fisher, M. Eager, and K. Kelly, "Operational Security Challenges and Tools for a Synchronous Power System with High Penetration of Non-conventional Sources," *CIGRE Science & Engineering Journal*, vol. February, no. February, pp. 91–101, 2017.

[22] N. Troldborg and J. Sørensen, "A simple atmospheric boundary layer model applied to large eddy simulations of wind turbine wakes," *Wind Energy*, vol. 17, pp. 657–669, 2014, doi: 10.1002/we.

[23] H. Holttinen *et al.*, "Impacts of large amounts of wind power on design and operation of power systems, results of IEA collaboration," *Wind Energy*, vol. 14, no. 2, pp. 179–192, Mar. 2011, doi: 10.1002/we.410.

[24] World Bank Group, "A Guide to Operational Impact Analysis of Variable Renewables: Application to the Philippines," World Bank Group, Washington DC, USA, 2013.

[25] G. Balaban, G. Lazaroiu, V. Dumbrava, and C. Sima, "Analysing Renewable Energy Source Impacts on Power System National Network Code," *Inventions*, vol. 2, no. 3, pp. 1–18, Aug. 2017, doi: 10.3390/inventions2030023.

[26] E. Vilchez and J. Stenzel, "Impact of renewable energy generation technologies on the power quality of the electrical power systems," in *22nd International Conference and Exhibition on Electricity Distribution (CIRED 2013)*, 2013, vol. 5. doi: 10.1049/cp.2013.0791.

[27] I. Graabak and M. Korpås, "Variability Characteristics of European Wind and Solar Power Resources—A Review," *Energies (Basel)*, vol. 9, no. 449, pp. 1–31, Jun. 2016, doi: 10.3390/en9060449.

[28] F. Ueckerdt, R. Brecha, and G. Luderer, "Analyzing major challenges of wind and solar variability in power systems," *Renewable Energy*, vol. 81, pp. 1–10, Sep. 2015, doi: 10.1016/j.renene.2015.03.002.

[29] I. S. Jha, Y. K. Sehgal, S. Sen, and K. Bhambhani, "Grid Integration of Large Scale Renewable Generation-Initiatives in Indian Power System," 2014.

[30] W.-Y. Chang, "A Literature Review of Wind Forecasting Methods," *Journal of Power and Energy Engineering*,vol.02,no.04,pp. 161–168, 2014, doi:10.4236/jpee.2014.24023.

[31] H. S. Dhiman and D. Deb, "A Review of Wind Speed and Wind Power Forecasting Techniques," Sep. 2020.

[32] J. Lerner, M. Grundmeyer, and M. Garvert, "The importance of wind forecasting," *Renewable Energy Focus*, vol. 10, no. 2, pp. 64–66, Mar. 2009, doi: 10.1016/s1755-0084(09)70092-4.

[33] P. Li, X. Guan, and J. Wu, "Aggregated wind power generation probabilistic forecasting based on particle filter," *Energy Conversion and Management*, vol. 96, pp. 579–587, May 2015, doi: 10.1016/j.enconman.2015.03.021.

[34] M. Sun, C. Feng, and J. Zhang, "Aggregated Probabilistic Wind Power Forecasting Based on Spatio-Temporal Correlation," *IEEE Power and Energy Society General Meeting*, vol. 2019-Augus, pp. 1–5, 2019, doi: 10.1109/PESGM40551.2019.8973912.

[35] Q. Zhu, J. Chen, L. Zhu, X. Duan, and Y. Liu, "Wind speed prediction with spatio-temporal correlation: A deep learning approach," *Energies (Basel)*, vol. 11, no. 4, pp. 1–18, 2018, doi: 10.3390/en11040705.

[36] Z. Wang, W. Wang, C. Liu, B. Wang, and S. Feng, "Probabilistic forecast for aggregated wind power outputs based on regional NWP data," *The Journal of Engineering*, vol. 2017, no. 13, pp. 1528–1532, Jan. 2017, doi: 10.1049/joe.2017.0587.

[37] B. Alonzo, P. Tankov, P. Drobinski, and R. Plougonven, "Probabilistic wind forecasting up to three months ahead using ensemble predictions for geopotential height," *International Journal of Forecasting*, vol. 36, no. 2, pp. 515–530, Apr. 2020, doi: 10.1016/j.ijforecast.2019.07.005.

[38] P. Pinson, H. Aa. Nielsen, H. Madsen, and G. Kariniotakis, "Skill forecasting from ensemble predictions of wind power," *Applied Energy*, vol. 86, no. 7–8, pp. 1326–1334, Jul. 2009, doi: 10.1016/j.apenergy.2008.10.009.

[39] J. W. Taylor, P. E. McSharry, and R. Buizza, "Wind Power Density Forecasting Using Ensemble Predictions and Time Series Models," *IEEE Transactions on Energy Conversion*, vol. 24, no. 3, pp. 775–782, Sep. 2009, doi: 10.1109/TEC.2009.2025431.

[40] N. Chen, Z. Qian, I. T. Nabney, and X. Meng, "Wind Power Forecasts Using Gaussian Processes and Numerical Weather Prediction," *IEEE Transactions on Power Systems*, vol. 29, no. 2, pp. 656–665, Mar. 2014, doi: 10.1109/TPWRS.2013.2282366.

[41] Y. Zhang and J. Wang, "A distributed approach for wind power probabilistic forecasting considering spatiooral correlation without direct access to off-site information," *IEEE Transactions on Power Systems*, vol. 33, no. 5, pp. 5714–5726, 2018, doi: 10.1109/TPWRS.2018.2822784.

[42] A. Lenzi, I. Steinsland, and P. Pinson, "Benefits of spatiotemporal modeling for short-term wind power forecasting at both individual and aggregated levels," *Environmetrics*, vol. 29, no. 3, p. e2493, May 2018, doi: 10.1002/env.2493.

[43] M. Sun, C. Feng, and J. Zhang, "Conditional aggregated probabilistic wind power forecasting based on spatio-temporal correlation," *Applied Energy*, vol. 256, no. February, p. 113842, 2019, doi: 10.1016/j.apenergy.2019.113842.

[44] R. J. Bessa, V. Miranda, A. Botterud, J. Wang, and E. M. Constantinescu, "Time Adaptive Conditional Kernel Density Estimation for Wind Power Forecasting," *IEEE Transactions on Sustainable Energy*, vol. 3, no. 4, pp. 660–669, Oct. 2012, doi: 10.1109/TSTE.2012.2200302.

[45] A. Malvaldi, S. Weiss, D. Infield, J. Browell, P. Leahy, and A. M. Foley, "A spatial and temporal correlation analysis of aggregate wind power in an ideally interconnected Europe," *Wind Energy*, vol. 20, no. 8, pp. 1315–1329, Aug. 2017, doi: 10.1002/we.2095.

[46] K. Porter and J. Rogers, "Status of Centralized Wind Power Forecasting in North America: May 2009 - May 2010," 2010. [Online]. Available: http://www.osti.gov/bridge

[47] Ministry of Energy, "Memorandum from the Parliament Office," South Africa, 2012.

[48] A. Dalton, B. Bekker, and M. J. Koivisto, "Classified atmospheric states as operating scenarios in probabilistic power flow analysis for networks with high levels of wind power," *Energy Reports*, vol. 7, pp. 3775–3784, Nov. 2021, doi: 10.1016/j.egyr.2021.06.060.

[49] A. Dalton, B. Bekker, and M. J. Koivisto, "Simulation and detection of wind power ramps and identification of their causative atmospheric circulation patterns," *Electric Power Systems Research*, vol. 192, p. 106936, Mar. 2021, doi: 10.1016/j.epsr.2020.106936.

[50] A. Dalton, B. Bekker, and M. J. Koivisto, "Atmospheric circulation archetypes as clustering criteria for wind power inputs into probabilistic power flow analysis," in *2020 International Conference on Probabilistic Methods Applied to Power Systems (PMAPS)*, Aug. 2020, pp. 1–6. doi: 10.1109/PMAPS47429.2020.9183659.

[51] D. J. Brayshaw, A. Troccoli, R. Fordham, and J. Methven, "The impact of large scale atmospheric circulation patterns on wind power generation and its potential predictability: A case study over the UK," *Renewable Energy*, vol. 36, no. 8, pp. 2087–2096, Aug. 2011, doi: 10.1016/j.renene.2011.01.025.

[52] H. C. Bloomfield, D. J. Brayshaw, P. L. M. Gonzalez, and A. Charlton-Perez, "Sub-seasonal forecasts of demand and wind power and solar power generation for 28

European countries," *Earth System Science Data*, vol. 13, no. 5, pp. 2259–2274, May 2021, doi: 10.5194/essd-13-2259-2021.

[53] R. J. Davy, M. J. Woods, C. J. Russell, and P. A. Coppin, "Statistical Downscaling of Wind Variability from Meteorological Fields," *Boundary-Layer Meteorology*, vol. 135, no. 1, pp. 161–175, Apr. 2010, doi: 10.1007/s10546-009-9462-7.

[54] C. Wan, Z. Xu, P. Pinson, Z. Y. Dong, and K. P. Wong, "Probabilistic Forecasting of Wind Power Generation Using Extreme Learning Machine," *IEEE Transactions on Power Systems*, vol. 29, no. 3, pp. 1033–1044, May 2014, doi: 10.1109/TPWRS.2013.2287871.

[55] Y. Zhang, J. Wang, and X. Wang, "Review on probabilistic forecasting of wind power generation," *Renewable and Sustainable Energy Reviews*, vol. 32, pp. 255–270, Apr. 2014, doi: 10.1016/j.rser.2014.01.033.

[56] M. A. Ortega-Vazquez and D. S. Kirschen, "Estimating the Spinning Reserve Requirements in Systems With Significant Wind Power Generation Penetration," *IEEE Transactions on Power Systems*, vol. 24, no. 1, pp. 114–124, Feb. 2009, doi: 10.1109/TPWRS.2008.2004745.

[57] R. Doherty and M. O'Malley, "A New Approach to Quantify Reserve Demand in Systems With Significant Installed Wind Capacity," *IEEE Transactions on Power Systems*, vol. 20, no. 2, pp. 587–595, May 2005, doi: 10.1109/TPWRS.2005.846206.

[58] P. V. Swaroop, I. Erlich, K. Rohrig, and J. Dobschinski, "A stochastic model for the optimal operation of a wind-thermal power system," *IEEE Transactions on Power Systems*, vol. 24, no. 2, pp. 940–950, 2009, doi: 10.1109/TPWRS.2009.2016504.

[59] K. Methaprayoon, C. Yingvivatanapong, W.-J. Lee, and J. R. Liao, "An Integration of ANN Wind Power Estimation Into Unit Commitment Considering the Forecasting Uncertainty," *IEEE Transactions on Industry Applications*, vol. 43, no. 6, pp. 1441–1448, 2007, doi: 10.1109/TIA.2007.908203.

[60] E. D. Castronuovo and J. A. P. Lopes, "On the Optimization of the Daily Operation of a Wind-Hydro Power Plant," *IEEE Transactions on Power Systems*, vol. 19, no. 3, pp. 1599–1606, Aug. 2004, doi: 10.1109/TPWRS.2004.831707.

[61] S. Tewari, C. J. Geyer, and N. Mohan, "A Statistical Model for Wind Power Forecast Error and its Application to the Estimation of Penalties in Liberalized Markets," *IEEE*

Transactions on Power Systems, vol. 26, no. 4, pp. 2031–2039, Nov. 2011, doi: 10.1109/TPWRS.2011.2141159.

[62] H. Bludszuweit, J. A. Dominguez-Navarro, and A. Llombart, "Statistical Analysis of Wind Power Forecast Error," *IEEE Transactions on Power Systems*, vol. 23, no. 3, pp. 983–991, Aug. 2008, doi: 10.1109/TPWRS.2008.922526.

[63] J. M. Lujano-Rojas, G. J. Osorio, J. C. O. Matias, and J. P. S. Catalao, "Wind power forecasting error distributions and probabilistic load dispatch," in *2016 IEEE Power and Energy Society General Meeting (PESGM)*, Jul. 2016, pp. 1–5. doi: 10.1109/PESGM.2016.7741482.

[64] B. M. Hodge and M. Milligan, "Wind power forecasting error distributions over multiple timescales," *IEEE Power and Energy Society General Meeting*, no. December 2017, 2011, doi: 10.1109/PES.2011.6039388.

[65] B. S. Hodge, E. G. Ela, and M. Milligan, "Characterizing and modeling wind power forecast errors from operational systems for use in wind integration planning studies," *Wind Engineering*, vol. 36, no. 5, pp. 509–524, Oct. 2012, doi: 10.1260/0309-524X.36.5.509.

[66] B.-M. Hodge *et al.*, "Wind power forecasting error distributions: An international comparison," in *11th Annual International Workshop on Large-Scale Integration of Wind Power into Power Systems as well as on Transmission Networks for Offshore Wind Power Plants Conference*, 2012, no. September 2012.

[67] J. Wu, B. Zhang, H. Li, Z. Li, Y. Chen, and X. Miao, "Electrical Power and Energy Systems Statistical distribution for wind power forecast error and its application to determine optimal size of energy storage system," *International Journal of Electrical Power and Energy Systems*, vol. 55, pp. 100–107, 2014, doi: 10.1016/j.ijepes.2013.09.003.

[68] D. D. Tung and T. Le, "A statistical analysis of short-term wind power forecasting error distribution," *International Journal of Applied Engineering Research*, vol. 12, no. 10, pp. 2306–2311, 2017.

[69] B. Hodge and M. Milligan, "Wind power forecasting error distributions over multiple timescales," in *2011 IEEE Power and Energy Society General Meeting*, Jul. 2011, pp. 1–8. doi: 10.1109/PES.2011.6039388.

[70] P. Pinson, “Estimation of the uncertainty in wind power forecasting,” Mines ParisTech, Paris, France, 2006. [Online]. Available: http://paristech.bib.rilk.com/2187/

[71] G. Liao *et al.*, “Wind power prediction errors model and algorithm based on non-parametric kernel density estimation,” in *2015 5th International Conference on Electric Utility Deregulation and Restructuring and Power Technologies (DRPT)*, Nov. 2015, pp. 1864–1868. doi: 10.1109/DRPT.2015.7432551.

[72] A. Z. Zambom and R. Dias, “A review of kernel density estimation with applications to econometrics,” *International Econometric Review*, pp. 20–42, 2012.

[73] B. Mauch, J. Apt, P. M. S. Carvalho, and M. J. Small, “An effective method for modeling wind power forecast uncertainty,” *Energy Systems*, vol. 4, no. 4, pp. 393–417, Dec. 2013, doi: 10.1007/s12667-013-0083-3.

[74] N. Menemenlis, M. Huneault, and A. Robitaille, “Computation of Dynamic Operating Balancing Reserve for Wind Power Integration for the Time-Horizon 1–48 Hours,” *IEEE Transactions on Sustainable Energy*, vol. 3, no. 4, pp. 692–702, Oct. 2012, doi: 10.1109/TSTE.2011.2181878.

[75] W. Ko, D. Hur, and J.-K. Park, “Correction of wind power forecasting by considering wind speed forecast error,” *Journal of International Council on Electrical Engineering*, vol. 5, no. 1, pp. 47–50, Jan. 2015, doi: 10.1080/22348972.2015.1081581.

[76] A. Fabbri, T. GomezSanRoman, J. RivierAbbad, and V. H. MendezQuezada, “Assessment of the Cost Associated With Wind Generation Prediction Errors in a Liberalized Electricity Market,” *IEEE Transactions on Power Systems*, vol. 20, no. 3, pp. 1440–1446, Aug. 2005, doi: 10.1109/TPWRS.2005.852148.

[77] J. Zhang, B.-M. Hodge, J. Mierttinen, H. Holttinen, E. Gomez-Lazaro, and N. Cutulis, “Analysis of Variability and Uncertainty in Wind Power Forecasting: An International Comparison,” in *12th International Workshop on Large-Scale Integration of Wind Power into Power Systems*, 2013, pp. 1–16.

[78] M. Marquis *et al.*, “Forecasting the Wind to Reach Significant Penetration Levels of Wind Energy,” *Bull Am Meteorol Soc*, vol. 92, no. 9, pp. 1159–1171, Sep. 2011, doi: 10.1175/2011BAMS3033.1.

[79] I. González-Aparicio and A. Zucker, “Impact of wind power uncertainty forecasting on the market integration of wind energy in Spain,” *Applied Energy*, vol. 159, pp. 334–349, Dec. 2015, doi: 10.1016/j.apenergy.2015.08.104.

[80] B. Mauch, J. Apt, P. M. S. Carvalho, and P. Jaramillo, “What day-ahead reserves are needed in electric grids with high levels of wind power?,” *Environmental Research Letters*, vol. 8, no. 3, p. 034013, Sep. 2013, doi: 10.1088/1748-9326/8/3/034013.

[81] J. J. Miettinen and H. Holttinen, “Characteristics of day-ahead wind power forecast errors in Nordic countries and benefits of aggregation,” *Wind Energy*, vol. 20, no. 6, pp. 959–972, Jun. 2017, doi: 10.1002/we.2073.

[82] S. Bofinger, A. Luig, and H. G. Beyer, “Qualification of wind power forecasts,” 2002.

[83] A. T. Al-Awami and M. A. El-Sharkawi, “Statistical characterization of wind power output for a given wind power forecast,” in *41st North American Power Symposium*, Oct. 2009, vol. 0, no. 1, pp. 1–4. doi: 10.1109/NAPS.2009.5484044.

[84] P. Pinson, H. A. Nielsen, J. K. Møller, H. Madsen, and G. N. Kariniotakis, “Non-parametric probabilistic forecasts of wind power: required properties and evaluation,” *Wind Energy*, vol. 10, no. 6, pp. 497–516, Nov. 2007, doi: 10.1002/we.230.

[85] P. Pinson, G. Kariniotakis, H. A. Nielsen, T. S. Nielsen, and H. Madsen, “Properties of quantile and interval forecasts of wind generation and their evaluation,” in *European Wind Energy Conference and Exhibition*, 2006, pp. 1647–1656.

Paper 1

N. Mararakanye and B. Bekker, “Renewable energy integration impacts within the context of generator type, penetration level and grid characteristics,” *Renewable and Sustainable Energy Reviews*, vol. 108, no. March, pp. 441–451, 2019.

Citations up to date: 68

Quartile of the journal as calculated by Scimago (www.scimagojr.com): 1

To comply with the copyright requirements, the final pre-print version of the article is presented here, formatted in dissertation style.

The final published paper is available at: https://doi.org/10.1016/j.rser.2019.03.045.

Renewable energy integration impacts within the context of generator type, penetration level and grid characteristics

Ndamulelo Mararakanye [a] and Bernard Bekker [a]

[a] *Department of Electrical and Electronic Engineering, Stellenbosch University, Private Bag X1, Matieland, 7602, South Africa*

Abstract

There has been a worldwide rise in installations of grid-connected variable renewable energy (VRE) systems over the past few years. However, with the increasing share of these systems comes additional complexities that can affect planning and operation of a power system within a specific region. Several studies have been conducted across different regions with the general aim to identify the impacts of integrating high shares of VRE in the respective power grids. However, each region is different in terms of available renewable resources, VRE targets and grid characteristics. Therefore, the results of VRE integration studies are generally context specific and the impacts observed in one region might not be relevant to another. Given that conducting a full range of detailed VRE integration studies for each grid is costly, there is value in effectively identifying likely issues relevant to the specific region under consideration, towards a smaller set of detailed VRE integration studies. This paper presents a literature review based on international experience that aims to provide an understanding on the VRE integration impacts within the context of generator type, penetration level and grid characteristics. This can be used to identify the VRE integration impacts that are relevant to the region under consideration.

Keywords: Variable renewable energy; grid integration; penetration level; grid characteristics

1. Introduction

The integration of variable renewable energy (VRE) sources such as wind and solar photovoltaic (PV) requires appropriate planning to avoid possible operational impacts that may compromise reliability of the power system. The output power from VRE sources is variable and uncertain in all time scales, which complicates the requirement for the power system to continuously balance generation with varying load demand [1]. Experience has shown that as the share of VRE power becomes relatively high, and assuming no VRE power curtailment, conventional resources may be required to increase or decrease their power output quickly to compensate for the additional variability introduced by VRE generators [2-7]. In addition, latest

technologies of wind and PV generators are connected to the grid through power electronic based converters, which ultimately reduce the rotating mass (inertia) in the system, resulting in possible frequency stability issues [5,7,8]. Furthermore, VRE generators are available in different sizes ranging from a few kWp to several MWp and often connected to distribution networks. However, distribution networks are typically not planned nor designed for large uptake of generators and can easily experience over-voltages and power quality problems as a result of VRE generators [5]. Another related challenge is that VRE generators are usually located where the renewable resource is high, which may be far away from the load centres, resulting in weak interconnection between the central grid and the VRE generator [1,9,10]. This may lead to voltage fluctuations exceeding the stipulated limits in the grid code, which if not properly accounted for, may result in equipment damage and trigger instability or cascading blackouts [1,11].

Grid integration studies are usually the first step in identifying the feasible VRE targets of a region. The outcome of these studies informs the policymakers, regulators, utilities and system operators on the possible impacts of integrating high shares of VRE on the power system as well as the cost of actions required to mitigate these impacts. Within the technical context there are three general studies that are typically conducted depending on the questions to be answered and priorities of the study. These are capacity expansion, electricity production cost and power flow studies [1,12,13]. The common practice is to firstly conduct a capacity expansion study, which identifies the infrastructure required to achieve certain targets of VRE. This is followed by an electricity production cost study, which assesses the impact of VRE on unit commitment and economic dispatch. The focus of capacity expansion and electricity production cost studies is usually on a system level, and do not consider local and regional characteristics of the grid. As a result, potential impacts arising from these studies are usually verified by a more detailed power flow study, which assesses the impact of VRE on the ability of the power system to withstand disturbances (both steady-state and dynamic) [12,14-16]. The typical simulation horizon for each of these types of study, together with examples of studies in the literature conducted in different countries, are detailed in Table 1.

Table 1: Three common types of grid integration studies conducted across the world.

	Capacity Expansion	**Production Cost**	**Power Flow**
Problem investigated	System adequacy	System operation	System security
Analysis timeframe	Long term (20 to 40 years)	Weeks to years	Snapshot

Study examples	Renewable electricity futures study (United States) [17], Transformation of Europe's power system until 2050 (Europe) [18], Electricity capacity expansion modeling, analysis, and visualization: a summary of selected high-renewable modeling experiences (United States) [19], Integrated Resource Plan (IRP) 2018 (South Africa) [20], Greening the grid (India) [21,22].	The western wind and solar integration study phase 2 (United States) [14], European wind integration study (Europe) [16], Grid integration of photovoltaic power generation (Europe) [23], Power plant cycling costs (United States) [24], Flexibility study (South Africa) [25].	Integrating renewable energy-wind integration studies report (Australia) [26], Western wind and solar integration study phase 3-frequency response and transient stability (United States) [15], Grid and system integration study (El Salvador) [27], Grid integration of wind energy in the Western Cape (South Africa) [28].

Figure 1 diagrammatically presents some issues that have been assessed in literature for each type of VRE integration study. The issues are classified according to their time constant and the geographic extent to which these issues impact the power system (local, regional or system-wide).

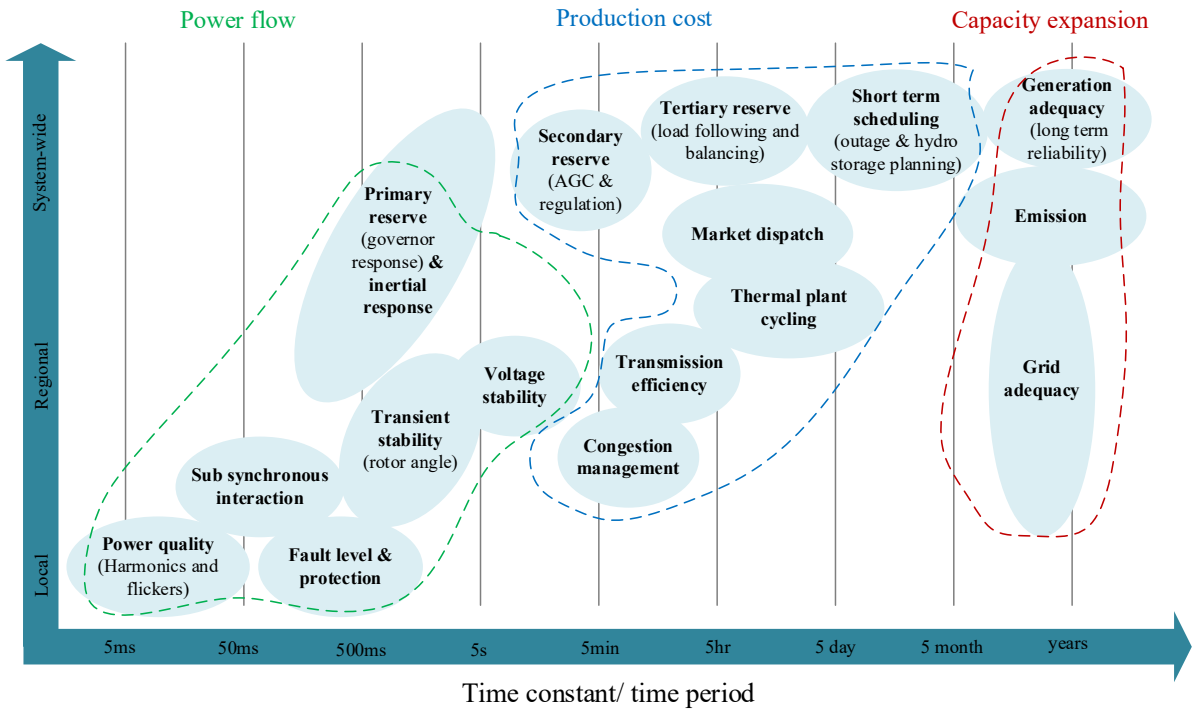

Figure 1: VRE grid integration issues assessed in the literature (Note that the diagram was adapted from [29]).

In general, issues shown in Figure 1 address different VRE integration impacts and hence, require different input data, models and simulation tools to study [30]. It is thus resource intensive to study all these issues, leading to a need to effectively identify and study only those issues that are most relevant to the region under consideration. However, each region is different in terms of available renewable resources, VRE targets (or penetration level) and grid

characteristics. International experience shows that these are the three main factors that influenced the VRE integration issues experienced in different regions [6,29,31-35]. Therefore, understanding how these factors contributed to the issues that were experienced in different regions can be the first step in prioritizing VRE integration issues for detailed VRE grid integration studies.

This paper presents a comprehensive literature review on how the three factors (generator type, penetration level and grid characteristics) contributed to VRE grid integration issues that were experienced in different regions across the world. This review enables network planners and policymakers with a framework within which to understand VRE integration issues of concern to their region, before conducting detailed studies. As a result, detailed studies can focus on the issues most likely to be relevant, which can reduce the resources needed. In addition, distribution and transmission operators already conduct different technical studies under different scenarios to ensure that the real time system reliability is adequate. This review will assist these operators in understanding when additional studies are required to account for the technical issues introduced by grid integration of VRE. In a nutshell, this review can be used as a conceptual framework for identifying the VRE integration issues that are relevant to the region under consideration. The literature reviewed in this paper focuses primarily on wind and solar PV systems since these are the most common VRE sources.

2. Generator type

The properties of wind and PV generators that can affect planning and operation of a power system were introduced in Section 1 above and can be summarised as; variable, uncertain, non-synchronous and location dependent. Each property is generally a multi-faceted concept that is described by a range of distinct characteristics, which are different for wind and PV generators. This section reviews the extent to which these properties differs for wind and PV, in order to understand how these different sources can impact the power system.

To begin with, both wind and solar resources are variable and uncertain in all time scales (seconds to seasons). On a long time scale, a study conducted in the United States (US) using 10 year data collected from different wind plants across the country showed significant inter-annual changes, with the highest production year generating 40% more energy than the lowest production year [36]. In Europe, the inter-annual capacity factor for most onshore and offshore wind generation varies between 20-40% and 39-43% respectively [33]. The global analysis conducted by [37], found that the inter-annual variability of wind varies widely by location since the coefficient of variation can be less than 3% in some regions, while more than 10% in

others. Compared to wind, the long term variability of the solar resource is more consistent since it is largely caused by the earth's tilt during different times of the year. This is confirmed by significantly lower inter-annual variability of solar irradiation (coefficient of variation less than 5%) in most countries across the world [38-41].

On a short time scale, Figure 2 shows maximum wind and PV power output variations (as a percentage of total wind or PV capacity) experienced in various countries and regions. It is clear from Figure 2 that maximum wind and PV power output variations experienced in various countries increased as longer time scales were considered. The experienced 15-minute maximum power output variations are less than 10% for most countries, while the 8-hour maximum variations are above 40% for most countries. In essence, dispatchable generators in these regions should be able to ramp up and down the power equivalent to 10% and 40% of wind or PV capacity in 15 minutes and 8 hours respectively. However, not all dispatchable generators can ramp up and down a significant amount of power within a short period of time. Thus, from the system operator point of view and given the generation mix of the power system, it might be easier to accommodate 40% variations over 8 hour period than 10% variations over 15 minutes period.

Power output variations are significantly reduced when a large region covering a wide range of micro-climates such as the EU28 is considered as opposed to geographically small or climatically relatively homogeneous regions such as South Australia. It can be observed in Figure 2 when looking at EU28 versus individual EU member states that this potential smoothing effect is higher for wind than solar. This is because wind power output variations are very location dependent as seen by wide range of values measured in various countries. On the other hand, PV power output variations are relatively consistent across all considered regions, because the variations are largely due to the movement of earth relative to the sun throughout the day.

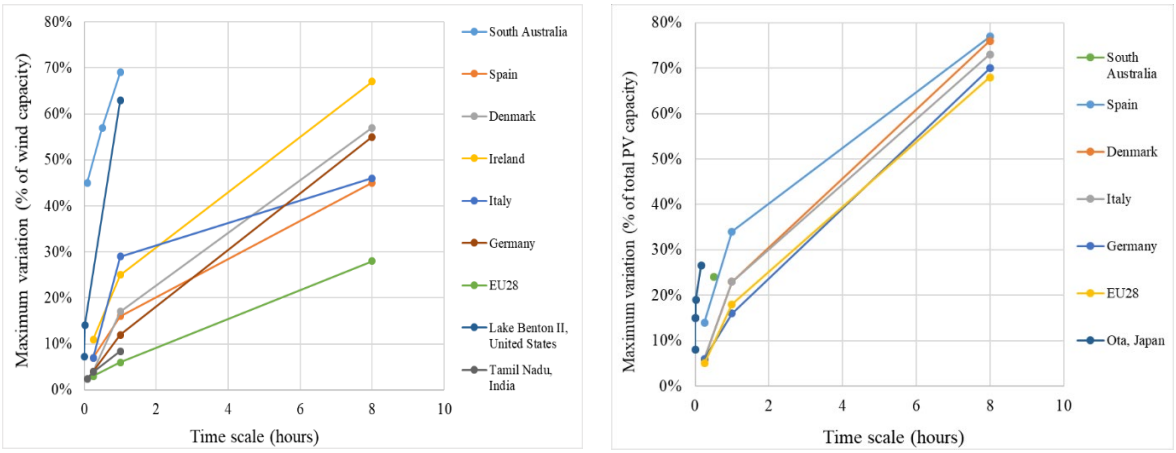

a) Wind b) PV

Figure 2: Maximum wind and PV power output variations experienced in various countries [42-46].

The worst case wind power output variations occur during a passing storm where the wind speed exceeds the cut-out speed of the wind turbine, resulting in rapid power shutdown of a turbine [33]. However, due to the averaging effect across a wind farm, the output takes several minutes to reduce to zero. Such an incident happened in Denmark on the 8th of January 2005 and it took 6 hours for the installed wind power to drop from 2GW to 200MW, which corresponds to a 15% reduction per hour [33]. On the other hand, the worst case solar variations occur when clouds pass over the PV plant, resulting in shading of some or all modules [47,48] . The output of a module underneath the cloud can drop to 20-30% of the output before the cloud passed in a matter of seconds [48]. However, the time it takes to cover the entire plant depends on the size and layout of the plant, cloud speed, height and other factors. Thus, the time it would take to shade an entire 100 MW PV plant, for example, will typically be in the order of minutes not seconds [47].

It is also important to understand how the variability of both wind and solar sources correlates with the load demand. In a study conducted in EU28 countries using 2014 data, wind-load and solar-load showed a positive correlation coefficient ranging between 0.03-0.32 and 0.02-0.34 respectively [42]. When the whole EU28 region was considered, both solar and wind showed a 0.25 correlation to the load. Wind and solar, on the other hand, showed a negative correlation ranging between -0.04 and -0.24 and when considering the whole EU28 region, the correlation was -0.24. This shows that wind and solar variability in the EU28 region has a complementary behaviour. This behaviour was also confirmed by other studies conducted in different regions across the world [49-53]. In fact, a study conducted in South Africa showed that if a balanced

combination of wind and PV is connected to the grid, up to 30% annual energy share of wind and PV can be achieved without increasing the fluctuations of the system [54].

It is clear from the sample case studies provided above that wind and solar variations are reduced if the installations are distributed over large areas. This is important because system operators only need to deal with aggregated output from large group of VRE plants and not individual plants. According to the case studies considered, this smoothing effect is generally higher for wind than solar. However, there is a challenge in the fact that wind resource tend to be heavily dependent on the location as compared to solar resource that tend to be distributed evenly across the country or region. Thus, siting wind farms across the country to minimise variability rather than to maximise energy output might significantly reduce the overall energy output, which is less attractive to the developers. A study done in South Africa highlighted the need to spread the wind plants across the country, even if the overall output would reduce [54]. The study showed that if wind farms are widely distributed, a 50% share of wind energy in South Africa electricity mix would not increase inter-hour gradients.

As highlighted earlier, modern wind and PV generators are interfaced to the grid through power electronic converters and therefore do not contribute natural inertia to the system. In addition, both wind and PV generators are usually operated at maximum power point (MPP) and thus do not have power reserve to support the system with frequency control. Therefore, one way to emulate inertia is by shifting the operating point of these generators from the MPP curve to a reduced level using a de-loading controller [8,55,56]. However, this option reduces the efficiency of the generators, which can have negative financial implications depending on the regulations of the region. Another option of emulating inertia for wind generators is to extract the stored kinetic energy from its rotating mass using controllers [8,55,57]. This option is not available for PV generators since there is no rotating mass in such generators.

To summarise the review in terms of how the generator type contributed to VRE grid integration issues experienced in different regions, the following can be noted:

- The long-term (inter-annual) variability of wind is largely uncorrelated as compared to solar variability that is well correlated. This affects the long term generation adequacy of the grid and thus the potential inter-annual wind energy deficits that should be taken into account on capacity expansion studies of regions that are planning to integrate high shares of wind generators.
- On a short time frame, the maximum wind and PV power output variations recorded in the literature increase with the increase in the time interval under consideration. This

implies that the minute-minute power variations of wind and PV plants are small, while the hourly and eight-hourly power variations of wind and PV plants can be significantly high. However, not all dispatchable generators have the capability to ramp up and down significant power on a minute-minute basis. Thus, to account for these small variations usually calls for expensive regulation and load following reserves. The high eight-hourly power variations can be easier to account for with adequate day-ahead unit commitment.

- The maximum wind power output variations are significantly reduced when installations across large area are considered. In addition, wind and solar have a complimentary behaviour, which can further reduce the need for reserve requirements at different time scales.
- Wind resource is location dependent, while solar resource is usually distributed more evenly across the country. Thus, there is a higher chance of weakly interconnected wind plants as compared to solar, which can increase the likelihood of violation of power quality parameters as well as transmission congestion.
- Finally, both wind and PV generators do not contribute natural inertia to the system. However, by operating both these generators at de-loading curve instead of following the MPP, the reserve power can be used to emulate system inertia. Wind generators also have stored kinetic energy contained in their rotating mass that can be extracted through controllers. This provide additional options for frequency control that is not available in solar generators.

Now that the impact of the generator type on the power system has been reviewed, the next section will review how penetration level contributed to the VRE integration issues experienced in different regions.

3. Penetration level of VRE

It is technically possible to integrate high shares of wind and solar into the grid. However, there is a limit on the acceptability of the additional costs that are required to account for impacts introduced by these sources. Currently, there are several countries approaching or exceeding 10% VRE share in annual energy generation - see Figure 3. Experience from these countries and results from studies in the literature can provide an insight on the potential impacts of VRE integration as the penetration level increases. The following sub-sections describe the penetration levels reported in literature at which countries with high share of wind and solar started experiencing different VRE integration issues.

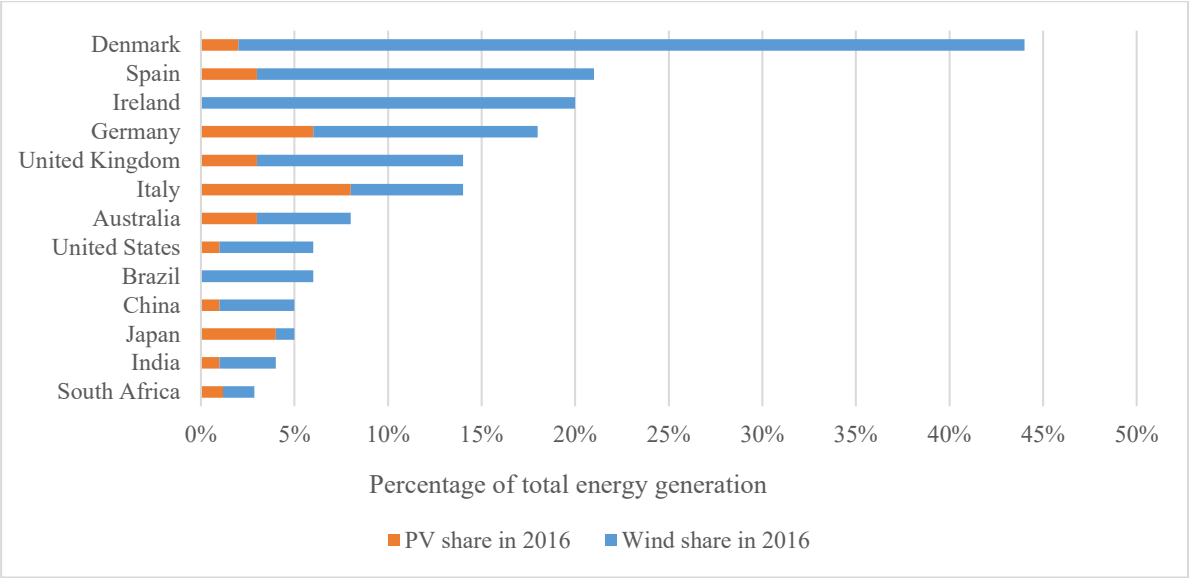

Figure 3: The VRE share in annual energy generation for a selection of countries [58,59].

3.1.Fault level

Fault level is the product of pre-fault voltage magnitude and post-fault current. The fault current is only limited by the impedance in the path between the power source and the fault location (source impedance) and hence fault levels are different at different points in the network. As a result, fault levels can provide information on interconnection strength at any point in the network. In addition, protection devices are rated based on the fault level of their respective location within the network.

Studies focused on the fault level contribution of power electronic based sources have found that inverters are capable of disconnecting from the power system within the first cycle following a fault [60,61]. Therefore, the behavior of power electronic based sources is controllable even during the worst-case fault scenarios. As a result, grid codes in most countries include low voltage ride through (LVRT) specifications, which force the power electronic based sources to remain connected to the power system for a certain period of time subsequent to a fault before disconnecting [62-64]. In addition, even if the control strategies are disabled, tests have shown that the fault level contribution from power electronic based sources ranges between 1.1 and 1.5 times their nominal currents, which is significantly lower than the 4 to 10 times fault to nominal current ratio caused by typical rotating machines [61].

3.2.Harmonics and Flicker

Harmonic currents are caused by non-linear loads such as inverters, static VAR compensators, furnaces, etc. The flow of harmonic currents through the source impedance creates voltage harmonics, which can affect all the loads between the source and the harmonic-causing load.

Voltage flicker, on the other hand, occur when the voltage magnitude varies due to fast load changes or power fluctuations from VRE sources. Flicker emitted by VRE sources depend on source type, characteristics and impedance.

Harmonics and flicker usually affect the local network and can become a challenge at any VRE penetration level if they are not effectively mitigated. However, these phenomena are difficult to evaluate using available simulation tools and are only easily measurable when the VRE plant is already installed. The measurements done in India found that wind plants connected in areas with low fault levels (or high source impedances) can cause ±6% voltage and current harmonic emissions at the point of connection [65]. Similar results were obtained in measurements conducted in the Rockampton distribution network in Australia [66]. The measurements in this reference showed that the current harmonic distortion exceeded the regulatory standard in both HV and LV distribution networks. Harmonics and flicker exceeding the required specifications can be managed by effective utilization of harmonic filters and different dynamic voltage stabilizers respectively.

3.3.Sub-synchronous interactions

As explained earlier, wind turbines are usually installed far from the load centres through long distance transmission lines. These lines make use of series capacitors (also referred to as series compensation) to compensate for the high inductance introduced by long transmission lines. This results in increased transmission line capacity, increased fault levels and improved system stability. However, series capacitors can introduce series resonances below the fundamental frequency that can interact with neighbouring wind turbine converter control systems.

Sub-synchronous interactions are local issues and can occur at any penetration level. In 2009, sub-synchronous resonance was observed on a wind farm in Texas (USA) [67]. An unplanned contingency resulted in direct interconnection between the doubly fed induction generator (DFIG) wind farm and a 345kV series compensated transmission line. After the fault was cleared, the current and voltage sub-synchronous resonance with a frequency of 20 Hz occurred on the transmission system. The system voltage exceeded 300% of the nominal value, forcing the turbines to enter crowbar state. The crowbar circuits of several turbines were damaged by the associated excessive current. Similarly, in 2012, several sub-synchronous resonance incidences with frequencies of 6-8 Hz occurred in wind farms of Hibei Province (China), which resulted in turbines tripping [68]. Sub-synchronous interactions can be managed by effective utilization of flexible AC transmission system (FACTS) devices, control of series capacitor and

converter, sub-synchronous frequency relays, pole face damper winding as well as bypass and blocking filters [69,70].

3.4.Voltage stability

Voltage stability is associated with the ability of the network to meet local reactive power requirements, so as to maintain the voltage at acceptable levels during steady state and following disturbances. Voltage stability is also a local issue and can be a problem to the network within the vicinity of the point of connection irrespective of penetration level. The latest solar and wind technologies are manufactured with some reactive power capability together with advanced control strategies, which can effectively mitigate voltage stability issues if adequate connection specifications are in place [71]. As a result, grid codes of most countries require VRE plants above a certain rating connected to distribution and transmission networks to have voltage and/or reactive power control capability at their terminals [10].

3.5.VRE Power Curtailments

Several countries have experienced power curtailments as a result of an increased share of RE. These curtailments can be due to transmission congestion (local network constraints) or challenges with system balancing in cases when VRE generation is high during low loading conditions and conventional units cannot be pushed further down due to minimum operating constraints. In isolated or medium sized interconnected grids, limits can be placed on RE plants in order to maintain frequency requirements and address other stability issues [71].

A literature review conducted in [72] compared wind and PV curtailment levels of various regions across the world. Countries such as Spain, Germany and Ireland have managed more than 10% share of VRE with less than 4% of curtailments between 2008 and 2011, while Portugal and Denmark managed 24% and 43% shares of VRE respectively, with almost 0% curtailment in 2014 [72]. In Portugal, the legislation does not allow VRE curtailment unless there is a technical problem [73]. High instantaneous penetration of VRE is managed by the flexibility of hydro power plants, exporting excess power to Spain and halting power imports from France [73]. On the other hand, Denmark relies on strong interconnections with neighbouring power systems to achieve high penetration of VRE without curtailments [73].

China, ERCOT and Italy, have experienced more than 10% curtailments with even less VRE share (less than 5%) [72]. The curtailments in China are attributed to wind plants concentrated far away from the load centres, short planning to construction time of wind turbine as compared to the planning and construction time of transmission network upgrades, and wind plants

concentration in the north of China where there is a lack of flexible generation such as gas power stations and pumped storage [74]. To address this challenge, China improved on generation scheduling, forecasting and the use of wind power for heating in order to increase local load of areas with high wind resources. In addition, China is constructing new transmission lines to strengthen the grid [73,74]. In Italy, the curtailments were usually introduced to relieve transmission congestion and maintain reserve margins during the periods when there was consistent wind and solar production and dispatchable generators have reached their minimum operating state [73]. Italy, as with China, made significant investment on the transmission network and VRE curtailments have since reduced as seen in Figure 4. Similarly, the VRE curtailments in ERCOT were mainly caused by local transmission network congestion [73,75]. ERCOT invested on additional transmission network and also changed the market design from 15-minute to 5-minute dispatch intervals, which significantly reduced the VRE curtailments [73,75].

In short, the case studies above show that system operators implement VRE curtailment for various reasons and that curtailment can happen at any penetration level. Typically, these curtailments are attributed to transmission network congestion and lack of flexible generation in the power system. Common measures for reducing curtailments include; constructing new transmission lines, improving on generation scheduling and forecasting, using VRE power for heating and changing market design.

3.6.Reserves

Variability and uncertainty associated with VRE affect the power reserves and level of flexibility that should be available at different time scales. It was shown earlier that the daily maximum wind and solar power output variations experienced increases with the increase in time interval under consideration – see Figure 2. However, accounting for large variations over longer period of time might be easier than accounting for small variations over shorter period of time depending on the ramping capability of the dispatchable generators on the grid.

A review conducted in [71] looked at how the reserve requirements of different regions (Nordic countries, Ireland, UK, Germany, Minnesota and California) increased in relation to the increase in wind penetration. The results showed that the reserve requirement increased with the increase in analysis time scale, which agrees with the findings in Figure 2. In addition, the reserve requirement increased with the increase in penetration level of wind plants. If only inter-hourly wind variability is considered, the increase in short term reserve requirement obtained from most regions is less than 4% of installed wind capacity, with wind shares of up to 20% of

gross demand. If 4-hour and day-ahead uncertainties are taken as the basis, the reserve requirement increases to between 6% and 18% of installed wind capacity for the same wind share. This experience shows that the variations introduced by wind plants do not significantly increase the regulating and load following reserve requirement when the penetration level is less than 20% of total VRE capacity.

Since maximum PV power variations followed a curve similar to wind in Figure 2, it follows that the reserve requirement at different PV penetration levels will also be similar. In addition, studies in the literature also confirm that uncertainty of solar and wind is not a serious issue for penetration level up to 20%, since any interconnected power system is planned to accommodate load demand uncertainty as well as different contingencies [76-79].

3.7.Transient stability

Transient stability is associated with the ability of the power system to continue operating in a stable condition and maintain its synchronism after being subjected to severe disturbances. The maximum time duration of a disturbance during which the generator does not lose its synchronism is called critical clearing time. This depends on the system inertia constant, generator parameters, reactance to resistance ratio, initial conditions prior to disturbance and fault location.

Recent PV and wind technologies have fault ride through capability, and can provide some level of support to the system restoration process depending on the local characteristics of the affected network [71,80]. A study conducted in New Zealand concluded that high penetration of PV generation is unlikely to cause any negative effect on the transient stability of the grid [81]. The Western Wind and Solar Integration Study Phase 3 concluded that transient stability can be maintained with high share of wind and solar, provided that local issues are addressed adequately [15]. A similar study was conducted in Ireland, showed that the transient stability of the system improves for wind penetration of up to 60% and starts deteriorating thereafter [10].

3.8.Frequency stability

Frequency stability has to do with the ability of the power system to maintain a steady frequency following a significant imbalance between the load demand and supply. Wind and PV generators are interfaced to the network through power converters and thus do not inherently contribute to the inertia of the power system. However, as mentioned earlier, controllers can be incorporated to these generators to provide some synthetic inertia. This is important because

with low inertia, there is a risk that during sudden supply-demand imbalances, the frequency will drop too low before primary reserves intervene, resulting in cascading tripping of generators or power system blackout.

Frequency stability is a system wide phenomenon that depends heavily on the size of the power system, share of VRE and control strategies being applied. The study conducted in the Western Interconnection (USA) found that the loss of system inertia due to increased wind and solar sources is of little significance to the rate of change of frequency (ROCOF) for up to 50% instantaneous penetration [15]. In addition, the results were significantly improved when various frequency control methods were simulated. The study conducted in Spain found that ROCOF limit of 0.1 Hz/s can be maintained for wind instantaneous penetration of 66-79% during peak and minimum load scenarios [82]. Similarly, the study conducted in Australia showed that the ROCOF of 0.5 Hz/s can be maintained at 60% instantaneous penetration of wind and solar sources [83]. Another study based on measured data concluded that a maximum instantaneous penetration of 74% can be maintained in Germany and Austria without violating the ROCOF limit [84]. Ireland has been increasing the non-synchronous RE instantaneous penetration level on a trial basis while observing resultant frequency stability issues. As of November 2017, the maximum instantaneous penetration level allowed in Ireland grid is set to 65% [85].

3.9.Summary

In summary, the intensity of local, regional and system-wide VRE integration impacts are influenced by wind and solar penetration levels. The international experiences discussed above provides some insight on the penetration levels at which different impacts can occur. Figure 4 maps different impacts with minimum instantaneous penetration level at which they are likely to occur based on international experience. In general, issues that affect the local and regional networks can occur at any penetration level depending on the local characteristics of the network and implemented VRE control strategies. On the other hand, issues affecting the balancing operation of the power system are likely to become significant when the instantaneous penetration level of VRE is above 20%. Transient and frequency stability issues typically become significant when the instantaneous penetration level is above 50%.

4. Characteristics of the grid

In the previous sections, the impacts of VRE are attributed to the type of VRE as well as the penetration level. However, every power grid is unique in terms of its size, interconnection

capacity, market structure, size of balancing area and geographical distribution of generation and load demand. These characteristics give rise to network constraints that cannot be ignored when studying the impact of integrating VRE into the grid.

From the findings of the previous section it can be concluded that local and regional issues arising at any penetration level can typically be attributed to constrained transmission network. System-wide issues that can arise at penetration levels higher than 20% can typically be attributed to constrained flexibility. Stability issues predicted to arise at penetration level higher than 50% can typically be attributed to constrained inertia. These constrained aspects are based on grid characteristics that are important when integrating high share of VRE and are further elaborated below.

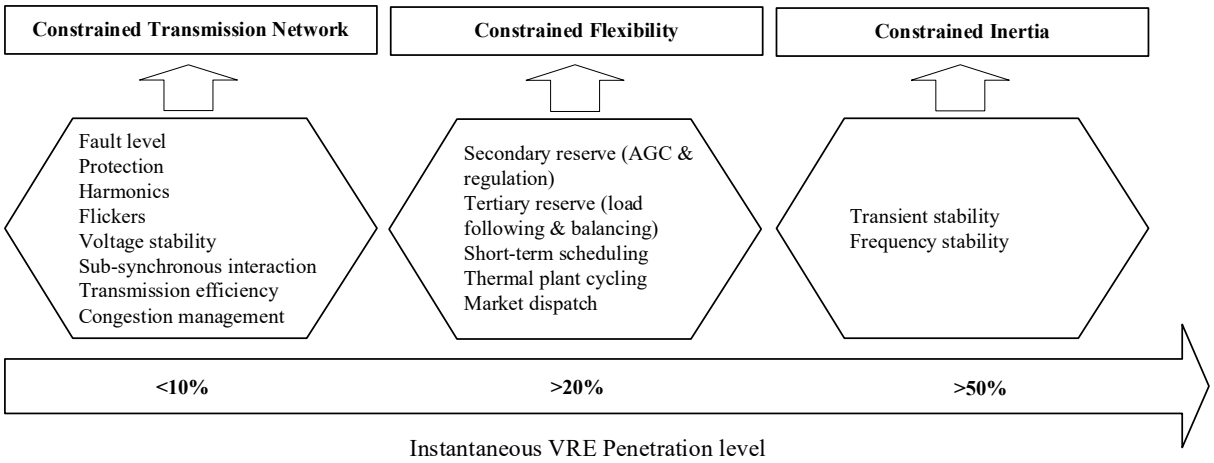

Figure 4: VRE integration impacts and minimum penetration level of occurrence based on the international experience.

4.1.Transmission Network

In order to achieve high share of VRE, transmission network should have sufficient capacity to dispatch required power with limited bottlenecks and be able to access broad range of balancing resources (e.g. sharing with neighbouring power systems) [2]. Transmission network can be described in terms of its strength (weak or strong), which is determined by impedance of the network. Weak grids are characterised by high impedance (or low fault levels), which can be due to sparsely distributed transmission lines or lack of interconnectivity in that part of the network [86]. High system impedance also indicate a lack of synchronous generators in the local area. This is the common scenario for off shore wind plants, which are usually far away from load centres and are usually connected to the grid through a single long transmission line, resulting in very low fault levels at the point of connection. At such point of connection, there is strong dependency between voltage and real or reactive power, meaning that a small change

in real or reactive power results in a large change in voltage, resulting in violation of voltage regulation and other power quality limits. These technical violations can, in turn, influence essential aspects of the wind turbine such as technical performance, safety and lifetime of both mechanical and electrical components [65]. Other issues associated with weak grids include increased transmission losses due to high impedance and lack of transmission capacity.

The common ways to evaluate the strength of the network is to consider the short circuit ratio (SCR) and reactance to resistance ratio (X/R) of the network [86]. The SCR is nothing more than a ratio of the system short circuit AC power to DC power injection at the specified bus. On the other hand, X/R ratio is the ratio of the system reactance to system resistance, looking from any point in a power circuit to the power source. It must be noted that SCR and X/R ratio are not a strength indicators of an entire system, but a measure of the system strength at the specified point. Therefore a system consisting of numerous generators and transmission lines will have a different value of the SCR and X/R ratio at each busbar. If the SCR is less than 10 or X/R ratio is less than 0.5, then the grid is considered weak [87-89].

Issues affecting the local and regional networks, discussed in the previous section, can easily be associated with the strength of the network. In strong networks, large RE plants can be integrated into the network without violating local and regional network operational limits while in weak networks, even small RE plants may result in violation of local and regional network operational limits. The grid codes in weak network regions are characterised by wider range of operating power factor (reactive power capability) and more demanding when it comes to fault ride-through requirements and the restoration time after a fault [89].

4.2.Power System Flexibility

Flexibility has to do with the ability of a power system to respond to change in demand and supply. To achieve high level of flexibility, all elements of a power system (generation, transmission, demand-side and system operation) should be able to provide some level of response to different changes in the network [2]. Generating plants should have the ability to operate at low power output level and ramp up and down quickly. Plants that are known to have this capability are pumped storage, hydro, combined cycle gas turbine (CCGT) and combined heat and power (CHP) plants [2]. Transmission network flexibility has been discussed in the previous section. Demand-side should incorporate technologies such as smart grids, storage and other means of consumers to respond to market signals or direct load control. System operators should implement close to real time decision making, improve forecasting methods and better collaborate with neighbouring grids.

As already explained, wind and solar introduce another source of variability and uncertainty that has to be balanced out by conventional resources. A study conducted by [90] evaluated the generation flexibility of various areas using five parameters, namely; capacity (% of peak load) of pumped storage, hydro, CCGT, CHP and interconnection capacity. The demand-side response was neglected because it is currently difficult to estimate its capacity. The results of the study were presented in flexibility charts, showing potential flexibility sources of various regions as of the end of 2011. Figure 5 shows the flexibility charts (blue polygons) of various regions that were plotted using the latest data (mostly 2016). Note that the orange polygons within the flexibility charts represent the wind and solar capacity (also as % of peak load).

It is clear from the charts that most regions with high share of VRE have some strategy to maintain flexibility in the power system. Regions such as Ireland, Italy and ERCOT rely on CCGT for flexibility while Australia, Portugal and Spain have plenty of hydro resources. Denmark relies on the strong interconnection with the neighbouring power systems. Germany, on the other hand, relies on CCGT, CHP and interconnection with neighbouring power systems. Although this is not easily observable in Germany flexibility chart, the cumulative contribution of these three strategies is 61% (of GW per peak). These findings highlight the importance of considering generation flexibility when planning for a grid with high share of VRE.

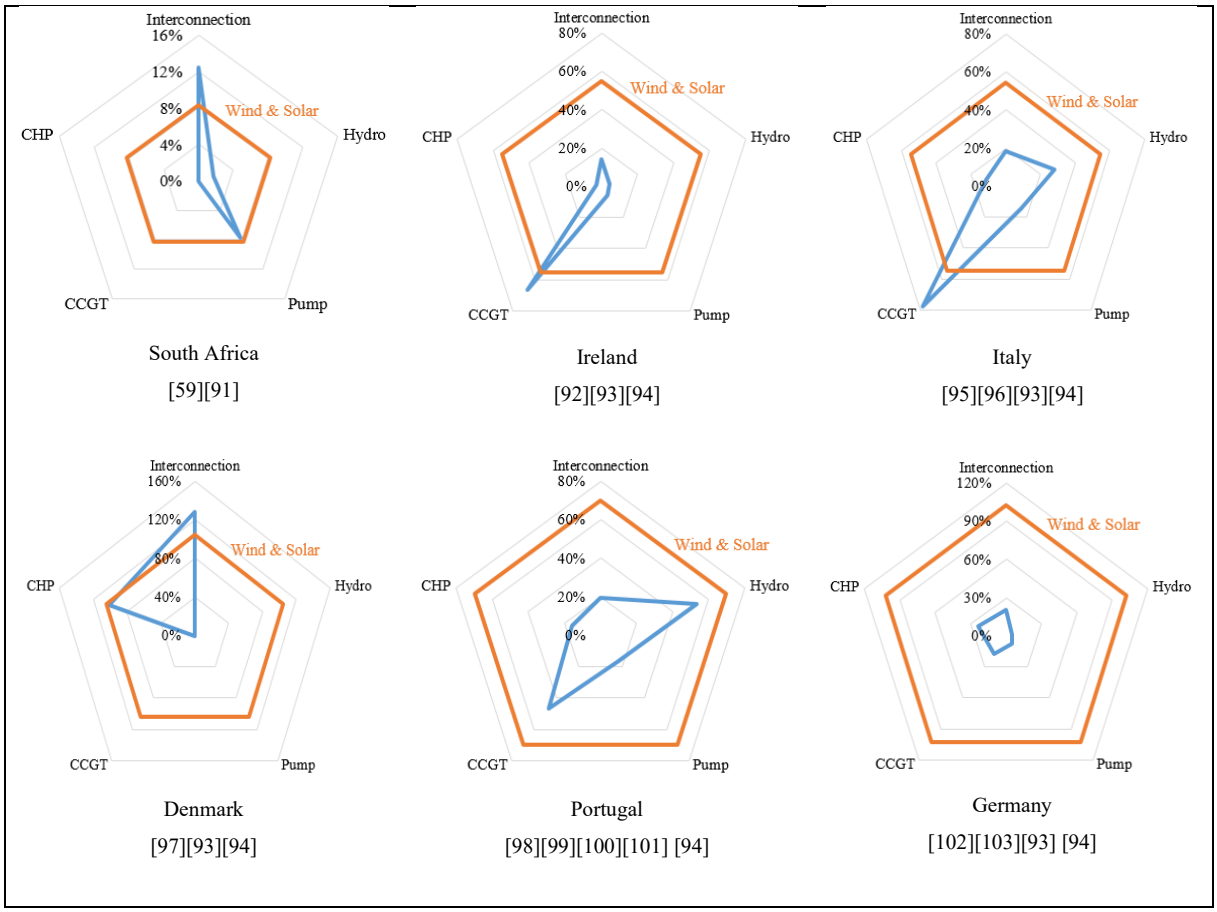

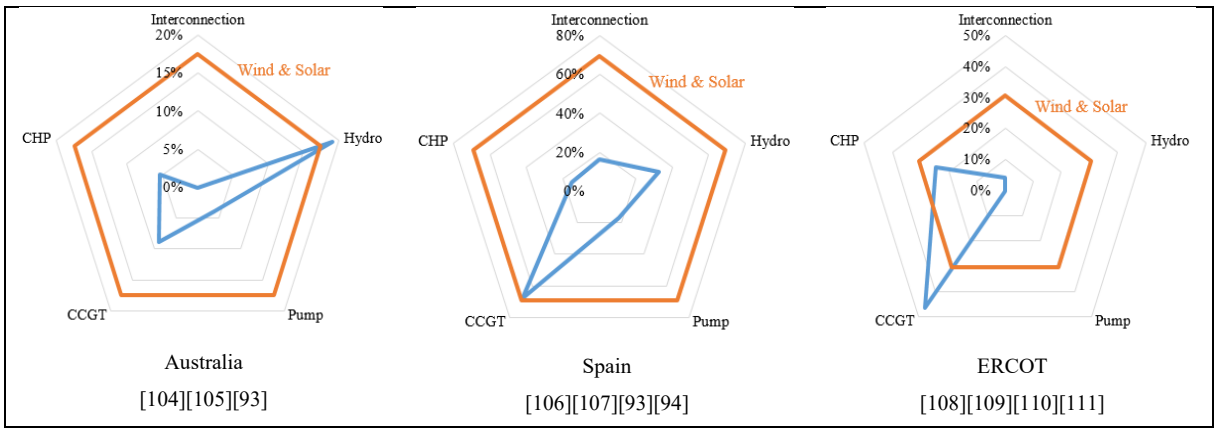

Figure 5: Flexibility charts of various areas with wind and solar penetration ratio (% of GW per peak as of the end of 2016).

4.3.System Inertia

Large synchronous machines consist of large rotating masses (inertia) that resist to change their speed in case of supply and demand imbalances. System inertia reduces the ROCOF and frequency nadir as well as providing the primary reserve with time to make relevant power adjustments. Increasing a share of wind and solar sources will reduce the number of synchronous generators operating in a power system and thus reduce the overall system inertia.

The well-known incident related to system inertia is the South Australian blackout on the 28th of September 2016, where the ROCOF of 6 Hz/s was recorded and this was caused by lack of inertia on the South Australian power system [112]. Before the blackout, wind and solar where generating more that 50% of total demand while there were only three thermal plants online at the time. Apart from the South Australian blackout, incidents attributed to system inertia are rare because most countries do not have enough shares of converter based sources. As a result, the current grid code procedures for various countries do not impose a minimum system inertia required to ensure secure operation of the power systems [82]. However, the studies conducted in various regions show that a minimum system inertia is required to safely operate the grid during potential contingency events [82,112,113]. For example, the current minimum inertia requirements for Ireland and Northern Ireland power system is set to 23 000 MWs while a study conducted in South Australia recommended that two largest synchronous machines should remain online at all times in order to maintain adequate system strength in case the region is islanded as was the case when the blackout occurred [85,113].

5. Conclusions

This paper reviewed a body of literature from the perspective of how type of VRE generator, penetration level and grid characteristics attributed to VRE integration issues experienced

across the world. Based on this review a conceptual framework was then derived that aims to inform decision makers (network planners, regulators, policymakers, utilities and system operators) on the VRE integration issues that can be of concern to the region under consideration. The findings are summarized in Figure 6.

The main findings are listed below:

- Local and regional VRE integration issues can affect the power system at any penetration level depending on the strength of the transmission network and its capacity to dispatch the VRE power whenever required. In order to achieve high shares of VRE, there is a need to continuously investigate local and regional characteristics of the power system and make necessary transmission upgrades. In addition, adequate grid code procedures are also important in mitigating some of these issues.
- Variability and uncertainty of VRE plants start affecting the balancing operation of the power system when the instantaneous penetration level is above 20%. At this level, there is a need for power system flexibility. It was found that countries with high share of VRE have some strategy to maintain flexibility in the power system. Some countries are CCGT-oriented while others are hydro-oriented or interconnection-oriented. It was also found that the need for flexibility can be reduced if VRE plants are spread across a large area and also if there is a balanced combination of wind and solar sources.
- Transient and frequency stability issues are expected to start affecting the power system when the instantaneous penetration level is 50%. This is because there will not be adequate inertia on the power system. Currently, incidents attributed to system inertia are rare because most regions do not have enough shares of power electronic-based sources. However, from the studies conducted in different regions there is a general agreement that a level of system inertia must be maintained to safely operate the grid during potential contingency events. Studies also foresee a major role that can be played by VRE control strategies as well as grid code procedures in maintaining the stability of power system.

The findings highlight the importance of grid planning that is aligned to the VRE targets of the specific region. This is because most solutions required to solve various VRE integration issues have longer lead time as compared to the installation of VRE generators. If proper planning is not done then the grid upgrades necessary for VRE integration will risk lagging the addition of new VRE developments onto the grid. This usually result in VRE power curtailments as seen

in different case studies presented, which may impede any further development of VRE in the region.

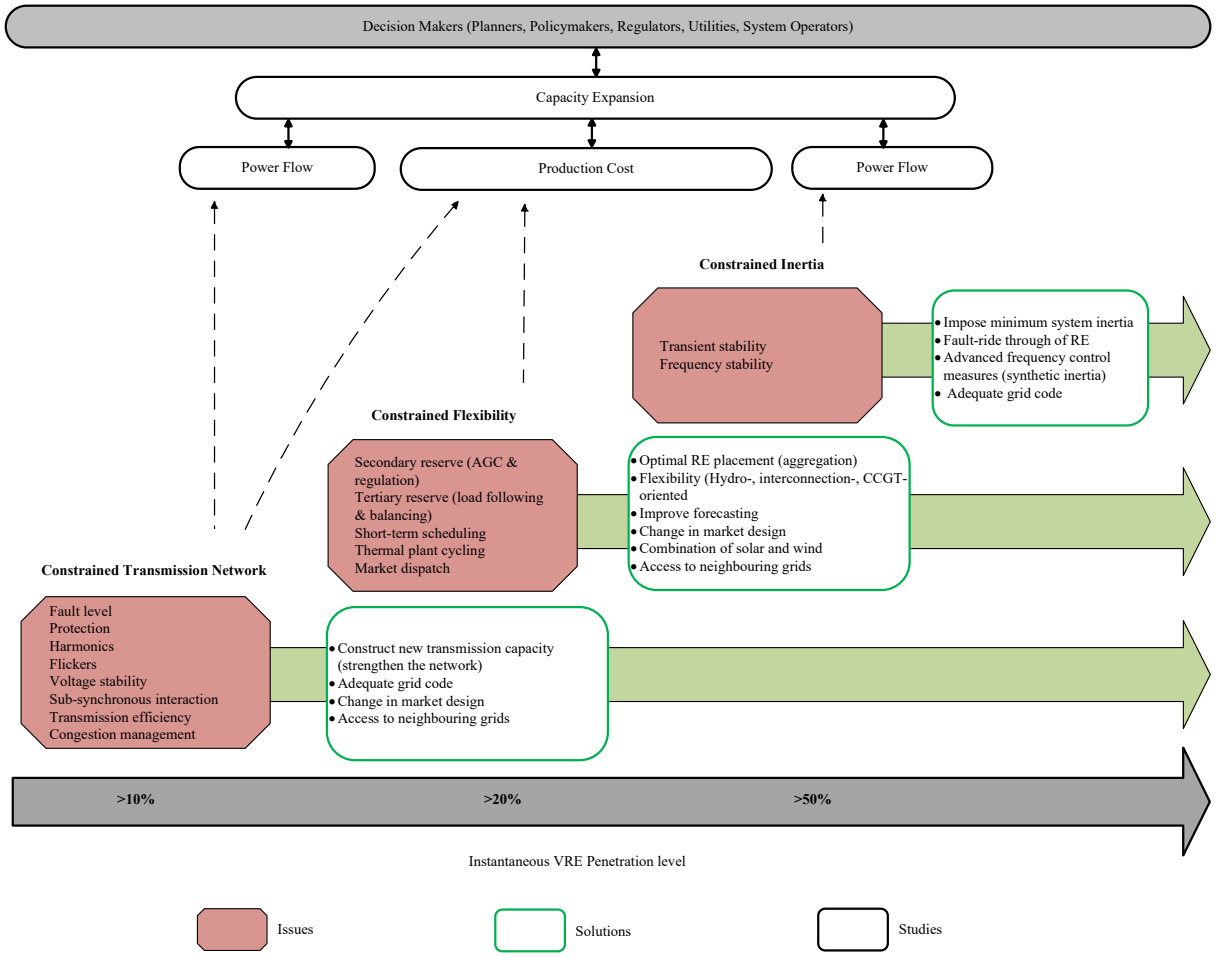

Figure 6: Summary of the literature review findings.

References

[1] Jain P (Innovative Wind Energy, Jacksonville, Florida, USA), Wijayatunga P (Asian Development Bank, Mandaluyong City, Philippines). Grid Integration of Wind Power: Best Practices for Emerging Wind Markets. Mandaluyong City, Philippines: Asian Development Bank; 2016.

[2] Cochran J, Miller M, Zinaman O, Milligan M, Arent D, Palmintier B, et al. Flexibility in 21st Century Power Systems. Golden, Colorado, USA: National Renewable Energy Laboratory; 2014. doi:10.2172/1130630.

[3] Denholm P, Hand M. Grid flexibility and storage required to achieve very high penetration of variable renewable electricity. Energy Policy 2011;39:1817–30. doi:10.1016/j.enpol.2011.01.019.

[4] Cochran J, Milligan M, Katz J. Sources of operational flexibility. Golden, Colorado,

USA: National Renewable Energy Laboratory; 2015.

[5] International Energy Agency. System Integration of Renewables: Implications for Electricity Security. Paris, France: International Energy Agency; 2016.

[6] Koltsaklis NE, Dagoumas AS, Panapakidis IP. Impact of the penetration of renewables on flexibility needs. Energy Policy 2017;109:360–9. doi:10.1016/j.enpol.2017.07.026.

[7] Vithayasrichareon P, Riesz J, MacGill I. Operational flexibility of future generation portfolios with high renewables. Appl Energy 2017;206:32–41. doi:10.1016/j.apenergy.2017.08.164.

[8] Dreidy M, Mokhlis H, Mekhilef S. Inertia response and frequency control techniques for renewable energy sources: A review. Renew Sustain Energy Rev 2017;69:144–55. doi:10.1016/j.rser.2016.11.170.

[9] De Mello P, Van Dam CP (California Wind Energy Collaborative, University of California, Davis, California, USA). Summary of recent wind integration studies: Experience from 2007-2010. Sacramento, California, USA: California Energy Commision; 2012.

[10] Dudurych I, Burke M, Fisher L, Eager M, Kelly K. Operational Security Challenges and Tools for a Synchronous Power System with High Penetration of Non-conventional Sources. CIGRE Sci Eng J 2017;February:91–101.

[11] Troldborg N, Sørensen J. A simple atmospheric boundary layer model applied to large eddy simulations of wind turbine wakes. Wind Energy 2014;17:657–69. doi:10.1002/we.

[12] Katz J, Chernyakhovskiy I. Grid Integration Studies: Advancing Clean Energy Planning and Deployment. Golden, Colorado, USA: National Renewable Energy Laboratory; 2016.

[13] International Renewable Energy Agency. Planning for the Renewable Future: Long-term modelling and tools to expand variable renewable power in emerging economies. Abu Dhabi, United Arab Emirates: International Renewable Energy Agency; 2017.

[14] Lew D, Brinkman G, Ibanez E, et al (National Renewable Energy Laboratory, Golden, Colorado, USA), King J (RePPAE, Wexford, Pennsylvania, USA), Lefton SA, Kumar N, Agan D (Intertek-APTECH, Sunnyvale, California, USA), Jordan G, Venkataraman (GE Energy Management, Schenectady, New York, USA) . The Western Wind and Solar Integration Study Phase 2. Golden, Colorado, USA: National Renewable Energy

Laboratory; 2013. doi:10.2172/1095399.

[15] Miller NW, Shao M, Pajic S, D'Aquila R (GE Energy Management, Schenectady, New York, USA). Western Wind and Solar Integration Study Phase 3 – Frequency Response and Transient Stability. Golden, Colorado, USA: National Renewable Energy Laboratory; 2014. doi:10.2172/1167065.

[16] Winter W, editor. European Wind Integration Study: Towards a successful integration of large scale wind power into European electricity grids. Brussels, Belgium: European Commission; 2010.

[17] Milligan M, Ela E, Hein J, Schneider T, Brinkman G, Denholm P. Vol 4 of Renewable Electricity Futures Study - Bulk Electric Power Systems: Operations and Transmission Planning. Golden, Colorado, USA: National Renewable Energy Laboratory; 2012.

[18] Feldhaus P, Furstenwerth D, Gohl M, Schroter B, Vahlenkamp T, editors. Transformation of Europe's power system until 2050, including specific considerations for Germany. Dusseldorf, Germany: Mckinsey&Company; 2010.

[19] Blair N, Zhou E, Getman D (National Renewable Energy Laboratory, Golden, Colorado, USA), Arent DJ (Joint Institute for Strategic Energy Analysis, Denver, Colorado, USA). Electricity Capacity Expansion Modeling, Analysis, and Visualization: A Summary of Selected High-Renewable Modeling Experiences. Golden, Colorado, USA: National Renewable Energy Laboratory; 2015.

[20] Department of Energy. Integrated Resource Plan 2018. Pretoria, South Africa: Department of Energy; 2018.

[21] Palchak A, Cochran J, Ehlen A, et al (National Renewable Energy Laboratory, Golden, Colorado, USA), Deshmukh R, Abhyankar N (Lawrence Berkeley National Laboratory, Berkeley, California, USA), Soonee SK, Narasimhan SR, Joshi M (Power System Operation Corporation, New Delhi, India), Sreedharan P (United States Agency for International Development, Washington, D.C., USA). Greening the grid: Pathways to integrate 175 gigwatts of renewable energy into India's electric grid, Vol II - Regional Study. Washington, D.C., USA and New Dehli, India: United States Agency for International Development and Ministry of Power; 2017.

[22] Palchak A, Cochran J, Ehlen A, et al (National Renewable Energy Laboratory, Golden, Colorado, USA), Deshmukh R, Abhyankar N (Lawrence Berkeley National Laboratory, Berkeley, California, USA), Soonee SK, Narasimhan SR, Joshi M (Power System

Operation Corporation, New Delhi, India), Sreedharan P (United States Agency for International Development, Washington, D.C., USA). Greening the grid: Pathways to integrate 175 gigwatts of renewable energy into India's electric grid, Vol I - National Study. Washington, D.C., USA and New Dehli, India: United States Agency for International Development and Ministry of Power; 2017.

[23] Pudjianto D, Djapic P, Dragovic J, Strbac G (Imperial College, London, England). Direct Costs Analysis related to Grid Impacts of Photovoltaics. Brussels, Belgium: European Commission; 2013.

[24] Kumar N, Besuner P, Lefton S, Agan D, Hilleman D (Intertek APTECH, Sunnyvale, California). Power Plant Cycling Costs. Golden, Colorado, USA: National Renewable Energy Laboratory; 2012. doi:10.2172/1046269.

[25] Obert M, Poller M (Moeller & Poeller Engineering, Tubingen, Germany). Assessing the impact of increasing shares of variable generation on system operations in South Africa. Pretoria, South Africa: Department of Energy and Eskom; 2017.

[26] Australian Energy Market Operator. Integrating renewable energy - Wind integration studies report. Melbourne, Australia: Australian Energy Market Operator; 2013.

[27] Horne J, Orellana ST, Poller M (Moeller & Poeller Engineering, Tubingen, Germany). Grid and System Integration Study for El Salvador. Bonn, Germany: Gesellschaft für international Zusammenarbeit (GIZ) GmbH; 2013.

[28] Poller M (DigSilent GmbH, Gomaringen, Germany). Grid Integration of Wind Energy in the Western Cape. Frankfurt, Germany and Pretoria, South Africa: Deutsche Gesellschaft für Technische Zusammenarbeit (GTZ) GmbH, Department of Environmental Affairs and Eskom; 2009.

[29] World Bank Group. A Guide to Operational Impact Analysis of Variable Renewables: Application to the Philippines. Washington DC, USA: World Bank Group; 2013.

[30] Holttinen H, Meibom P, Orths A, Lange B, O'Malley M, Tande JO, et al. Impacts of large amounts of wind power on design and operation of power systems, results of IEA collaboration. Wind Energy 2011;14:179–92. doi:10.1002/we.410.

[31] Balaban G, Lazaroiu GC, Dumbrava V, Sima CA. Analysing Renewable Energy Source Impacts on Power System National Network Code. Inventions 2017;2:23. doi:10.3390/inventions2030023.

[32] Vilchez E, Stenzel J. Impact of renewable energy generation technologies on the power quality of the electrical power systems. 22nd Int. Conf. Exhib. Electr. Distrib., vol. 5, Institution of Engineering and Technology; 2013. doi:10.1049/cp.2013.0791.

[33] Graabak I, Korpås M. Variability Characteristics of European Wind and Solar Power Resources—A Review. Energies 2016;9:449. doi:10.3390/en9060449.

[34] Ueckerdt F, Brecha R, Luderer G. Analyzing major challenges of wind and solar variability in power systems. Renew Energy 2015;81:1–10. doi:10.1016/j.renene.2015.03.002.

[35] Jha IS, Sehgal YK, Sen S, Bhambhani K. Grid Integration of Large Scale Renewable Generation-Initiatives in Indian Power System. CIGRE, 2014.

[36] Wan YH. Long-Term Wind Power Variability. Golden, Colorado, USA: National Renewable Energy Laboratory; 2012.

[37] Brower MC, Barton MS, Lledo L, Dubois J. A study of wind speed variability using Global Reanalysis data. Albany, New York: AWS Truepower; 2013.

[38] Darez P, Baudry J, Darr C. Summary for Policymakers. Clim Chang 2013 - Phys Sci Basis 2007;53:1689–99. doi:10.1017/CBO9781107415324.004.

[39] World Bank Group. Utility-Scale Solar Photovoltaic Power Plants. Washington DC, USA: World Bank Group; 2015.

[40] Ryberg DS, Freeman J, Blair N. Quantifying Interannual Variability for Photovoltaic Systems in PVWatts Quantifying Interannual Variability for Photovoltaic Systems in PVWatts. Golden, Colorado, USA: National Renewable Energy Laboratory; 2015.

[41] Kariuki BW, Sato T. Interannual and spatial variability of solar radiation energy potential in Kenya using Meteosat satellite. Renew Energy 2018;116:88–96. doi:10.1016/j.renene.2017.09.069.

[42] Buttler A, Dinkel F, Franz S, Spliethoff H. Variability of wind and solar power – An assessment of the current situation in the European Union based on the year 2014. Energy 2016;106:147–61. doi:10.1016/j.energy.2016.03.041.

[43] Wan Y-H, Bucaneg D. Short-Term Power Fluctuations of Large Wind Power Plants. J Sol Energy Eng 2002;124:427. doi:10.1115/1.1507762.

[44] Australian Energy Market Operator. South Australian Renewable Energy Report.

Melbourne, Australia: Australian Energy Market Operator; 2017.

[45] Phadke AA, Abhyankar N, Rao P (Lawrence Berkeley National Laboratory, Berkeley, California, USA). Empirical Analysis of the Variability of Wind Generation in India: Implications for Grid Integration. Washington, D.C., USA: United States Department of Energy; 2014.

[46] Stein JS, Miyamoto Y, Nakashima E, Lave M. Ota City : characterizing output variability from 553 homes with residential PV systems on a distribution feeder. Albuquerque, NM, and Livermore, California, USA: Sandia National Laboratories; 2011. doi:10.2172/1035324.

[47] Mills A, Ahlstrom M, Brower M, Ellis A, George R, Hoff T, et al. Dark Shadows. IEEE Power Energy Mag 2011;9:33–41. doi:10.1109/MPE.2011.940575.

[48] International Energy Agency. Getting Wind and Sun onto the Grid. Paris, France: International Energy Agency; 2017.

[49] Yi Li, Agelidis VG, Shrivastava Y. Wind-solar resource complementarity and its combined correlation with electricity load demand. 2009 4th IEEE Conf. Ind. Electron. Appl., IEEE; 2009, p. 3623–8. doi:10.1109/ICIEA.2009.5138882.

[50] Widén J. Correlations between large-scale solar and wind power in a future scenario for Sweden. IEEE Trans Sustain Energy 2011;2:177–84. doi:10.1109/TSTE.2010.2101620.

[51] Solbakken K, Babar B, Boström T. Correlation of wind and solar power in high-latitude arctic areas in Northern Norway and Svalbard. Renew Energy Environ Sustain 2016;1:42. doi:10.1051/rees/2016027.

[52] Miglietta MM, Huld T, Monforti-Ferrario F. Local Complementarity of Wind and Solar Energy Resources over Europe: An Assessment Study from a Meteorological Perspective. J Appl Meteorol Climatol 2017;56:217–34. doi:10.1175/JAMC-D-16-0031.1.

[53] Santos-Alamillos FJ, Pozo-Vázquez D, Ruiz-Arias JA, Lara-Fanego V, Tovar-Pescador J. Analysis of spatiotemporal balancing between wind and solar energy resources in the southern Iberian Peninsula. J Appl Meteorol Climatol 2012;51:2005–24. doi:10.1175/JAMC-D-11-0189.1.

[54] Knorr K, Zimmermann B, Bofinger S, Gerlach A (Fraunhofer Institute for Wind Energy Systems, Germany), Bischof-Niemz T, Mushwana C (Council for Scientific and

Industrial Research, Pretoria, South Africa). Wind and Solar PV Resource Aggregation Study for South Africa. Pretoria, South Africa: Council for Scientific and Industrial Research; 2016.

[55] Gonzalez-Longatt F, Chikuni E, Rashayi E. Effects of the Synthetic Inertia from wind power on the total system inertia after a frequency disturbance. 2013 IEEE Int. Conf. Ind. Technol., IEEE; 2013, p. 826–32. doi:10.1109/ICIT.2013.6505779.

[56] Jietan Z, Linan Q, Pestana R, Fengkui L, Libin Y. Dynamic frequency support by photovoltaic generation with "synthetic" inertia and frequency droop control. 2017 IEEE Conf. Energy Internet Energy Syst. Integr., IEEE; 2017, p. 1–6. doi:10.1109/EI2.2017.8245445.

[57] Dharmawardena H, Uhlen K, Gjerde SS. Modelling wind farm with synthetic inertia for power system dynamic studies. 2016 IEEE Int. Energy Conf., IEEE; 2016, p. 1–6. doi:10.1109/ENERGYCON.2016.7514098.

[58] International Energy Agency. Renewables 2017. https://www.iea.org/publications/renewables2017/ (accessed April 20, 2018).

[59] Eskom. Integrated Report. Johannesburg, South Africa: Eskom; 2017.

[60] Neumann T, Erlich I. Short Circuit Current Contribution of a Photovoltaic Power Plant. IFAC Proc., vol. 45, 2012, p. 343–8. doi:10.3182/20120902-4-FR-2032.00061.

[61] Turcotte D, Katiraei F. Fault contribution of grid-connected inverters. 2009 IEEE Electr. Power Energy Conf., IEEE; 2009. doi:10.1109/EPEC.2009.5420365.

[62] Keller J, Kroposki B. Understanding Fault Characteristics of Inverter-Based Distributed Energy Resources. Golden, Colorado, USA: National Renewable Energy Laboratory; 2010. doi:10.2172/971441.

[63] González JA, Dyśko A, Iberdrola GL. The impact of renewable energy sources and distributed generation on substation protection and automation. CIGRE, 2010.

[64] Luo X, Wang J, Wojcik J, Wang J, Li D, Draganescu M, et al. Review of Voltage and Frequency Grid Code Specifications for Electrical Energy Storage Applications. Energies 2018;11:1070. doi:10.3390/en11051070.

[65] Sørensen P, Unnikrishnan AK, Mathew SA. Wind farms connected to weak grids in India. Wind Energy 2001;4:137–49. doi:10.1002/we.52.

[66] Shafiullah GM, Oo AMT, Ali ABMS, Stojcevski A. Influences of Wind Energy Integration into the Distribution Network. J Wind Energy 2013;2013:1–21. doi:10.1155/2013/903057.

[67] Adams J, Carter C, Huang S-H. ERCOT experience with Sub-synchronous Control Interaction and proposed remediation. PES T&D 2012, IEEE; 2012, p. 1–5. doi:10.1109/TDC.2012.6281678.

[68] Wang L, Xie X, Jiang Q, Liu H, Li Y, Liu H. Investigation of SSR in Practical DFIG-Based Wind Farms Connected to a Series-Compensated Power System. IEEE Trans Power Syst 2015;30:2772–9. doi:10.1109/TPWRS.2014.2365197.

[69] Virulkar VB, Gotmare GV. Sub-synchronous resonance in series compensated wind farm: A review. Renew Sustain Energy Rev 2016;55:1010–29. doi:10.1016/J.RSER.2015.11.012.

[70] Ghasemi H, Gharehpetian GB, Nabavi-Niaki SA, Aghaei J. Overview of subsynchronous resonance analysis and control in wind turbines. Renew Sustain Energy Rev 2013;27:234–43. doi:10.1016/j.rser.2013.06.025.

[71] International Energy Agency. Design and operation of power systems with large amounts of wind power. Paris, France: International Energy Agency; 2012.

[72] Yasuda Y, Bird L, Maria Carlini E, Estanqueiro A, Flynn D, Forcione A, et al. International Comparison of Wind and Solar Curtailment Ratio. 14th Wind Intergration Work., 2015.

[73] Bird L, Lew D, Milligan M, Carlini EM, Estanqueiro A, Flynn D, et al. Wind and solar energy curtailment: A review of international experience. Renew Sustain Energy Rev 2016;65:577–86. doi:10.1016/j.rser.2016.06.082.

[74] Fan X, Wang W, Shi R, Li F. Analysis and countermeasures of wind power curtailment in China. Renew Sustain Energy Rev 2015;52:1429–36. doi:10.1016/j.rser.2015.08.025.

[75] Bird L, Cochran J, Wang X. Wind and Solar Energy Curtailment: Experience and Practices in the United States. Golden, Colorado, USA: National Renewable Energy Laboratory; 2014. doi:10.2172/1126842.

[76] Weisser D, Garcia RS. Instantaneous wind energy penetration in isolated electricity grids: concepts and review. Renew Energy 2005;30:1299–308. doi:10.1016/j.renene.2004.10.002.

[77] Quanta Technology. Grid Impacts and Solutions of Renewables at High Penetration Levels. Westchase, United States: Quanta Technology; 2009.

[78] Lew D (National Renewable Energy Laboratory, Golden, Colorado, USA), Piwko D, Miller N, Jordan G, Clark K, Freeman L (GE Energy Management, Schenectady, New York, USA). How Do High Levels of Wind and Solar Impact the Grid? The Western Wind and Solar Integration Study. Golden, Colorado, USA: National Renewable Energy Laboratory; 2010. doi:10.2172/1001442.

[79] Huber M, Dimkova D, Hamacher T. Integration of wind and solar power in Europe: Assessment of flexibility requirements. Energy 2014;69:236–46. doi:10.1016/j.energy.2014.02.109.

[80] Ayodele TR, Jimoh AA, Munda JL, Agee JT. The impact of wind power on power system transient stability based on probabilistic weighting method. J Renew Sustain Energy 2012;4. doi:10.1063/1.4771998.

[81] Transpower. Effect of Solar PV on Transient Stability of the New Zealand Power System. Wellington, New Zealand: Transpower; 2017.

[82] Fernandez-Bernal F, Egido I, Lobato E. Maximum wind power generation in a power system imposed by system inertia and primary reserve requirements. Wind Energy 2015;18:1501–14. doi:10.1002/we.1773.

[83] Ahmadyar AS, Riaz S, Verbic G, Chapman A, Hill DJ. A Framework for Assessing Renewable Integration Limits with Respect to Frequency Performance. IEEE Trans Power Syst 2017;8950:1–10. doi:10.1109/TPWRS.2017.2773091.

[84] Xypolytou E, Gawlik W, Zseby T, Fabini J. Impact of Asynchronous Renewable Generation Infeed on Grid Frequency: Analysis Based on Synchrophasor Measurements. Sustainability 2018;10:1605. doi:10.3390/su10051605.

[85] Eirgrid and SONI. Operational Constraints Update. Dublin, Ireland and Belfast, Northern Ireland: Eirgrid and SONI; 2017.

[86] Guide for Planning DC Links Terminating at AC Locations Having Low Short-Circuit Capacities. IEEE Std 1204-1997; 1997.

[87] Grunau S, Fuchs FW. Effect of Wind-Energy Power Injection into Weak Grids. EWEA 2012 Conf. Proc., 2012.

[88] Strachan NPW, Jovcic D. Stability of a variable-speed permanent magnet wind generator with weak AC grids. IEEE Trans Power Deliv 2010;25:2779–88. doi:10.1109/TPWRD.2010.2053723.

[89] Etxegarai A, Eguia P, Torres E, Iturregi A, Valverde V. Review of grid connection requirements for generation assets in weak power grids. Renew Sustain Energy Rev 2015;41:1501–4. doi:10.1016/j.rser.2014.09.030.

[90] Yasuda Y, Rygg Årdal A, Huertas Hernando D, Maria Carlini E, Estanqueiro LNEG A, Damian Flynn P, et al. Evaluation on diversity of flexibility in various areas. 12th Wind Integr. Work., 2013.

[91] Southern African Power Pool. Interconnection Transfer Limits n.d. http://www.sapp.co.zw/transfer-limits (accessed August 22, 2018).

[92] EirGrid Group. All-Island Generation Capacity Statement. Dublin, Ireland: EirGrid Group; 2017.

[93] International Energy Agency. Global CHP/DHC Data - Current Baseline n.d. http://www.iea.org/chp/data/globalchpdhcdata-currentbaseline/ (accessed August 22, 2018).

[94] European Commission. Communication on strengthening Europe's energy networks. Brussels, Belgium: European Commission; 2017.

[95] International Energy Agency. Energy Policies of IEA Countries - Italy 2016 Review. Paris, France: International Energy Agency; 2016.

[96] Kougias I, Szabó S. Pumped hydroelectric storage utilization assessment: Forerunner of renewable energy integration or Trojan horse? Energy 2017;140:318–29. doi:10.1016/j.energy.2017.08.106.

[97] International Energy Agency. Energy Policies of IEA Countries - Denmark 2017 Review. Paris, France: International Energy Agency; 2017.

[98] International Energy Agency. Energy Policies of IEA Countries - Portugal 2016 Review. Paris, France: International Energy Agency; 2016.

[99] Wind Europe. Wind in power 2016: Eurpoean Statistics. Brussels, Belgium: Wind Europe; 2017.

[100] International Energy Agency. National Survey Report of PV Power Applications in

Portugal. Paris, France: International Energy Agency; 2016. doi:10.13140/RG.2.1.2305.4968.

[101] European Commission. Final Cogeneration Roadmap non pilot Member State: Portugal. Brussels, Belgium: European Commission; 2014.

[102] Energy Charts. Net installed electricity generation capacity in Germany 2016. https://www.energy-charts.de/power_inst.htm?year=2016&period=annual&type=power_inst (accessed August 22, 2018).

[103] Schill W-P, Pahle M, Gambardella C. Start-up costs of thermal power plants in markets with increasing shares of variable renewable generation. Nat Energy 2017;2:17050. doi:10.1038/nenergy.2017.50.

[104] Australian Energy Market Operator. Generation information page 2018. https://www.aemo.com.au/Electricity/National-Electricity-Market-NEM/Planning-and-forecasting/Generation-information (accessed August 22, 2018).

[105] Australian Energy Regulator. Generation capacity and peak demand 2016. https://www.aer.gov.au/wholesale-markets/wholesale-statistics/generation-capacity-and-peak-demand (accessed August 22, 2018).

[106] International Energy Agency. Energy Policies of IEA Countries - Spain 2015 Review. Paris, France: International Energy Agency; 2015.

[107] Barbour E, Wilson IAG, Radcliffe J, Ding Y, Li Y. A review of pumped hydro energy storage development in significant international electricity markets. Renew Sustain Energy Rev 2016;61:421–32. doi:10.1016/j.rser.2016.04.019.

[108] Potomac Economics. 2017 State of the Markert Report for the ERCOT Electricity Markets. Austin, Texas, USA: Electric Reliability Council of Texas; 2018.

[109] Magness B. ERCOT in 2018: Challenges and Opportunities. Austin, Texas, USA: Electric Reliability Council of Texas; 2018.

[110] Lasher W. Transmission Planning in the ERCOT Interconnection. Austin, Texas, USA: Electric Reliability Council of Texas; 2011.

[111] United States Department of Energy. The state of CHP: Texas. Washington, D.C., USA: United States Department of Energy; 2016.

[112] Gu H, Yan R, Saha TK. Minimum Synchronous Inertia Requirement of Renewable Power Systems. IEEE Trans Power Syst 2018;33:1533–43. doi:10.1109/TPWRS.2017.2720621.

[113] Australian Energy Market Operator. South Australia system strength assessment. Melbourne, Australia: Australian Energy Market Operator; 2017.

Paper 2

N. Mararakanye and B. Bekker, "Incorporating spatial and temporal correlations to improve aggregation of decentralized day-ahead wind power forecasts," *Revised and resubmitted to IEEE Access.*

Quartile of the journal as calculated by Scimago (www.scimagojr.com): 1

To comply with the copyright requirements, the final pre-print version of the article is presented here, formatted in dissertation style.

Incorporating spatial and temporal correlations to improve aggregation of decentralized day-ahead wind power forecasts

Ndamulelo Mararakanye [a], Amaris Dalton [a] and Bernard Bekker [a]

[a] *Department of Electrical and Electronic Engineering, Stellenbosch University, Private Bag X1, Matieland, 7602, South Africa*

Abstract

In some electricity markets, individual wind farms are obliged to provide point forecasts to the power purchaser or system operator. These decentralized forecasts are usually based on on-site meteorological forecasts and measurements, and thus optimized for local conditions. Simply adding decentralized forecasts may not capture some of the spatial and temporal correlations, thereby lowering the potential accuracy of the aggregated forecast. This paper proposes the explanatory variables that are used to train the kernel density estimator and conditional kernel density estimator models to derive day-ahead aggregated point and probabilistic wind power forecasts from decentralized point forecasts of geographically distributed wind farms. The proposed explanatory variables include (a) decentralized point forecasts clustered using the clustering large applications algorithm to reduce the high-dimensional matrices, (b) hour of day and month of year to account for diurnal and seasonal cycles, respectively, and (c) atmospheric states derived from self-organizing maps to represent large-scale synoptic circulation climatology for a study area. The proposed methodology is tested using the day-ahead point forecast data obtained from 29 wind farms in South Africa. The results from the proposed methodology show a significant improvement as compared to simply adding the decentralized point forecasts. The derived predictive densities are shown to be non-Gaussian and time-varying, as expected given the time-varying nature of wind uncertainty. The proposed methodology provides system operators with a method of not only producing more accurate aggregated forecasts from decentralized forecasts, but also improving operational decisions such as dynamic operating reserve allocation and stochastic unit commitment.

Keywords: Aggregated wind power forecasting; diurnality; large-scale atmospheric circulations; probabilistic; seasonality

1. Introduction

The electricity generation from wind energy is increasing worldwide, as different regions continue with the transition towards a decarbonized future. Wind power forecasting remains

one of the most effective methods of reducing the impacts of wind power intermittency on power system operations. Traditionally, wind power forecasts consist of one value (also called point or deterministic forecasts) for each wind farm [1]–[3]. These are usually based on on-site meteorological forecasts and measurements, and thus optimized for local conditions [4]. However, as wind capacity continues to increase in a region, producing accurate aggregated wind power forecasts becomes a concern for system operators. One of the key considerations in aggregated wind power forecasting is spatial-temporal correlations between wind farms that are geographically distributed. The power from geographically distributed wind farms exhibit spatial-temporal correlations, the degree of which can vary based on numerous factors such as separation distance and direction, timescale, diurnal weather variations and movement of synoptic weather systems [1], [2], [5]. Recent literature has shown the potential benefit of incorporating spatial-temporal correlations in wind forecasting, especially in terms of improving forecasting accuracy [1]–[3], [6]–[8]. Another factor to consider is that uncertainty in wind power forecasting are unavoidable due to time-varying meteorological conditions, weather-to-power conversion process, and dynamic behavior of wind turbines [7]. Based on this realization, utilities are moving away from only focusing on increasing the accuracy of wind power forecasts towards also quantifying the uncertainty inherent in the forecast and incorporating this into their decisions [1], [2], [7], [9], [10], i.e. attaching a risk metric to the forecast. This is also referred to as probabilistic forecasting.

Probabilistic wind power forecasting approaches that incorporate spatial-temporal correlations can be divided into two main categories: physical and statistical [1], [7], [11]–[13]. Physical approaches typically use numerical weather prediction (NWP) models and current weather conditions to predict wind speed [7], [8], [14]. NWP models formulate the problem of wind speed prediction as a set of mathematical equations describing the atmosphere and oceans. In [7], a recursively backtracking framework based on the particle filter was used to estimate the atmospheric state (with near-surface measurements) and forecast samples of aggregated wind power. The samples were used to derive predictive densities using a kernel density estimator (KDE). In [3], weighted Euclidean distance was proposed to search for similar wind characteristics in historical NWP data, and used corresponding aggregated wind power measurements to construct probabilistic forecasts based on distance-weighted KDE. Weather ensemble predictions based on atmospheric models and time series were used together with Gaussian KDE [15], normalized prediction risk index [16], and generalized autoregressive conditional heteroscedasticity [17] to derive wind power forecasts and associated uncertainty. In [18], Gaussian processes combined with NWP were used to derive day-ahead wind power

forecasts. In [19], the poor man's ensemble was used to estimate forecast errors for one wind farm while in [20] used input from 16 different European met services for Previento to derive probabilistic forecasts for Germany. More studies based on physical models can be found in literature reviews conducted in [11], [12], [21]–[23]. Statistical approaches, on the other hand, take historical wind power data and/or NWP as inputs and use machine learning algorithms to generate aggregated wind forecasts [7], [8], [14]. These approaches assume that historical data can be used to infer spatial-temporal correlations among wind farms. In [8], machine learning algorithms were used to generate point forecasts of wind farms, the copula method to build spatial-temporal correlated aggregated wind power forecasts, and Bayesian theory to derive predictive densities. In [2], Bayesian hierarchical models were used for obtaining spatial-temporal correlated probabilistic wind power forecasts. In [1], the alternating direction method of multipliers was proposed to capture spatial-temporal correlations of geographically distributed wind farms and used multiple quantile regression to derive predictive densities. In [24][25], the resampling approach is used to estimate the confidence intervals for wind power forecasts. In [26], local quantile regression is compared with the local Gaussian model and the Nadaraya-Watson Estimator. In [27], historical forecast error distributions were used to obtain scenarios for stochastic wind power generation. In [10], time adaptive conditional KDE was proposed for probabilistic wind power forecasting. In [28]–[30], the beta distribution was used to estimate forecast errors at different wind power forecast bins while in [31] the gamma-like distributions were used to achieve the same. In [32], the logit transformation approach was used to estimate the confidence intervals of forecast errors. More studies based on statistical models can be found in literature reviews conducted in [11], [12], [21]–[23].

The first observation made from the literature is that the majority of proposed forecasting methodologies assume that the problem of aggregated wind power forecasting is solved in a centralized manner, i.e. forecasts of all wind farms in a region are derived centrally by one forecasting company (facilitated by the system operator). A centralized forecaster will often use a consistent forecasting approach for all wind farms, leading to more consistent results [33]. In addition, a forecaster will have access to measurements from all wind farms, making it easier to incorporate spatial-temporal correlations between wind farms into their forecasting methodologies [1]. However, in some markets (e.g. South Africa), individual wind farms are obliged to provide point forecasts to the power purchaser or system operator [34]. These decentralized point forecasts are optimized for local conditions and therefore simply adding these decentralized point forecasts may not capture some of the well-known spatial and temporal correlations, thereby lowering the potential accuracy of the aggregated wind power

forecast. It is well known that the correlation of wind power from geographically distributed wind farms depends on the proximity of wind farms [2]. Wind farms in close proximity are highly correlated, whereas wind farms that are further apart are not. In addition, wind power profiles exhibit a high degree of statistical regularity along diurnal and seasonal timescales in the literature [35]–[41]. These spatial and temporal correlations form the basis of understanding wind power variability and ultimately improving wind power forecasting. Therefore, there is a need for a model that aggregates decentralized point forecasts while considering these correlations.

The second observation made from the literature is that most forecasting methodologies are based on the microscale and/or mesoscale NWP models. However, it was illustrated in [42]–[44] that the probabilistic properties of wind power generators' output, along with the level of correlation between wind generators' output, are dependent on the dominant large-scale atmospheric circulation archetypes. Thus, the information contained in large-scale atmospheric circulations can be useful in improving wind power forecasting. Large-scale atmospheric circulations have been incorporated in medium- to long-term wind forecasting [15], [45], [46], but have only been alluded to in short-term wind forecasting [7], [15], [47]. There is a need for more applied research on the potential benefits of incorporating large-scale atmospheric circulations in short-term wind power forecasting.

In light of the two aforementioned needs, the primary hypothesis of this paper is that: decentralized wind power point forecasts are optimized for local conditions, and this reduces the accuracy of aggregated forecasts when these forecasts are simply added together. The accuracy of aggregated forecasts can be improved by training machine learning models with features that account for some of the common spatial and temporal correlations of wind power, including those correlations caused by large-scale atmospheric circulations.

To test this hypothesis, a methodology is proposed that trains machine learning models using the explanatory variables listed below to derive aggregated point and probabilistic wind power forecasts:

(a) Decentralized point forecasts – To eliminate duplicate features and reduce the high dimension matrices required to model a high number of wind farms in a region (without losing important spatial information), the correlated point forecasts are first clustered into k clusters using the clustering large applications algorithm (CLARA).
(b) The hour of day and month of year – These are included to model the well-known statistical regularity of wind profiles along diurnal and seasonal timescales.

(c) Atmospheric states – These are derived from self-organizing maps (SOMs) to represent large-scale synoptic circulation climatology for a study area.

The machine learning models proposed to test the hypothesis are: (a) the *k*-nearest neighbor (*k*-NN) to derive the aggregated wind power point forecast and (b) conditional KDE to derive aggregated wind power predictive densities. It should be noted here that there are numerous machine learning models that have been applied for wind power forecasting as shown in the literature review conducted above. However, the *k*-NN- and KDE-based approaches are proposed to test this hypothesis because they are common and easy to implement. In addition, the conditional KDE is a nonparametric approach for predicting wind power densities and thus can account for time-varying and non-Gaussian nature of wind power uncertainty (caused by time-varying meteorological conditions, weather-to-power conversion process, and dynamic behavior of wind turbines [7]). The proposed methodology is demonstrated using the day-ahead point forecast data obtained from 29 wind farms in South Africa.

An overview of this paper is shown in Figure 1, with the paper organized as follows: Section 2 provides a theoretical framework of the methodology for aggregated wind power forecasting. Section 3 defines the forecasting evaluation framework used in this paper. Section 4 introduces the case study used for illustrating the proposed methodology and presents the results and discussions. Section 5 gives conclusions and identifies further research that may arise from this work.

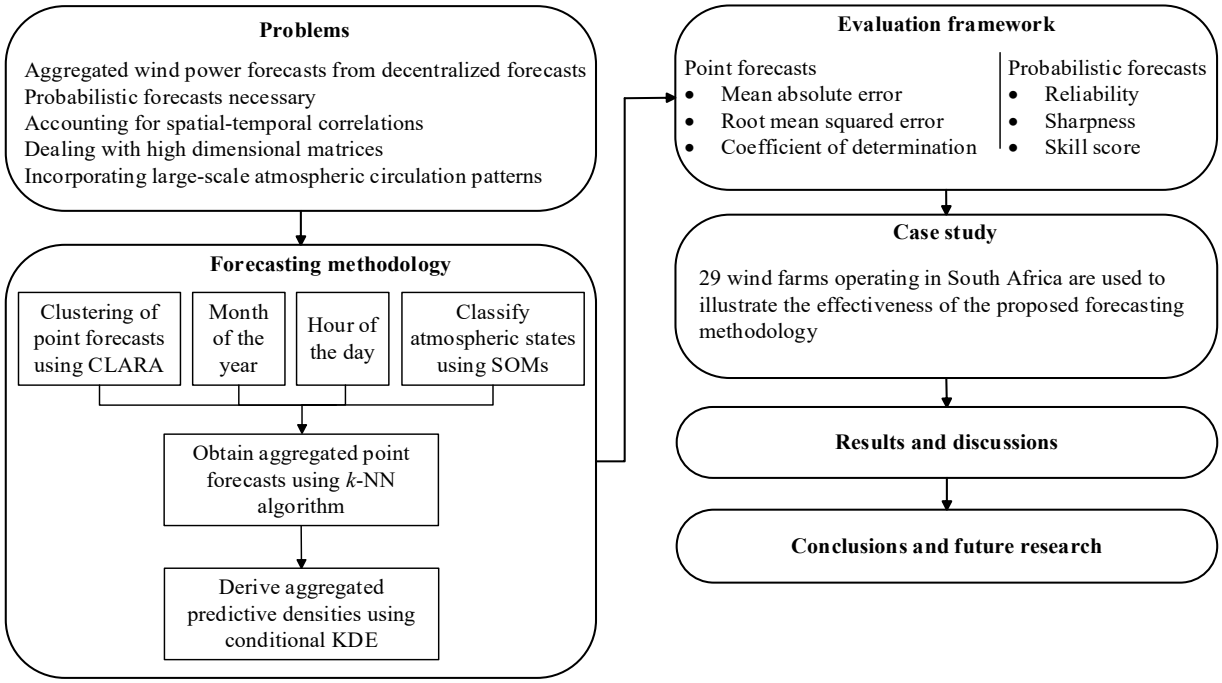

Figure 1: Outline of this paper.

The most significant contribution made by this paper is in proposing a simple approach to improve the accuracy of aggregated point and probabilistic wind power forecasts that can be derived from decentralized point forecasts. This is particularly important in regions where individual wind farms generate their own forecasts and do not necessarily have access to the measurements from other wind farms. The proposed approach provides system operators with a way of aggregating these forecasts while taking into account spatial and temporal correlations. In addition, the derived predictive densities can be used to improve operational decisions such as dynamic operating reserve allocation and stochastic unit commitment.

An additional contribution of the paper is contained in the proposed approach towards atmospheric states, derived from SOMs, which demonstrates another way in which large-scale atmospheric circulation patterns can be incorporated into short-term wind power forecasting.

2. Forecasting methodology

2.1.Feature selection

(a) Clusters of wind power point forecasts

There can be hundreds of wind farms within a region and thus the dataset containing individual wind power point forecasts can be high dimensional. In most machine learning algorithms, as the number of features grows, the amount of data required to generalize accurately grows exponentially (also known as the 'curse of dimensionality'). In addition, wind farms that are in close proximity are highly correlated as (mentioned in Section 1) and therefore, the machine learning model might not learn anything insightful by considering these wind farms independently. To mitigate against this phenomena, this paper clusters wind farms with correlated point forecasts together. Some of the most common clustering algorithms that can be used to achieve this include; partitioning, include hierarchical, k-means, partitioning around medoids (PAM) and the clustering large applications algorithm (CLARA). Recent studies have shown that CLARA algorithm produces better clustering results for large datasets [48], [49], and hence it is used in this paper. The CLARA algorithm can be summarised in the following steps:

- Creating random subsets with fixed size from original dataset;
- Choosing the number of clusters k and corresponding k medoids for each subset;
- Calculating the dissimilarity matrix and assigning each observation of the dataset to the closest medoid;
- Calculating the mean of the dissimilarities of the observations to their closest medoid; and
- Repeating the process while retaining the sub-dataset for which the mean is minimal.

The silhouette coefficient is used in this paper to find the optimal number of clusters k, while the distance metric used is the Euclidean distance (as also recommended for wind resource clustering in [48]).

(b) Atmospheric states

A useful way to classify atmospheric circulation is by using SOMs, which are a class of self-learning artificial neural networks [50]. The classification output from the SOM procedure is a two-dimensional array of nodes, spaced on a lattice topology, which may be interpreted as maps showing typical patterns within a dataset. SOMs have often been used in meteorology and climatology [51], and may indeed be preferential to other commonly employed classification procedures, notably principal components analysis, as it does not discretise data and does not force orthogonality [52].

The SOM training process is based on a competitive learning algorithm which successively measures the Euclidean distance between a predefined set of SOM-nodes (or reference vectors) and the input feature vectors. For each iteration of the training process, the best matching unit's (BMU) weight, along with the weights of nodes located in the BMUs proximity on the SOM lattice, is updated towards that of the feature vector. Reference nodes on the SOM lattice thereby develop towards a generalized configuration of the training dataset. Once the training process has been completed, each feature vector in the classification time-series may be clustered based on the weighted Euclidean to each node on the SOM map. In other words, each time-step in the input-data is retroactively clustered by being assigned the node number (or atmospheric state in this instance), to which it is most similar.

(c) Hour of day and month of year

The cyclical nature of the processes responsible for diurnal and seasonal variability – i.e., the rotation of the earth around its axis and around the sun – however does imbue these processes with a measure of statistical regularity. This statistical regularity increases the wind power predictability associated with such cyclical diurnal and seasonal processes. The value of modelling these variations in wind power forecasting has been shown in the recent literature [53]. This paper captures these variations by including the attributes 'hour of day' (for diurnal variations) and 'month of year' (for seasonal variations), which takes the values 0,1,…23 and 0,1,…11, respectively.

2.2. *k*-NN algorithm

The *k*-NN algorithm is a non-parametric method that averages the k closest training examples in feature space to predict the new data point (also known as the query point). This method resembles the similar-day approach that is still used by many system operators for short term load demand forecasting [53]. The similar-day approach predicts the load demand using historical days with similar weather conditions and day types to the day of forecast. In the same way, the k-NN algorithm is used in this paper to predict the aggregated wind power using historical examples with similar month of year, hour of day, point forecasts (of wind farm clusters) and atmospheric states. The k-NN algorithm can be summarised in three steps:

- Calculating the distance between the query point and each training point;
- Selecting the k nearest neighbors from the training set with k smallest distances; and
- Predicting the aggregated wind power output based on a weighted average of *k* nearest neighbors.

If $X_1, X_2, \dots, X_K$ are the k nearest neighbors and $P_1, P_2, \dots, P_K$ are their corresponding aggregated wind power observations, then the aggregated wind power prediction $\hat{p}\,(x)$ can be derived using the estimator given by:

$$\hat{p}(x) = \frac{\sum_{k=1}^{K} K(x, X_k).P_k}{\sum_{k=1}^{K} K(x, X_k)} \tag{1}$$

Where $K(x, X_k)$ is a kernel function that assigns weights on aggregated wind power observations P_k based on the distance from the neighbor X_k to the query point x. The distance metric used in this paper is the Manhattan distance. The aggregated wind power observations of the neighbor with the smallest distance from the query point has more influence on the final point prediction $\hat{p}(x)$, as compared to the other observations. For a Gaussian kernel function (which is used in this paper) with a smoothing bandwidth h, the function $K(x, X_k)$ can be written as:

$$K(x, X_k) = e^{-\frac{(x-X_k)^2}{2h^2}} \tag{2}$$

2.3. Conditional kernel density estimator

Once the aggregated wind power point forecasts have been determined using (5), the KDE-based approach is used to derive the conditional aggregated wind power predictive density. This involves estimating the conditional probability density function of aggregated wind power P, given that the explanatory variable X is equal to x. The main advantage of KDE is that it is a non-

parametric and data driven approach that can estimate the density of a random variable without distribution hypothesis. As a result, KDE-based approaches are becoming popular in recent developments of probabilistic wind power forecasting [3], [10], [53]–[56]. The main drawback of KDE-based approaches is the difficulty in selecting good bandwidths, especially in the presence of large datasets and high dimensionality. For this reason, this paper considers different combinations of explanatory variables (explained in 2.1) to avoid using all variables at once (and thus reducing the dimensionality of the dataset).

The standard conditional KDE (also known as the Nadaraya-Watson Conditional Estimator) can be written as:

$$\hat{f}(p|X=x) = \frac{1}{h_p}\sum_{i=1}^{N} K\left(\frac{p-P_i}{h_p}\right).w_i(x) \tag{3}$$

Having

$$w_i(x) = \frac{K\left(\frac{x-X_i}{h_x}\right)}{\sum_{i=1}^{N} K\left(\frac{x-X_i}{h_x}\right)} \tag{4}$$

Where h_p and h_x are bandwidths controlling the smoothness of each conditional density in p and x directions, respectively, X_i is a point in a training set and P_i is the corresponding aggregated wind power observation, and K is a kernel function.

The choice of a kernel function K and bandwidths h_p and h_x has a significant influence on estimated conditional densities. For most applications, Gaussian kernel function is the popular choice. However, it is well known that wind power output follows a non-Gaussian distribution [10], [53]. In general, the mean squared error of the Epanechnikov kernel function is optimal [55][57], and hence it is used in this paper. The Epanechnikov kernel function can be written as:

$$K(\partial) = \begin{cases} \frac{3}{4}(1-\partial^2), & \partial \in [-1,1] \\ 0, & otherwise \end{cases} \tag{5}$$

Where $\partial = \frac{p-P_i}{h_p}$ and $\partial = \frac{x-X_i}{h_x}$ in p and x directions, respectively.

To select the bandwidths h_p and h_x, this paper uses the least-squares cross-validation (LSCV) method. The method is based on selecting h_p and h_x that minimises the integrated squared error (ISE) given by:

$$ISE(h_p, h_x) = \int \left(\hat{f}(p|x) - f(p|x)\right)^2 dp \tag{6}$$

$$= \int (\hat{f}(p|x))^2 dp - 2\int \hat{f}(p|x) f(p|x) dp + \int (f(p|x))^2 dp$$

Therefore, minimising ISE is equivalent to minimising the first two terms, $\int (\hat{f}(p|x))^2 dp - 2\int \hat{f}(p|x) f(p|x) dp$, since the last term does not involve h_p and h_x. Thus, a cross-validated estimate of ISE is given by:

$$LSCV(h_p, h_x) = \frac{1}{n}\sum_{i=1}^{n} \int (\hat{f}_{-i}(p|X_i))^2 dp - \frac{2}{n}\sum_{i=1}^{n} \hat{f}_{-i}(P_i|X_i) \tag{7}$$

Where, $\hat{f}_{-i}$ is $\hat{f}$ evaluated with (X_i, P_i) left out.

2.4.Summary of the proposed methodology

In summary, a methodology is proposed that trains k-NN and conditional KDE models to derive aggregated point and probabilistic wind power forecasts, respectively. The explanatory variables considered in training these models include: decentralized point forecasts (clustered using CLARA), atmospheric states (derived using SOMs), month of year and hour of day. Figure 2 shows the flowchart summarising the proposed methodology for aggregated wind power forecasting.

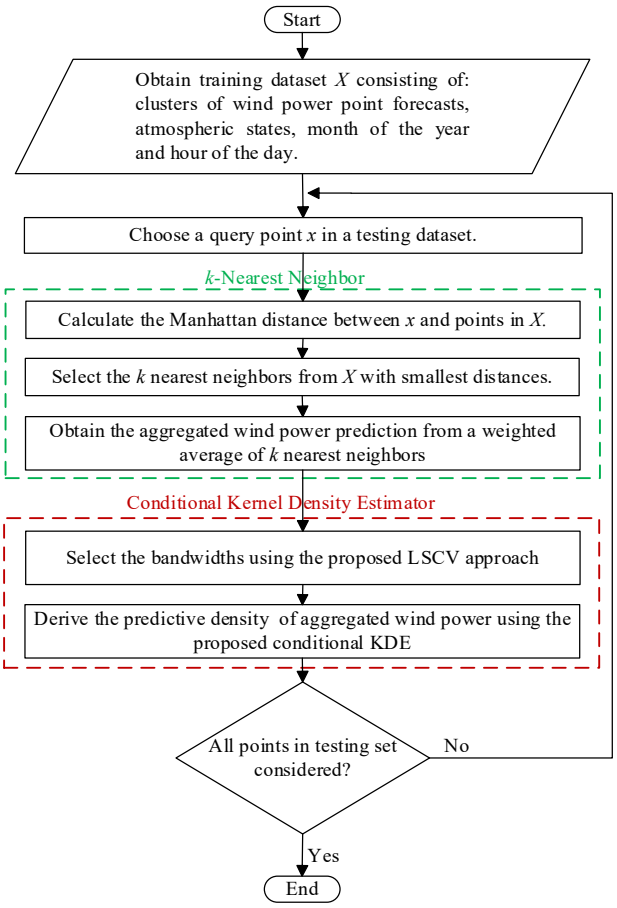

Figure 2: Flowchart summarizing the proposed methodology.

3. Evaluation framework

3.1.Point forecasts

There are many metrics that can be used to evaluate the accuracy of wind power point forecasts. The most frequently used metrics are mean absolute error (MAE), root mean squared error (RMSE) and coefficient of determination (R^2) [8], [14], [55], [58]. The same metrics are used in this paper to evaluate the accuracy of aggregated wind power point forecasts, and are calculated as:

$$MAE = \frac{1}{N}\sum_{i=1}^{N}\left|\frac{P_i - \hat{p}_i}{C_t}\right| \tag{8}$$

$$RMSE = \sqrt{\frac{1}{N}\sum_{i=1}^{N}\left(\frac{P_i - \hat{p}_i}{C_t}\right)^2} \tag{9}$$

$$R^2 = 1 - \frac{\sum_{i=1}^{N}(P_i - \hat{p}_i)^2}{\sum_{i=1}^{N}(P_i - \bar{P})^2} \tag{10}$$

Where P_i and $\hat{p}_i$ are the i-th actual and forecasted values of aggregated wind power, respectively, N is the total number of forecasting samples and C_t is the total wind capacity in a region. Note that the total wind capacity C_t is used as a denominator for (8) and (9) instead of actual wind power P_i to avoid the effects of aggregated wind power that is close to zero. In general, smaller MAE and RMSE, and R^2 value that is close to 1, indicate better performance of the forecasting model.

3.2.Probabilistic forecasts

To evaluate the aggregated wind power predictive densities, this paper adopts the framework defined in [59]. The framework is based on three metrics; reliability or calibration, sharpness and skill score. Evaluating probabilistic forecasts based on these metrics requires the evaluation set consisting of quantile forecasts (of various nominal proportions) and observations.

(a) Reliability or calibration

This metric measures the statistical consistency between quantile forecasts and observations. For example, a quantile forecast with a nominal level of 0.5 should contain 50% of the observed values lower or equal to its value. For a given quantile forecast $\hat{q}_t^{(\alpha)}$ at time t with nominal level α, and the corresponding observation p_t, the indicator variable $\xi_t^{(\alpha)}$ is given by:

$$\xi_t^{(\alpha)} = \begin{cases} 1, & if\ p_t < \hat{q}_t^{(\alpha)} \\ 0, & otherwise \end{cases} \tag{11}$$

The empirical level $a_k^{(\alpha)}$ is obtained by calculating the mean of indicator variable $\xi_t^{(\alpha)}$ over a set of T quantile forecasts.

$$a_k^{(\alpha)} = \frac{1}{T}\sum_{t=1}^{T} \xi_t^{(\alpha)} \tag{12}$$

In a 'perfect' calibration, the empirical levels match the nominal proportions.

(b) Sharpness

This metric measures how tight or concentrated the predictive densities are. Let $\delta_t^{(\beta)} = \hat{q}_t^{(1-\alpha/2)} - \hat{q}_t^{\alpha/2}$ be the width of a given prediction interval estimated at time t. The sharpness is obtained by calculating the average width $\bar{\delta}_t^{(\beta)}$ of the prediction interval over a set of T quantile forecasts. Mathematically, this is given by:

$$\bar{\delta}_t^{(\beta)} = \frac{1}{T}\sum_{t=1}^{T} \delta_t^{(\beta)} \tag{13}$$

In general, narrow prediction intervals (subject to calibration) are preferred because they suggest that predictions have more information content.

(c) Skill score

This metric assesses probabilistic forecasts by a single score, just like MAE and RMSE for the point forecasts. This score incorporates a variety of aspects of probabilistic forecast evaluation and hence allows for easier comparison between probabilistic forecasting approaches. In this paper, the skill score S_c for a set of M quantiles is calculated as:

$$S_c = \frac{1}{T}\sum_{t=1}^{T}\sum_{i=1}^{M} (\xi_t^{\alpha_i} - \alpha_i).(p_t - \hat{q}_t^{\alpha_i}) \tag{14}$$

This score cannot be decomposed to provide contributions of calibration, sharpness and other aspects of probabilistic forecast evaluation. In general, a higher score means higher skill of the probabilistic forecast approach and the score is zero for a 'perfect' probabilistic forecast.

4. Case study

4.1.Description of case study

The proposed methodology for aggregated wind power forecasting is tested using the data obtained from 29 wind farms in South Africa from 01 January 2018 to 31 March 2021. The

average installed capacity of these wind farms is 92 MW (ranging between 13 MW and 140 MW) and their geographical locations are shown in Figure 3. Since the individual wind power point forecast data is sensitive and confidential, Eskom (the utility company in South Africa) was only able to send the day-ahead wind power point forecasts in groups of three nearest wind farms (summed together). The challenge here is that some of the wind farms may not fall in the same cluster as its two nearest neighbors if CLARA was applied to the original dataset, instead of applying it to already clustered dataset (as received from the utility). This implies a drop in resolution of the data, which may have impacted the performance of the proposed methodology in this particular case study.

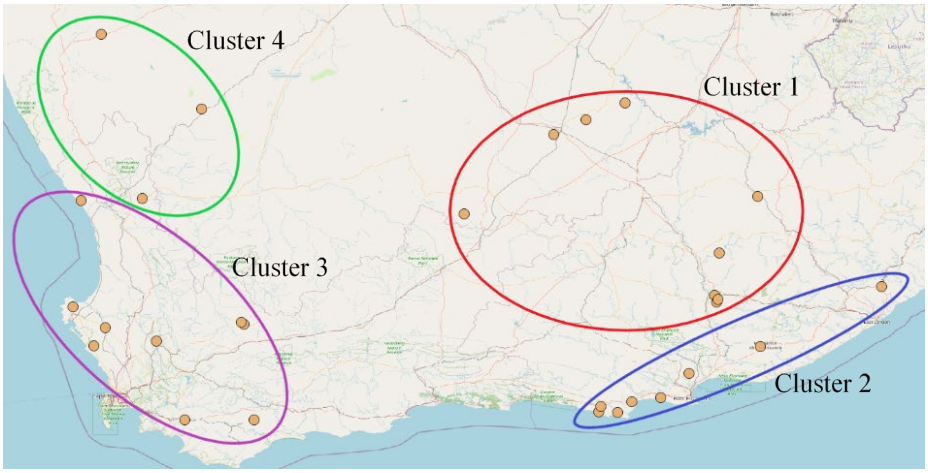

Figure 3: Geographical locations of wind farms used for testing the methodology.

The SOM Toolbox developed for Matlab by Helsinki University of Technology was used [60] for the classification of atmospheric states. As classification parameter, the hourly ERA5 850hPa geopotential height reanalysis dataset [61] was selected, as geopotential heights provide a good representation of large scale atmospheric circulation, and is a wind speed predictor e.g. [62], [63]. It was further deemed that the 850 hPa pressure level provides sufficient elevation to capture circulation above the South African escarpment. The classification area was bounded between 22-40°S and 5-40°E, which includes the South African subcontinent along with significant areas of the Indian and Atlantic oceans so as to adequately capture the large-scale circulation impacting the study area. To illustrate the proposed aggregation methodology, a 4x5 SOM-node topology was selected, which was deemed to provide sufficient detail. It should however be noted that the number of SOM nodes chosen represents what is often a subjective trade-off between level of generalization or detail required and quantization error.

The SOM was trained in two phases with a batch training algorithm, using a rectangular lattice as recommended for batch training [64]. The first (rough) training phase consisted of 1000

iterations with the neighborhood decreasing from 5 to 1, which was followed by a fine-tuning phase of 5000 iterations where the neighborhood function decreased from 2 to 1, thereafter remaining fixed after which only the BMU was updated. A number of studies have showed the starting point of the neighborhood function to have little impact on patterns produced [65], however in continuing the training once the radius parameter equals 1, the SOM approach becomes the equivalent of the *k*-means clustering procedure, which has been shown to be advantages in terms of average classification error [66]. The Epanechikov neighborhood function was used, as recommended by [64] when training small SOM maps.

The full dataset (consisting of hour of day, month of year, actual wind power generation, clusters of wind power point forecasts, and atmospheric states) was split into a training set (by randomly picking 90% rows from the full dataset) and testing set (remaining 10% from the full dataset). The seven-fold cross validation was used to determine the optimal value of *k* in *k*-NN algorithm. The aggregated wind power point forecast results obtained by training the *k*-NN algorithm with the proposed explanatory variables were compared to the results obtained by simply summing up the point forecasts. In addition, the *k*-NN algorithm was trained using different combinations of explanatory variables to evaluate the impact of each variable on the accuracy of the resulting aggregated forecasts. Furthermore, in order to assess the proposed model under various conditions, its performance evaluated during different hours of the day, months of the year, and atmospheric states.

This paper trained the conditional KDE using various combinations of proposed explanatory variables, and the results were compared to those obtained by training the conditional KDE with just the sum of point forecasts. This was done because it was difficult to train the conditional KDE using all proposed explanatory variables at once (due to bandwidth selection as explained in Section 2.3).

4.2.Evaluation of point forecasts

In Table 1, the overall performance of training the *k*-NN model with proposed explanatory variables is compared to simply adding the point forecasts by individual wind farms. The proposed methodology performs better than the sum of point forecasts within the context of the proposed evaluation metrics. The MAE and RMSE of the proposed methodology are 55% and 47% less than those achieved by adding the point forecasts, respectively. Likewise, the R^2 values show that 94% of the observed data fit the proposed model, while 77% of the data fit the sum of point forecasts model. Therefore, taking into account the spatial and temporal correlations

through the proposed explanatory variables improves the accuracy of aggregating decentralized point forecasts.

Table 1: Overall point prediction results of the proposed methodology.

Method	Sum of point forecasts	Proposed methodology
MAE	7.12	3.18
RMSE	9.11	4.63
R^2	0.77	0.94

Table 2 displays the results of the various scenarios for explanatory variables to show how the proposed explanatory variables affect forecasting accuracy. As shown in Table 2, taking into account the spatial information found within various clusters result in better forecasting accuracy compared to the sum of point forecasts. The accuracy improves further when taking into account diurnal and seasonal cycles as well as large-scale atmospheric circulations. The seasonal cycles shows superior impact followed by the large-scale atmospheric circulations.

Table 2: Scenarios for explanatory variables to show how explanatory variables affect forecasting accuracy.

Explanatory variables	Clusters	Clusters + time of day	Clusters + month of year	Clusters + atmospheric state	All
MAE	6.25	5.81	4.62	4.92	3.18
RMSE	8.45	8.03	6.70	7.08	4.63
R^2	0.80	0.82	0.87	0.86	0.94

Tables 3, 4 and 5 shows the performance of the proposed model during different hours of the day, months of the year and atmospheric states, respectively. The proposed model seems to perform better in the hours between 4h and 14h and in the months between March and July (which is the autumn and winter seasons). Figure 4 shows the hourly average wind power generation for January (summer), April (autumn), July (winter) and October (spring). The average wind generation profile shows daily ramp-up in wind power, especially during summer, autumn, and spring seasons, from approximately 9h to 18h, which is in turn followed by an equivalent ramp-down during the evening. This ramp-up is likely associated with daily surface heating due to the diurnal cycle. A possible reason that prediction errors are comparatively small during a period associated with significant variability in the wind power profile (4h-14h), is due to the cyclical nature of said variability, which is a function diurnal surface heating and cooling. Notwithstanding diurnal variability, Figure 4 shows that the autumn and winter wind power profiles are comparatively flat throughout the day, which is in turn a possible reason for the better model performance during these seasons.

The model also performs better during the atmospheric states (2,4), (2,5), (3,1), (3,3), (3,4), (3,5), (4,2), (4.3) and (4.4). Figure 5 shows the 20 (4x5) node SOM representing the 20 classified atmospheric states together with the frequency of SOM node occurrence as a percentage above each node. It is evident that the nodes where the proposed model performs better tends to represent atmospheric circulation dominated by high pressure conditions. Such conditions are associated with clear skies and more stable weather conditions, and thus less variability over different timescales which increases predictive skill.

Table 3: Point prediction results for different hours of the day.

Hour	0	1	2	3	4	5	6	7	8	9	10	11
MAE	5.22	4.83	3.18	3.19	2.65	1.97	2.43	2.46	3.14	2.61	2.92	2.75
RMSE	6.96	6.82	4.43	5.04	3.98	3.12	3.56	3.84	4.74	3.38	4.30	3.70
R^2	0.86	0.83	0.93	0.91	0.94	0.97	0.95	0.95	0.91	0.96	0.92	0.95

Hour	12	13	14	15	16	17	18	19	20	21	22	23
MAE	2.53	3.21	2.94	3.66	3.11	3.57	3.74	3.43	3.37	3.79	3.50	3.27
RMSE	3.28	5.05	4.5	5.19	4.6	4.96	5.43	5.29	4.38	5.88	4.85	4.56
R^2	0.97	0.94	0.96	0.93	0.95	0.95	0.93	0.92	0.95	0.88	0.93	0.92

Table 4: Point prediction results for different months of the year.

Month	1	2	3	4	5	6	7	8	9	10	11	12
MAE	3.77	3.17	2.87	2.68	2.63	2.87	2.82	3.06	2.74	3.78	3.89	4.46
RMSE	5.22	4.65	3.89	3.82	4.10	4.71	4.09	4.63	3.80	5.81	5.37	6.23
R^2	0.91	0.91	0.95	0.96	0.95	0.94	0.96	0.94	0.96	0.92	0.90	0.87

Table 5: Point prediction results for different atmospheric states.

Atmospheric state	1,1	1,2	1,3	1,4	1,5	2,1	2,2	2,3	2,4	2,5
MAE	3.77	4.04	4.09	3.67	3.07	3.37	3.34	4.2	2.58	2.85
RMSE	5.37	5.84	5.80	5.48	4.27	4.47	4.65	6.24	3.61	4.22
R^2	0.89	0.88	0.90	0.92	0.93	0.94	0.92	0.92	0.96	0.93

Atmospheric state	3,1	3,2	3,3	3,4	3,5	4,1	4,2	4,3	4,4	4,5
MAE	2.59	3.61	2.61	2.88	2.74	3.54	2.62	2.80	2.80	3.03
RMSE	3.57	5.60	3.87	4.25	4.21	5.07	4.08	3.81	3.96	4.56
R^2	0.96	0.94	0.95	0.92	0.94	0.95	0.93	0.95	0.93	0.94

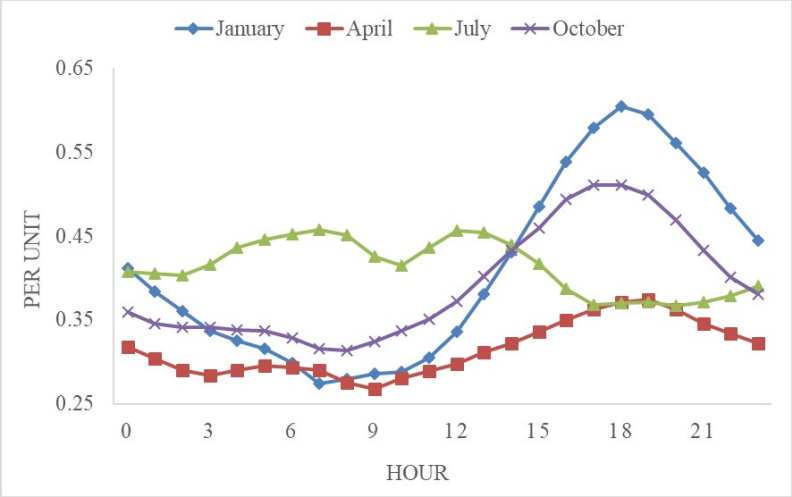

Figure 4: Hourly average wind generation for different months representing different seasons.

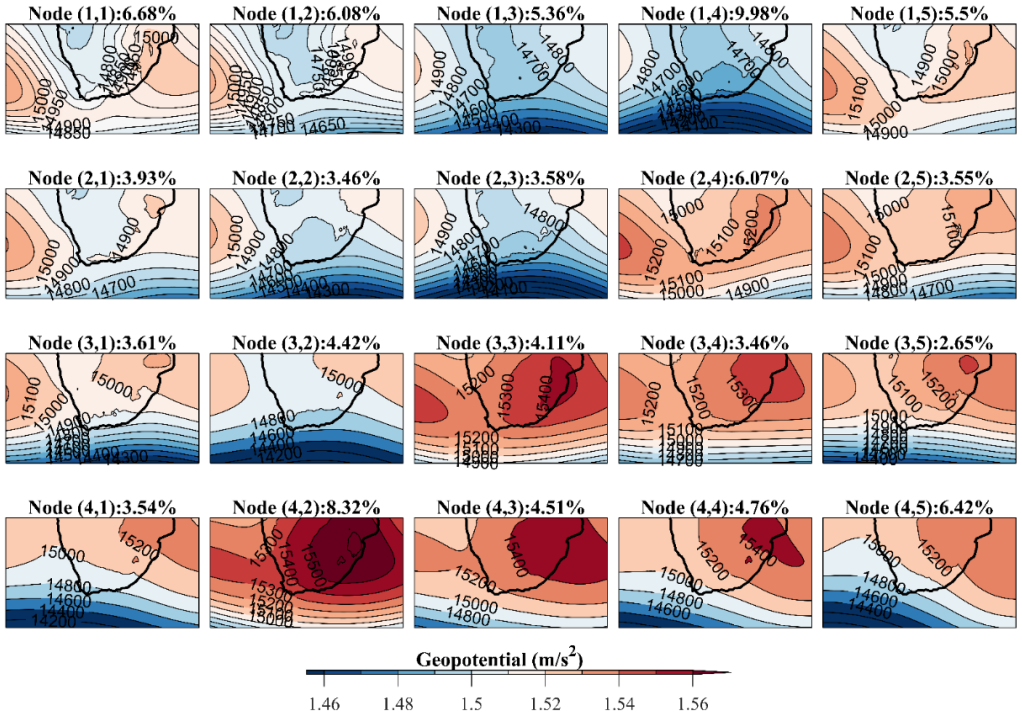

Figure 5: SOM geopotential heights together with frequency of SOM node occurrence over Southern Africa.

4.3.Evaluation of probabilistic forecasts

Figure 6 shows the day-ahead prediction intervals (10-90%) together with the actual observations of aggregated wind power generation on 30 March 2021 (which is reflective of a 'typical' autumn day in South Africa). Note that for Figure 6 only clusters of wind power point forecasts were used as the explanatory variables for illustration purposes. It can be seen that only two observations (at 7h and 21h) falls outside the 90% prediction intervals. The width of the prediction intervals is time-varying with the actual observations as expected. To get a different view on these results,

Figure 7 shows the aggregated wind power generation predictive densities at 1h, 8h, 14h and 20h on 30 March 2021. It can be seen from Figure 7 that the predictive densities are not only time-varying, but also multimodal and asymmetric (and thus non-Gaussian).

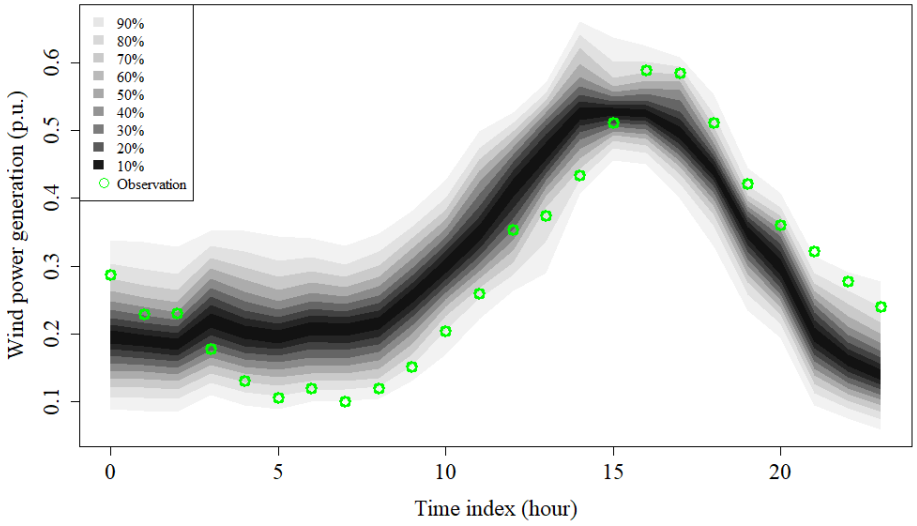

Figure 6: Day-ahead prediction intervals of aggregated wind power and actual observations on 30 March 2021 using clusters of point forecasts as explanatory variables.

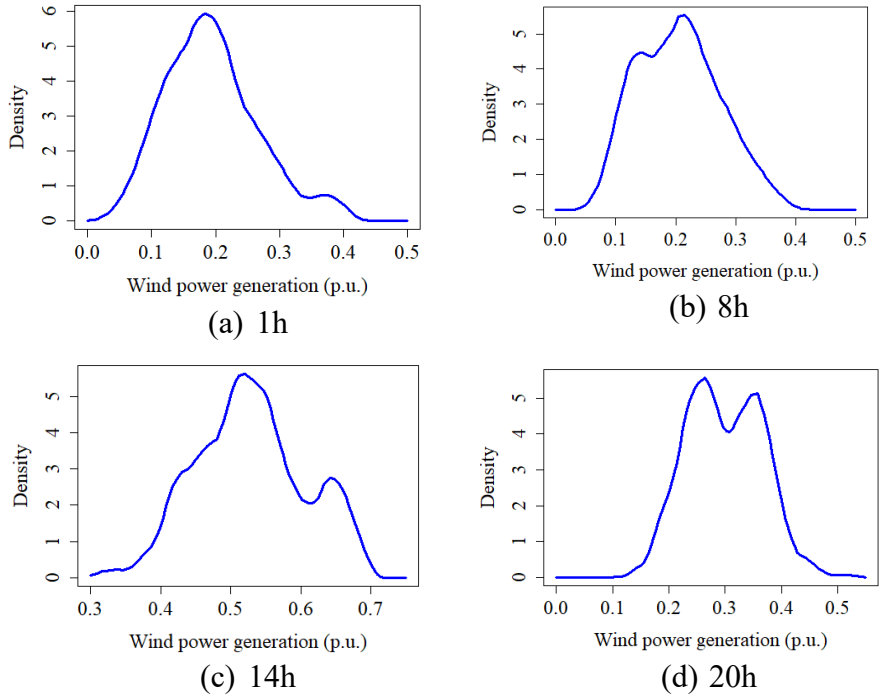

Figure 7: Day-ahead predictive densities of the aggregated wind power generation at 1h, 8h, 14h and 20h on 30 March 2021 using clusters of point forecasts as explanatory variables.

Figure 8 shows the reliability diagrams of the probabilistic forecasts using the proposed model for different explanatory variables scenarios. In Figure 8 (a), the empirical levels are plotted against the nominal proportions while also showing the desired line (where the empirical levels are equal to the nominal proportions). It can be seen from Figure 8 (a) that results achieved from all considered scenarios aligns well with the desired line (indicating reliable probabilistic

forecasts). To conduct a comparative analysis between considered scenarios, Figure 8 (b) plots the errors between empirical levels and desired outcomes, against the nominal proportions. A general conclusion from Figure 8 (b) is that the 'sum' scenario produces better reliability results than all other scenarios. In addition, the reliability of forecasts seems to drop with the increase in explanatory variables considered in a scenario. One possible explanation for this is the bandwidths selection that becomes more complex for high number of explanatory variables. As seen through negative reliability results, the proposed model tends to underestimate the aggregated wind power generation for the 'sum' scenario. For the rest of scenarios, the model tends to underestimate the aggregated wind power generation when nominal proportion is below 60% and overestimate for larger nominal proportions.

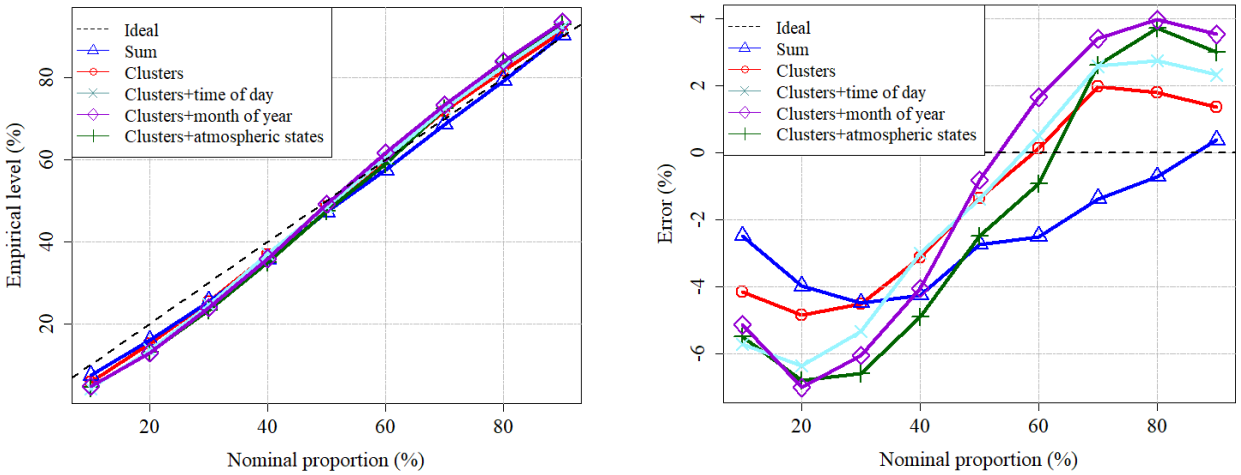

(a) Empirical level

(b) Error

Figure 8: Reliability diagrams of prediction intervals provided by the proposed model for different combinations of explanatory variables.

Figure 9 shows the sharpness results of prediction intervals for different explanatory variables scenarios. It can be seen that the 'clusters + month of year' scenario achieves the best sharpness results (ranging between 2% and 20%) while the 'sum' scenario achieves the worst sharpness results (ranging between 2% and 28%). The results show a significant improvement from the 'sum' scenario to the 'clusters' scenario, followed by noticeable improvements from the 'clusters' scenario to the rest of scenarios. This highlights the importance of considering spatial correlations, larger atmospheric circulations, inter-hour and seasonal variations in aggregated wind power forecasting. However, good sharpness results may lead to underestimation and overestimation of aggregated wind power uncertainty as deduced from the reliability diagram in Figure 8. Therefore, there is a need for a trade-off between reliability and sharpness depending on the specific requirements of the grid and its customers.

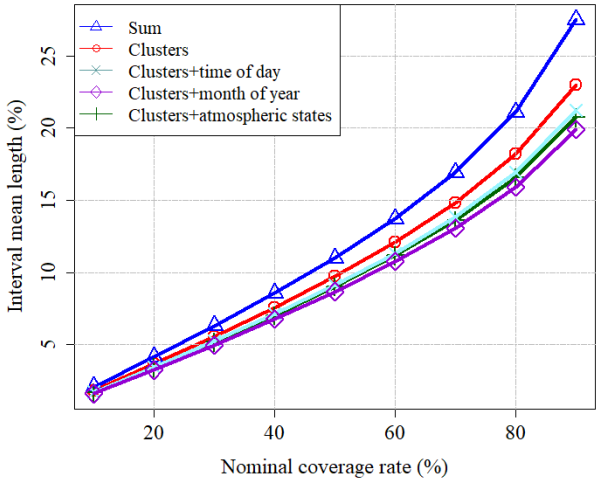

Figure 9: Sharpness results with different nominal coverage rates for different combinations of explanatory variables.

Table 6 shows the skill score results for different combinations of explanatory variables. It can be seen that the 'clusters + month of year' scenario achieves the best skill score (-0.148) while, the lowest skill score (-0.283) is achieved on 'sum' scenario. The results show a significant improvement from the 'sum' scenario to the 'clusters' scenario, followed by smaller improvements from the 'clusters' scenario to the rest of scenarios.

Table 6: Skill score results for different explanatory variables scenarios.

Explanatory variables	Sum	Clusters	Clusters + time of day	Clusters + month of year	Clusters + atmospheric states
Skill score	-0.283	-0.174	-0.157	-0.148	-0.153

The results above show that taking into account the spatial and temporal correlations through the proposed explanatory variables also improves the accuracy of aggregated probabilistic forecasts that can be derived from decentralized forecasts.

5. Conclusion

This paper proposed explanatory variables that were used to train the *k*-NN and conditional KDE models to derive day-ahead aggregated point and probabilistic wind power forecasts from decentralized point forecasts of geographically distributed wind farms. The proposed explanatory variables include clusters of point forecasts (to account for spatial correlations between wind farms), hour of day (to account for diurnal cycles), month of year (to account for seasonal cycles) and, atmospheric states (to account for correlations due to large-scale atmospheric circulations). The main findings of this paper can be summarized as follows:

- The results from the proposed approach showed a significant improvement (47% less RMSE) as compared to simply adding the decentralized point forecasts. Therefore, the

proposed well-known spatial and temporal correlations as well as large-scale atmospheric circulations can be effective in capturing some spatial and temporal correlations that are not accounted for by simply adding the decentralized forecasts.

- In the case study, the proposed approach performed better in hours between 4h and 14h. One possible reason for this can be that the variability of the wind power profile between these hours is a function of diurnal surface heating and cooling, and this was incorporated by including the hour of day feature in the proposed approach. In addition, the autumn and winter wind power profiles are comparatively flat throughout the day, which can be a possible reason for the better performance of the approach during these seasons. Furthermore, the proposed approach performed better in SOM nodes that tends to represent atmospheric circulation dominated by high pressure conditions.
- The predictive densities obtained from the proposed approach were shown to be non-Gaussian and time-varying as expected given the time-varying nature of wind uncertainty. The probabilistic forecasts from the considered scenarios were relatively reliable (less than 8% in error between empirical levels and desired outcomes). However, the reliability of forecasts appears to drop with the increase in explanatory variables considered in a scenario. This can be due to bandwidths selection that becomes more complex in the proposed KDE approach for a high number of explanatory variables.
- The sharpness and skill score results showed a significant improvement when the proposed explanatory variables were considered as compared to simply adding decentralized forecasts. In addition, the month of year feature produce slightly better sharpness and skill scores compared to the hour of day and atmospheric state features, which highlights the importance of incorporating effects of seasonality in aggregated forecasting.

The most significant contribution made by this paper is in proposing an approach for incorporating some spatial and temporal correlations to improve accuracy of aggregated forecasts derived from decentralized point forecasts. In addition, knowing the hours, months, and atmospheric states under which the proposed approach performs better together with the derived predictive densities can be used as inputs to operational processes such as stochastic unit commitment and dynamic operating reserve allocation. This paper also demonstrated a way in which large-scale atmospheric circulation patterns can be incorporated into short-term wind power forecasting – which has been lacking in the literature. In future, one can test the proposed methodology using ungrouped wind data to see if there can be further improvements on the results. In addition, more work needs to be done in terms of bandwidths selection of high dimensional dataset in KDE-based approaches.

References

[1] Y. Zhang and J. Wang, "A distributed approach for wind power probabilistic forecasting considering spatiooral correlation without direct access to off-site information," *IEEE Trans. Power Syst.*, vol. 33, no. 5, pp. 5714–5726, 2018.

[2] A. Lenzi, I. Steinsland, and P. Pinson, "Benefits of spatiotemporal modeling for short-term wind power forecasting at both individual and aggregated levels," *Environmetrics*, vol. 29, no. 3, pp. 1-17, 2018.

[3] Z. Wang, W. Wang, C. Liu, B. Wang, and S. Feng, "Probabilistic forecast for aggregated wind power outputs based on regional NWP data," *J. Eng.*, vol. 2017, no. 13, pp. 1528–1532, 2017.

[4] J. Tastu, P. Pinson, E. Kotwa, H. Madsen, and H. A. Nielsen, "Spatio-temporal analysis and modeling of short-term wind power forecast errors," *Wind Energy*, vol. 14, pp. 43–60, 2011.

[5] A. Malvaldi, S. Weiss, D. Infield, J. Browell, P. Leahy, and A. M. Foley, "A spatial and temporal correlation analysis of aggregate wind power in an ideally interconnected Europe," *Wind Energy*, vol. 20, no. 8, pp. 1315–1329, 2017.

[6] M. Sun, C. Feng, and J. Zhang, "Aggregated Probabilistic Wind Power Forecasting Based on Spatio-Temporal Correlation," in *IEEE Power Energy Soc. Gen. Meet.*, 2019.

[7] P. Li, X. Guan, and J. Wu, "Aggregated wind power generation probabilistic forecasting based on particle filter," *Energy Convers. Manag.*, vol. 96, pp. 579–587, 2015.

[8] M. Sun, C. Feng, and J. Zhang, "Conditional aggregated probabilistic wind power forecasting based on spatio-temporal correlation," *Appl. Energy*, vol. 256, 2019.

[9] C. Wan, Z. Xu, P. Pinson, Z. Y. Dong, and K. P. Wong, "Probabilistic Forecasting of Wind Power Generation Using Extreme Learning Machine," *IEEE Trans. Power Syst.*, vol. 29, no. 3, pp. 1033–1044, 2014.

[10] R. J. Bessa, V. Miranda, A. Botterud, J. Wang, and E. M. Constantinescu, "Time Adaptive Conditional Kernel Density Estimation for Wind Power Forecasting," *IEEE Trans. Sustain. Energy*, vol. 3, no. 4, pp. 660–669, 2012.

[11] M. Lei, L. Shiyan, J. Chuanwen, L. Hongling, and Z. Yan, "A review on the forecasting of wind speed and generated power," *Renew. Sustain. Energy Rev.*, vol. 13, no. 4, pp. 915–920, May 2009.

[12] G. Giebel, G. N. Kariniotakis, and C. Draxl, “The State of the Art in Short-Term Prediction of Wind Power,” Reppenstedt, Germany, 2011.

[13] P. Mandal, H. Zareipour, and W. D. Rosehart, “Forecasting aggregated wind power production of multiple wind farms using hybrid wavelet-PSO-NNs,” *Int. J. Energy Res.*, vol. 38, no. 13, pp. 1654–1666, 2014.

[14] Q. Zhu, J. Chen, L. Zhu, X. Duan, and Y. Liu, “Wind speed prediction with spatio-temporal correlation: A deep learning approach,” *Energies*, vol. 11, no. 4, pp. 1–18, 2018.

[15] B. Alonzo, P. Tankov, P. Drobinski, and R. Plougonven, “Probabilistic wind forecasting up to three months ahead using ensemble predictions for geopotential height,” *Int. J. Forecast.*, vol. 36, no. 2, pp. 515–530, 2020.

[16] P. Pinson, H. A. Nielsen, H. Madsen, and G. Kariniotakis, “Skill forecasting from ensemble predictions of wind power,” *Appl. Energy*, vol. 86, pp. 1326–1334, 2009.

[17] J. W. Taylor, P. E. McSharry, and R. Buizza, “Wind Power Density Forecasting Using Ensemble Predictions and Time Series Models,” *IEEE Trans. Energy Convers.*, vol. 24, no. 3, pp. 775–782, 2009.

[18] N. Chen, Z. Qian, I. T. Nabney, and X. Meng, “Wind Power Forecasts Using Gaussian Processes and Numerical Weather Prediction,” *IEEE Trans. Power Syst.*, vol. 29, no. 2, pp. 656–665, 2014.

[19] L. Landberg, G. Giebel, L. Myllerup, J. Badger, H. Madsen, and T. S. Nielsen, “Poor-man’s ensemble forecasting for error estimation,” 2002

[20] M. Lange, U. Focken, R. Meyer, M. Denhardt, B. Ernst, and F. Berster, “Optimal combination of different numerical weather models for improved wind power predictions,” in *Sixth International Workshop on Large-Scale Integration of Wind Power and Transmission Networks for Offshore Wind Farms*, 2006.

[21] M. Negnevitsky, P. Mandal, and A. K. Srivastava, “An overview of forecasting problems and techniques in power systems,” in *2009 IEEE Power & Energy Society General Meeting*, 2009.

[22] Y. Zhang, J. Wang, and X. Wang, “Review on probabilistic forecasting of wind power generation,” *Renew. Sustain. Energy Rev.*, vol. 32, pp. 255–270, 2014.

[23] W. Chang, “A Literature Review of Wind Forecasting Methods,” *J. Power Energy Eng.*,

vol. 02, no. 04, pp. 161–168, 2014.

[24] P. Pinson and G. Kariniotakis, “On-line assessment of prediction risk for wind power production forecasts,” *Wind Energy*, vol. 7, no. 2, pp. 119–132, 2004.

[25] P. Pinson and G. N. Kariniotakis, “On-line adaption of confidence intervals based on weather stability for wind power forecsting,” in *Proc. ofthe 2004 Global Windpower Conference*, 2004.

[26] J. B. Bremnes, “A comparison of a few statistical models for making quantile wind power forecasts,” *Wind Energy*, vol. 9, no. 1–2, pp. 3–11, 2006.

[27] C. Yildiz, M. Tekin, A. Gani, O. F. Keçecioğlu, H. Açikgöz, and M. Şekkeli, “A day-aheadwind power scenario generation, reduction, and quality test tool,” *Sustain.*, vol. 9, no. 5, May 2017.

[28] H. Bludszuweit, J. A. Dominguez-Navarro, and A. Llombart, “Statistical Analysis of Wind Power Forecast Error,” *IEEE Trans. Power Syst.*, vol. 23, no. 3, pp. 983–991, Aug. 2008.

[29] A. Fabbri, T. GomezSanRoman, J. RivierAbbad, and V. H. MendezQuezada, “Assessment of the Cost Associated With Wind Generation Prediction Errors in a Liberalized Electricity Market,” *IEEE Trans. Power Syst.*, vol. 20, no. 3, pp. 1440–1446, Aug. 2005.

[30] S. Bofinger, A. Luig, and H. G. Beyer, “Qualification of wind power forecasts,” in *Proc. Global Wind Power Conf.*, 2002.

[31] N. Menemenlis, M. Huneault, and A. Robitaille, “Computation of Dynamic Operating Balancing Reserve for Wind Power Integration for the Time-Horizon 1–48 Hours,” *IEEE Trans. Sustain. Energy*, vol. 3, no. 4, pp. 692–702, Oct. 2012.

[32] B. Mauch, J. Apt, P. M. S. Carvalho, and M. J. Small, “An effective method for modeling wind power forecast uncertainty,” *Energy Syst.*, vol. 4, no. 4, pp. 393–417, Dec. 2013.

[33] K. Porter, J. Rogers, K. Porter, and J. Rogers, “Status of Centralized Wind Power Forecasting in North America Status of Centralized Wind Power Forecasting in North America May 2009 – May 2010,” Golden, CO (United States), 2010.

[34] Ministry of Energy, “Implementation agreement between the Seller and the Department of Energy pursuant to the Renewable Energy Independent Power Producer Procurement

Programme," South Africa, 2012.

[35] M. Fripp and R. H. Wiser, "Effects of Temporal Wind Patterns on the Value of Wind-Generated Electricity in California and the Northwest," *IEEE Trans. Power Syst.*, vol. 23, no. 2, pp. 477–485, 2008.

[36] S. Rehman, "Wind energy resources assessment for Yanbo, Saudi Arabia," *Energy Convers. Manag.*, vol. 45, pp. 2019–2032, 2004.

[37] B. Karki and R. Billinton, "Effects of seasonality and locality on the operating capacity benefits of wind power," in *2009 IEEE Electrical Power & Energy Conference (EPEC)*, 2009.

[38] K. Knorr, B. Zimmermann, S. Bofinger, A. Gerlach, T. Bischof-Niemz, and C. Mushwana, "Wind and Solar PV Resource Aggregation Study for South Africa," Council for Scientific and Industrial Research, Pretoria, South Africa, 2016.

[39] F. M. Mulder, "Implications of diurnal and seasonal variations in renewable energy generation for large scale energy storage," *J. Renew. Sustain. Energy*, vol. 6, no. 3, 2014.

[40] R. Carapellucci and L. Giordano, "The effect of diurnal profile and seasonal wind regime on sizing grid-connected and off-grid wind power plants," *Appl. Energy*, vol. 107, pp. 364–376, 2013.

[41] L. Zhou, Y. Tian, S. Baidya Roy, Y. Dai, and H. Chen, "Diurnal and seasonal variations of wind farm impacts on land surface temperature over western Texas," *Clim. Dyn.*, vol. 41, no. 2, pp. 307–326, 2013.

[42] A. Dalton, B. Bekker, and M. J. Koivisto, "Atmospheric circulation archetypes as clustering criteria for wind power inputs into probabilistic power flow analysis," in *2020 International Conference on Probabilistic Methods Applied to Power Systems (PMAPS)*, 2020.

[43] A. Dalton, B. Bekker, and M. J. Koivisto, "Simulation and detection of wind power ramps and identification of their causative atmospheric circulation patterns," *Electr. Power Syst. Res.*, vol. 192, 2021.

[44] A. Dalton, B. Bekker, and M. J. Koivisto, "Classified atmospheric states as operating scenarios in probabilistic power flow analysis for networks with high levels of wind power," *Energy Reports*, vol. 7, pp. 3775–3784, 2021.

[45] D. J. Brayshaw, A. Troccoli, R. Fordham, and J. Methven, "The impact of large scale atmospheric circulation patterns on wind power generation and its potential predictability: A case study over the UK," *Renew. Energy*, vol. 36, no. 8, pp. 2087–2096, 2011.

[46] H. C. Bloomfield, D. J. Brayshaw, P. L. M. Gonzalez, and A. Charlton-Perez, "Sub-seasonal forecasts of demand and wind power and solar power generation for 28 European countries," *Earth Syst. Sci. Data*, vol. 13, no. 5, pp. 2259–2274, May 2021.

[47] R. J. Davy, M. J. Woods, C. J. Russell, and P. A. Coppin, "Statistical Downscaling of Wind Variability from Meteorological Fields," *Boundary-Layer Meteorol.*, vol. 135, pp. 161–175, 2010.

[48] C. Y. Janse van Vuuren and H. J. Vermeulen, "Clustering of wind resource data for the South African renewable energy development zones," *J. Energy South. Africa*, vol. 30, no. 2, pp. 126–143, 2019.

[49] T. Gupta and S. Panda, "A Comparison of K-Means Clustering Algorithm and CLARA Clustering Algorithm on Iris Dataset," *Int. J. Eng. Technol.*, vol. 7, no. 4, pp. 4766–4768, 2018.

[50] T. Kohonen, "The self-organizing map," *Proc. IEEE*, vol. 78, no. 9, pp. 1464–1480, 1990.

[51] R. Huth *et al.*, "Classifications of Atmospheric Circulation Patterns," *Ann. N. Y. Acad. Sci.*, vol. 1146, pp. 105–152, 2008.

[52] C. Lennard and G. Hegerl, "Relating changes in synoptic circulation to the surface rainfall response using self-organising maps," *Clim. Dyn.*, vol. 44, pp. 861–879, 2015.

[53] Y. Zhang and J. Wang, "K-nearest neighbors and a kernel density estimator for GEFCom2014 probabilistic wind power forecasting," *Int. J. Forecast.*, vol. 32, no. 3, pp. 1074–1080, 2016.

[54] Y. He, R. Liu, H. Li, S. Wang, and X. Lu, "Short-term power load probability density forecasting method using kernel-based support vector quantile regression and Copula theory," *Appl. Energy*, vol. 185, pp. 254–266, 2017.

[55] Y. He and H. Li, "Probability density forecasting of wind power using quantile regression neural network and kernel density estimation," *Energy Convers. Manag.*, vol. 164, no. March, pp. 374–384, 2018.

[56] X. Yang, X. Ma, N. Kang, and M. Maihemuti, "Probability Interval Prediction of Wind

Power Based on KDE Method with Rough Sets and Weighted Markov Chain," *IEEE Access*, vol. 6, pp. 51556–51565, 2018.

[57] A. Araveeporn, "The Comparison of Bandwidth Selection Methods," *KMITL Sci. Tech. J.*, vol. 11, no. 2, pp. 64–78, 2011.

[58] P. Mandal, H. Zareipour, and W. D. Rosehart, "Forecasting aggregated wind power production of multiple wind farms using hybrid wavelet-PSO-NNs," *Int. J. Energy Res.*, vol. 38, no. 13, pp. 1654–1666, 2014.

[59] P. Pinson, H. A. Nielsen, J. K. Møller, H. Madsen, and G. N. Kariniotakis, "Non-parametric probabilistic forecasts of wind power: required properties and evaluation," *Wind Energy*, vol. 10, no. 6, pp. 497–516, 2007.

[60] E. Alhoniemi, J. Himberg, J. Parhankangas, and J. Vesanto, "SOM Toolbox." Laboratory of Information and Computer Science, Helsinki University of Technology, Helsinki, 2002.

[61] Copernicus Climate Change Service, "ERA5: Fifth generation of ECMWF atmospheric reanalyses of the global climate." Copernicus Climate Change Service Climate Data Store (CDS), 2017.

[62] J. Browell, D. R. Drew, and K. Philippopoulos, "Improved very short-term spatio-temporal wind forecasting using atmospheric regimes," *Wind Energy*, vol. 21, no. 11, pp. 968–979, 2018.

[63] R. J. Davy, M. J. Woods, C. J. Russell, and P. A. Coppin, "Statistical downscaling of wind variability from meteorological fields," *Boundary-Layer Meteorol.*, vol. 135, pp. 161–175, 2010.

[64] Y. Liu, R. H. Weisberg, and C. N. K. Mooers, "Performance evaluation of the self-organizing map for feature extraction," *J. Geophys. Res.*, vol. 111, 2006.

[65] P. B. Gibson, S. E. Perkins-Kirkpatrick, P. Uotila, A. S. Pepler, and L. V. Alexander, "On the use of self-organizing maps for studying climate extremes," *J. Geophys. Res.*, vol. 122, no. 7, pp. 3891–3903, 2017.

[66] N. Jiang, K. Luo, P. J. Beggs, K. Cheung, and Y. Scorgie, "Insights into the implementation of synoptic weather-type classification using self-organizing maps: An Australian case study," *Int. J. Climatol.*, vol. 35, no. 12, pp. 3471–3485, 2015.

Paper 3

N. Mararakanye, A. Dalton, and B. Bekker, “Characterizing Wind Power Forecast Error Using Extreme Value Theory and Copulas,” IEEE Access, vol. 10, pp. 58547–58557, Jun. 2022, doi: 10.1109/access.2022.3179697.

Citations up to date: 0

Quartile of the journal as calculated by Scimago (www.scimagojr.com): 1

To comply with the copyright requirements, the final pre-print version of the article is presented here, formatted in dissertation style.

The final published paper is available at: https://doi.org/10.1109/ACCESS.2022.3179697.

Characterizing wind power forecast error using extreme value theory and copulas

Ndamulelo Mararakanye [a], Amaris Dalton [a] and Bernard Bekker [a]

[a] *Department of Electrical and Electronic Engineering, Stellenbosch University, Private Bag X1, Matieland, 7602, South Africa*

Abstract

Wind energy is one of the fastest-growing renewable energy sources in the world. However, wind power is variable in all timescales. This variability is difficult to predict with perfect certainty, with potentially significant financial implications when rare extreme forecast errors occur. This paper focuses on three key aspects associated with the extreme errors of geographically distributed wind farms: suitable parametric distribution representation, effects of diurnality, seasonality and larger atmospheric circulations, and modeling multivariate distribution. The paper shows that some of the distributions commonly used for modeling forecast errors may be inappropriate in representing extreme errors. As the first contribution, this paper fits a Generalized Pareto distribution (GPD) from extreme value theory to achieve a better estimation of extreme errors. In the second contribution, this paper splits extreme errors by hour, month, and atmospheric states to investigate the statistical regularities of GPD parameters along diurnal and seasonal timescales and larger atmospheric circulations. In the third contribution, this paper uses copula functions to model multivariate extreme error distribution and investigates their effectiveness in providing a regional view of extreme errors. This paper tests the proposed methodology using the forecast error data obtained from 29 wind farms in South Africa. The results show that GPD outperforms commonly used distributions. Extreme errors have strong diurnal and seasonal components and vary significantly between SOM nodes. Copulas can be useful in providing a regional view of extreme errors. This paper improves the estimation of extreme errors, which is an important step toward better operating reserve allocation.

Keywords: Atmospheric state, copula, extreme value theory, Generalized Pareto distribution, wind power forecast error

1. Introduction

The use of wind energy for electricity generation is increasing worldwide. This is because there is a need to decarbonize the electricity industry and wind energy is becoming cost competitive. However, unlike conventional thermal power, wind power varies over time. This is a source of

concern for system operators, who must ensure that supply matches demand at all times. One way of mitigating the impacts of wind power variations in power system operations is wind power forecasting. These forecasts provide system operators with an estimate of future wind power generation, but they are rarely perfect. Small forecast errors are not always a concern for system operators since power systems can accommodate a certain level of variability and uncertainty from the load demand. However, during significant wind power ramp events, forecast errors from a day-ahead prediction can be as high as 60-80% of total wind capacity [1], [2]. If there is insufficient operating reserve to deal with these extreme forecast errors, the system operator may have to implement wind generation curtailment or load shedding – scenarios that system operators try to avoid due to the associated financial implications. In deregulated markets, extreme forecast errors can also affect energy traders since inaccurate bids during these events can result in costly penalties. As an example, on February 26, 2008, Electric Reliability Council of Texas reported a high forecast error event, forcing them to declare a system emergency, which is a high-cost system condition [3]. These potential implications justify the need for understanding and characterizing the magnitude and frequency of extreme wind power forecast errors, towards better operational decisions such as dynamic operating reserve allocation to account for wind power uncertainty.

In this paper, we analyze the tails of forecast error distributions of geographically distributed wind farms. We focus on three main aspects associated with extreme forecast errors: 1) suitable parametric distribution representation, 2) effects of diurnality, seasonality, and large atmospheric circulations, and 3) modeling the multivariate distribution.

The studies in the literature frequently used the normal distribution to model wind power forecast errors [4]–[11]. Other distributions considered in the literature include beta [12], Weibull [13], [14], Cauchy [14], [15] and hyperbolic [15], [16]. While these distributions are relatively suitable for representing the body of the forecast error distribution, the same assertion is not valid for the tails of the forecast error distribution. According to the findings in [1], [10]–[12], [17], normal, beta, and Weibull distributions are not fat-tailed enough, and therefore often underestimate the frequency of extreme forecast errors. On the other hand, the study in [15] demonstrated that the Cauchy distribution is overly fat-tailed and over-represents the frequency of extreme forecast errors. According to the findings in [14], [15], the hyperbolic distribution seems to perform better compared to normal, beta, Weibull, and Cauchy distributions in modeling extreme forecast errors. Given the severe financial implications of extreme forecast errors, finding models that best represent these extreme forecast errors remains critical. As a result, other studies in the literature have considered non-parametric approaches for modeling

wind power forecast errors [18], [19]. While non-parametric approaches can be accurate, extreme forecast errors often do not occur frequently enough to make accurate non-parametric inferences [15], [20]. This paper will investigate whether extreme forecast errors can be modeled accurately using the Extreme Value Theory (EVT) by fitting the Generalized Pareto distribution (GPD) on the extreme forecast errors. Recent literature has used the same approach to model the tail behavior of wind speed [21], [22] and wind power ramp [23], however, the approach has not been explored for wind power forecast error.

The second aspect of this paper is investigating the influence of diurnality, seasonality, and large atmospheric circulations on extreme forecast errors. Several studies (e.g. [24]–[30]) in the literature have demonstrated that wind power profiles exhibit a high degree of statistical regularity along diurnal and seasonal timescales. In addition, the study in [31] revealed that large atmospheric circulations are the major cause of wind power variations over timescales ranging from hours to days. These variables are the basis used to understand wind power variability and ultimately improve wind power forecasting (e.g. [32]–[34]). However, there is little to no investigation in the literature on how these variables affect forecast errors – towards improved estimation of extreme forecast errors. To investigate the diurnal and seasonal patterns of extreme forecast errors, this paper investigates the tail distribution (or fitted GPD) associated with each hour and month. Additionally, this paper assigns atmospheric states, derived from self-organizing maps (SOMs), to each historical forecast scenario and investigates the tail distribution associated with each state.

The third aspect of this paper is modeling multivariate forecast error distribution. While univariate analysis can be useful in certain applications (e.g. congestion management), other operational decisions such as operating reserve allocation need to consider all wind farms within a region. It is thus important to evaluate the dependence structure of forecast errors from geographically distributed wind farms. Copula theory is widely used to model dependence structure between variables, mostly in financial market analysis, portfolio investments, and risk assessments [35]. In recent years, copula theory has been applied in wind power analyses (e.g. [21], [32], [33], [35]–[38]). The majority of these studies used copula theory to model the spatial dependency of regional wind speeds or power outputs. However, there is little to no investigation on using copula theory to model forecast errors. This paper uses copula functions to model multivariate extreme forecast error distribution and investigates if this is effective in providing a region-wide view of extreme forecast errors using numerical examples. Fig. 1 shows an overview of this paper.

The remainder of this paper is organized as follows: Section 2 provides the theoretical framework of the proposed methodology. Section 3 introduces the case study of 29 wind farms in South Africa used for illustrating the proposed methodology and presents the results and discussion. Section 4 summarizes the findings before concluding the paper.

The main contributions of this paper can be summarized as finding a suitable parametric distribution for representing extreme forecast errors, improving understanding on some of the factors that may influence extreme forecast errors, and proposing a suitable model for representing spatial correlations of extreme forecast errors between wind farms. These contributions can assist system operators with a method of deriving conditional extreme forecast error distributions that changes based on various states (i.e. hour, month, atmospheric and spatial configuration of wind farms). These conditional distributions usually contain more probabilistic information (as compared to unconditional distribution), which can improve operating reserve allocation to account for wind power uncertainty. In addition, the classified atmospheric states represent larger atmospheric circulation, allowing inputs into reserve allocation based on physical meteorological phenomena.

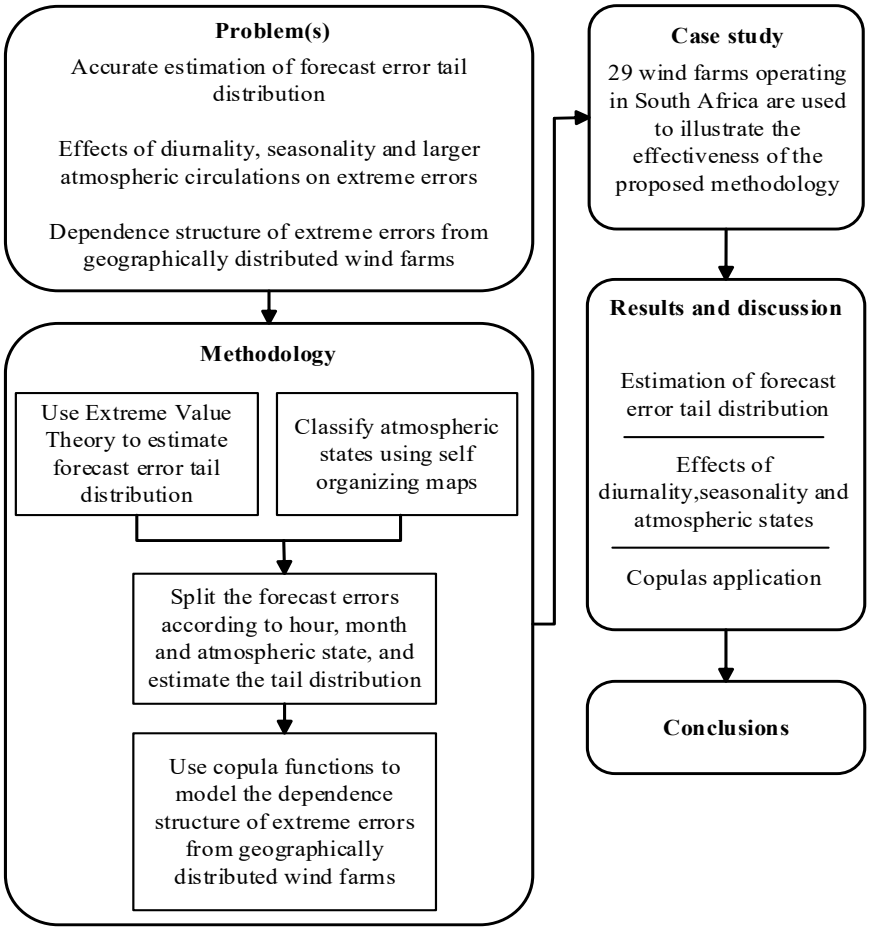

Figure 1: Paper overview.

2. Methodology

2.1.Fitting forecast error tail distribution

In EVT, there are two ways to sample extreme events: block maxima (BM) and peak-over-threshold (POT). The BM method divides the data into equal blocks, extracts the highest observation in each block, then fits a Generalized Extreme Value (GEV) distribution to the block maxima. The BM method has a significant limitation in that it retrieves only one observation from each block, regardless of whether the second-highest observation in a block exceeds the largest observations in adjacent blocks. As a result, adopting BM necessitates a large amount of data [43], [44]. The POT, on the other hand, entails setting a threshold, extracting the excess of observations over the threshold, and fitting a GPD to the exceedances. This is a more flexible technique that typically enables more observations to be retrieved (rather than just one in each block), resulting in reduced uncertainty [43], [44].

As a result, the POT approach is used in this paper to model the distribution of forecast error exceedances over a high threshold u. Assuming that $X_1, X_2, \dots, X_N$ (representing the forecast errors for individual clusters) is an independent and identically distributed sequence of random variables and N is the sample size, the distribution function $F_u(y)$ of exceedances X over a threshold u is defined by:

$$F_u(y) = P(X - u \leq y | X > u) = \frac{F(y+u) - F(u)}{1 - F(u)} \tag{1}$$

With high enough u, $F_u(y)$ can be approximated by a GPD with the following cumulative distribution function.

$$G_{\xi,\beta}(y) = \begin{cases} 1 - \left(1 + \frac{\xi y}{\beta}\right)^{-\frac{1}{\xi}} & if\ \xi \neq 0 \\ 1 - \exp\left(-\frac{y}{\beta}\right) & if\ \xi = 0 \end{cases} \tag{2}$$

$$\text{For} \begin{cases} \beta > 0\ and\ y \geq 0 & if\ \xi \geq 0 \\ 0 \leq y \leq -\frac{\beta}{\xi} & if\ \xi < 0 \end{cases}$$

Where ξ is the shape parameter and β is the scale parameter. To estimate the values of ξ and β, this paper uses the maximum likelihood estimation (MLE) approach. If $y_1, y_2, \dots, y_{N_u}$ is a sequence of N_u exceedances over a threshold u, the log-likelihood can be derived for $\xi \neq 0$ as:

$$l(\beta,\xi) = -N_u log\beta - (1+\frac{1}{\xi})\sum_{i=1}^{N_u} log\left(1+\xi\frac{y_i}{\beta}\right) \tag{3}$$

Provided $(1+\xi\, y_i/\beta) > 0$ for $i = 1,2,\ldots,N_u$; otherwise $l(\beta,\xi) = \infty$. When $\xi = 0$, the log-likelihood can be derived as:

$$l(\beta) = -N_u log\beta - (1/\beta)\sum_{i=1}^{N_u} y_i \tag{4}$$

The maximum likelihood estimates for GPD distributions are achieved by maximizing (3) and (4) with respect to parameters β and ξ.

After estimating the suitable parameters of the GPD, we can evaluate the forecast error x_m that is expected to be exceeded on average once every m observations (with probability $1/m$). The forecast error x_m is also known as the return level, while the m observations or inverse of the probability that the forecast error x_m will be exceeded is also known as the return period. The return level and return period can be useful to system operators to allocate reserves to account for wind power uncertainty. The return level x_m can be derived for $\xi \neq 0$ as:

$$x_m = u + \frac{\beta}{\xi}\left[(m\zeta_u)^{\xi} - 1\right] \tag{5}$$

Provided that m is large to ensure that $x > u$. When $\xi = 0$, the return level can be derived as:

$$x_m = u + \beta \log(m\zeta_u) \tag{6}$$

The parameter $\zeta_u = N_u/N$ is the proportion of observations that are greater than u.

2.2.Classification of atmospheric states

To investigate the relationship between large – or *synoptic*-scale atmospheric circulation and extreme forecast errors, atmospheric circulation was classified into a set of atmospheric states that serve as archetypical representations of weather regimes associated with the climatology of a region. The classification of atmospheric circulation, as a complexity reduction mechanism, is a common and well-established practice in the meteorological community. Classification techniques have evolved from subjective approaches, which are dependent on expert knowledge, toward objective computer-assisted methodologies such as principal component analysis, k-means clustering, and self-organizing maps (SOMs) [39].

This paper makes use of SOMs as a classification technique. A SOM is a class of self-learning artificial neural network that allows for the representation of high dimensional data onto what is typically a 2D lattice (or map), whilst preserving the topology of the higher dimensional data [40]. SOMs are trained using a competitive learning algorithm represented in (7) below. During training, a set of SOM nodes (n), established during the initialization process, are continually updated according to which node best matches (based on the Euclidean distance) each randomly selected iterative input vector ($R(s)$), for each step (t) of the training process. This most similar node is called the best matching unit (BMU). Subsequently, each BMU along with a number of nodes in a neighborhood (φ) stretching between nodes j and i, are adjusted to increase their similarity to that of the input vector. The size of the neighborhood decreases throughout the training process based on a monotonically decreasing learning coefficient (ρ). Thereby weight vector for each node P_n is updated as follows:

$$P_n(t+1) = P_n(t) + \varphi(i,j,t).\rho(t).(R(s) - P_n(t)) \tag{7}$$

2.3.Multivariate forecast error distribution

Once the forecast error distribution of exceedances over a high threshold for each cluster has been obtained, it is important to link these univariate distributions (to form multivariate distribution) to get a system-wide view of forecast error. The multivariate distribution should account for spatial-temporal correlations in forecast errors between various clusters.

This paper uses copula functions to model the bivariate joint distribution function $F_{D,S}(d,s)$, where D and S are forecast errors for clusters 1 and 2, respectively. According to the Sklar's Theorem, if $F_{D,S}(d,s)$ is a two-dimensional distribution function with marginal distributions $F_D(d)$ and $F_S(s)$, then there exists a copula C such that:

$$F_{D,S}(d,s) = C(F_D(d), F_S(s)) \tag{8}$$

Conversely, if C is a copula with $F_D(d)$ and $F_S(s)$ being the distribution functions, then the function $F_{D,S}(d,s)$ defined by (8) is a joint distribution function with marginal distributions $F_D(d)$ and $F_S(s)$. Section 3.4 will discuss the selection of an appropriate copula function for this particular application.

The derived copula-based joint forecast error distribution provides some important information about forecast error in a region. For example, the probability that forecast errors from both clusters exceed certain thresholds can be obtained in terms of copulas as follows:

$$P(D \geq d, S \geq s) = 1 - F_D(d) - F_S(s) + C(F_D(d), F_S(s)) \quad (9)$$

In addition, it may be of interest to system operators to evaluate the forecast error distribution of cluster 1 given that the forecast error of cluster 2 exceeds a certain threshold s'. This conditional distribution is given by:

$$P(D \leq d, S \geq s') = \frac{F_D(d) - C(F_D(d), F_S(s'))}{1 - F_S(s')} \quad (10)$$

Conversely, the conditional forecast error distribution of Cluster 2 given that the forecast error of Cluster 1 exceeds a certain threshold d' is given by:

$$P(S \leq s, D \geq d') = \frac{F_S(s) - C(F_D(d'), F_S(s))}{1 - F_D(d')} \quad (11)$$

3. Case study and results

3.1. Description of data used

To test the proposed methodology, this paper uses the day-ahead point forecast error data (between 01 January 2018 and 31 March 2021) from 29 wind farms, obtained from Eskom (the power utility company in South Africa). However, due to the confidentiality of individual point forecast error data, Eskom was only able to provide the data in clusters of wind farms summed together. This paper uses two of those clusters (with 18 wind farms) to demonstrate the concepts proposed in this paper. Figure 2 shows the locations of the wind farms within each of these clusters.

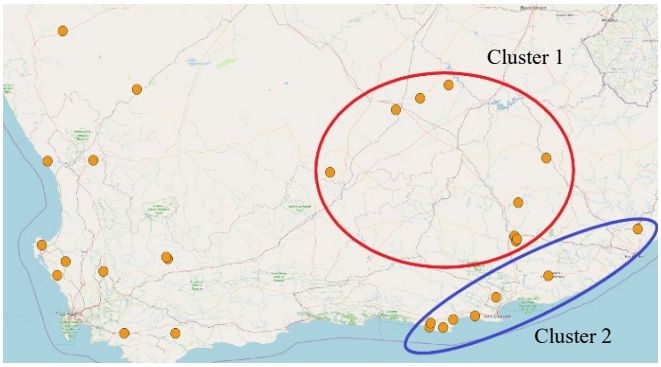

Figure 2: Geographical locations of operating wind farms in South Africa and clusters used for evaluating the proposed methodology.

The forecast errors range between -57.04% and 54.14% (of installed wind capacity) in Cluster 1, while the errors range between -63.71% and 67.31% in Cluster 2. To make comparisons between clusters easier, this paper represents the errors that are greater or equal to zero on a scale of [0, 1]

and negative errors on a scale of [-1, 0). Figure 3 shows the main characteristics of the forecast error data –the probability density function (PDF) and boxplot of forecast errors for both considered clusters. As seen in Figure 3, the observed error distribution from both clusters is positively skewed. In addition, there is a significant number of observations that are located outside the whiskers of boxplots (or outliers), which can be an indication of heavy-tailed distributions.

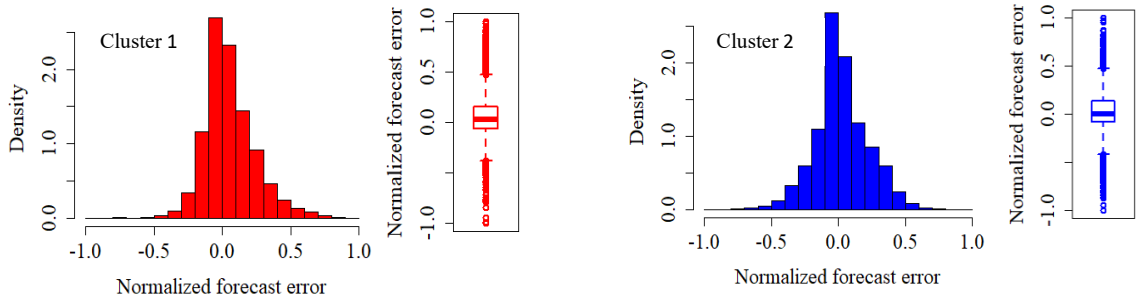

Figure 3: PDF and boxplot of forecast error for both considered clusters.

3.2.Parameter estimation of the forecast error tail distribution

As discussed in Section 1, common distributions used for representing forecast errors include, normal, hyperbolic, Weibull and beta. To see if these distributions can also represent the forecast error data described in Section 3.1, we consider the quantile-quantile (Q-Q) plot. This plot shows the quantiles of hypothesized distributions (in this case normal, beta, Weibull and beta) as a function of the observed quantiles. If the observed data is drawn from the hypothesized distribution, then the Q-Q plot is linear with a slope of 45 degrees. Figure 4 shows the Q-Q plot of normal, hyperbolic, Weibull, and beta distributions for both considered clusters. As seen from Figure 4, the considered distributions are relatively suitable for representing forecast errors in ranges -0.53 to 0.36 and -0.47 to 0.45 for clusters 1 and 2, respectively. However, the normal, Weibull, and beta distributions underestimate the extreme forecast errors in both clusters, while the hyperbolic distribution tends to overestimate the extreme forecast errors (except for negative extreme errors in Cluster 1). In other words, the observed data has heavier tails than estimates from the normal, Weibull, and beta distributions, and lighter tails than estimates from hyperbolic distribution.

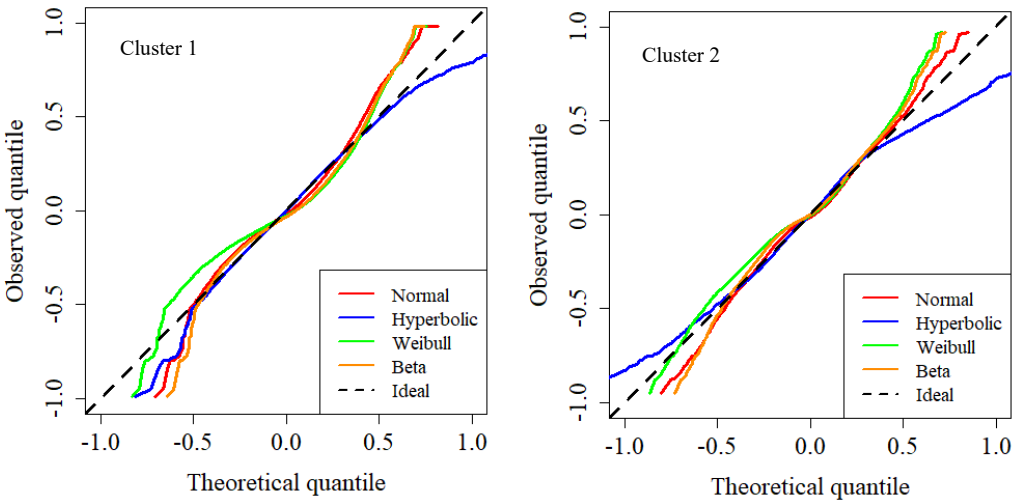

Figure 4: Q-Q plot of normal, hyperbolic, Weibull and beta distributions for both clusters.

In this paper, we propose fitting the tails of the forecast error distribution with a GPD. The forecast error data, as shown in figures 3 and 4, have both left and right tails. This study uses the right tail as an example; however, it is possible to apply the same approach to the left tail. The first step in the proposed approach is to identify the forecast error threshold above which we can fit the GPD. If the threshold is set too high, there will be few observations that exceed it, resulting in a significant variance [43]. If the threshold is too low, data with ordinary values will be included as extremes, making the asymptotic assumption less valid [43]. In this paper, the mean excess and parameter threshold stability plots (also used for example in [43], [46], [47]) are used to identify the right tail thresholds of 0.33 and 0.37 for clusters 1 and 2, respectively. After determining the thresholds, the parameters of the GPD for both clusters are calculated as outlined in Section 2.1.

Figure 5 shows the Q-Q plots of the GPD for both clusters. For comparative purposes, Figure 5 also shows the Q-Q plots of normal, hyperbolic, Weibull, and beta distributions (focused on the tails of the distribution) for both clusters. One can notice a significant improvement in fitting the GPD on the extreme forecast errors compared to the other distributions. To emphasize this finding, Figure 6 illustrates the cumulative distribution functions of observed data, normal, hyperbolic, Weibull, beta, and GPD for both clusters. The GPD is noticeably closer to the observed cumulative distribution function, whereas the other distributions significantly under- or overestimate the probabilities of extreme forecast errors as already observed on the Q-Q plots. We also examine the mean absolute error (MAE) and root mean squared error (RMSE) between cumulative distribution functions of normal, hyperbolic, Weibull, beta, and GPD in relation to the observed cumulative distribution function – see Table 1. This can be seen as a numerical confirmation that the GPD is closest to the observed data.

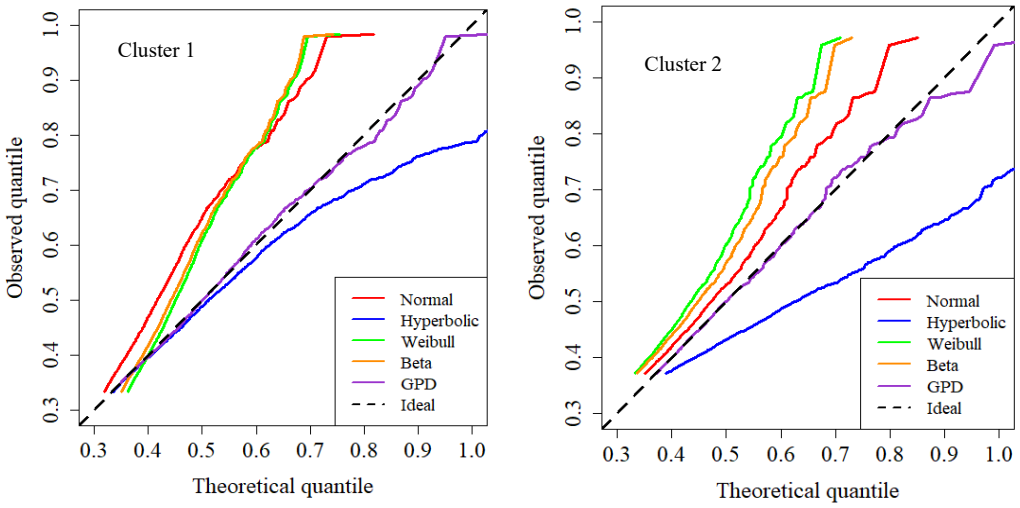

Figure 5: Q-Q plot of GPD compared with Q-Q plot of considered theoretical distributions for both clusters.

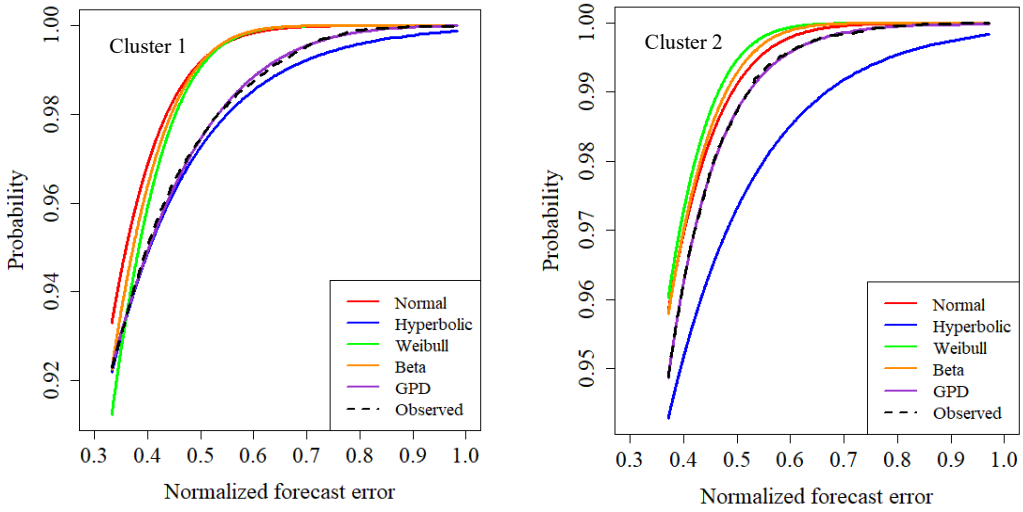

Figure 6: Comparison of cumulative distribution functions of observed data and considered theoretical distributions for both clusters.

Table 1: Comparison of MAE and RMSE between cumulative distribution functions for both clusters.

Cluster 1		
Distribution	MAE	RMSE
Normal	1.38e-2	1.45e-2
Hyperbolic	1.32e-3	1.56e-3
Weibull	2.58e-2	3.25e-2
Beta	2.49e-2	3.14e-2
GPD	6.55e-4	8.05e-4
Cluster 2		
Distribution	MAE	RMSE
Normal	6.72e-3	7.31e-3
Hyperbolic	1.11e-2	1.14e-2
Weibull	1.74e-2	2.11e-2
Beta	1.71e-2	2.07e-2
GPD	1.82e-4	2.19e-4

3.3.Effects of diurnality, seasonality, and atmospheric states on tail distribution

With the estimated parameters of the GPD in Section 3.2, we can calculate the return levels using (5) and (6). For example, the expectation is that the forecast error will exceed 0.53 and 0.45 on overage once every 48 hours (or a probability of 0.021) for clusters 1 and 2, respectively.

Similarly, if we split the data according to hour, month, and atmospheric state, we can estimate the parameters of the conditional GPD (and associated return level) to assess the impact of diurnality, seasonality, and larger atmospheric circulation on tail distribution of forecast errors. Figures 7 and 8 show the return level associated with each hour and month at different return periods (48 hours or 2 days, 168 hours or week, and 744 hours or month), respectively. The return level of both clusters fluctuates dramatically across different hours of the day. Cluster 1 has considerable spikes in return levels at 9h and 17h, while Cluster 2 has a dip at 10h. The return level of cluster 1 is often high during the day and low at night, whereas the return level of Cluster 2 is the reverse. The return level of Cluster 1 has a visible seasonal pattern – it drops during the winter months (May to July) and it is at its highest during the summer months (December to February). On the other hand, the return level of Cluster 2 remains relatively flat throughout the months, except for the noticeable dip in October.

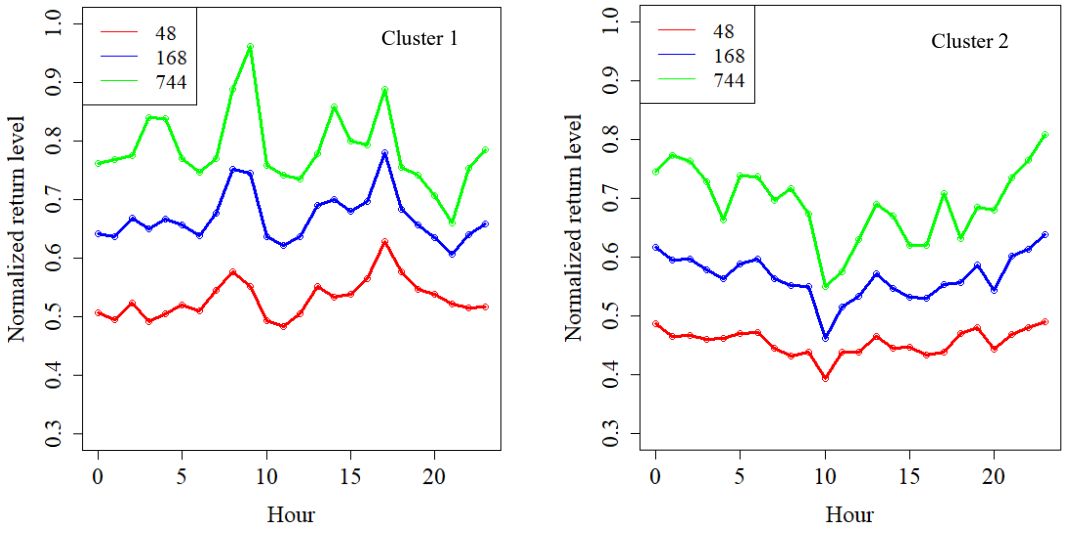

Figure 7: Conditional return level associated with each hour at different return periods for both considered clusters.

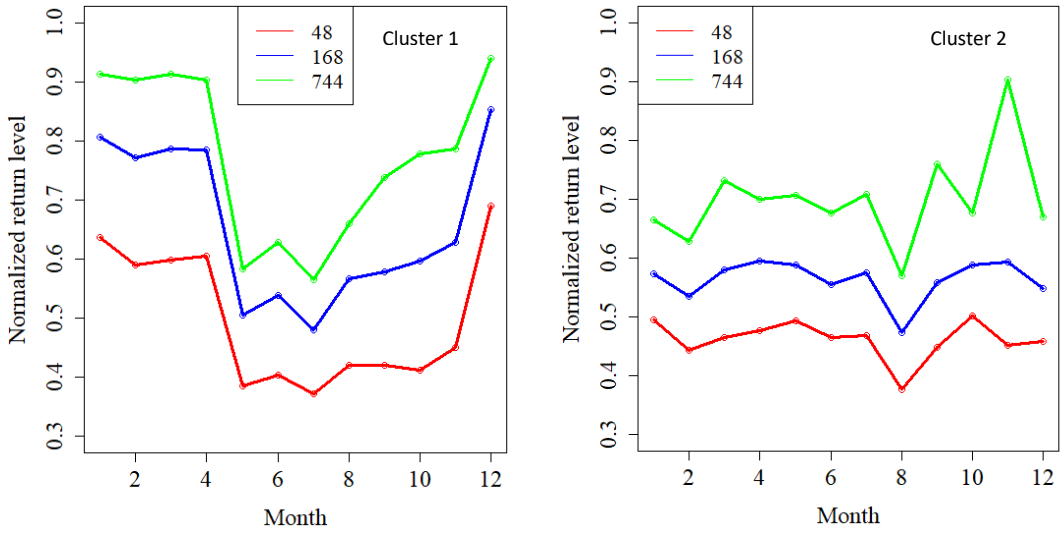

Figure 8: Conditional return level associated with each month at different return periods for both considered clusters.

To assess the impact of larger atmospheric circulations on extreme forecast errors, this paper selected a 4-by-5 SOM node lattice, resulting in a 20 node SOM. The SOM was trained in two phases using the batch training algorithm on a rectangular lattice – firstly a rough training phase consisting of 1000 iterations which was followed by a fine-tuning phase of 5000 iterations. During the rough training phase, the neighborhood function decreased from 5-to-1 and during the fine-tuning phase, it decreased from 2-to-1. Both training phases use the Epanechnikov neighborhood function, as recommended for small SOMs [45]. Once the training process was completed, and the SOM has been created, each input vector (i.e. each geopotential height time step) was assigned a 'label' based on which SOM node it is most similar to, likewise using the Euclidean distance as with the training phase. Accordingly, this allows firstly each time step in the input geopotential height time series, along with the corresponding wind power prediction error time series, to be clustered based on the atmospheric state that was concurrent to each time step.

Figure 9 shows the 20 (4x5) node SOM representing classified atmospheric states together with the frequency of SOM node occurrence as a percentage above each node. Table 2 shows the return level associated with each SOM node at different return periods. It is evident from Table II that the return level can change significantly due to changes in the SOM node. For example, the return level drops significantly (for all return periods) at SOM nodes (2,5), (3,4), and (4,2) for Cluster 1, while the same happens at (1,5) and (2,4) for Cluster 2. Each of these nodes illustrates dominant high-pressure circulation over the respective clusters, particularly the ridging of the Indian Ocean High-Pressure System.

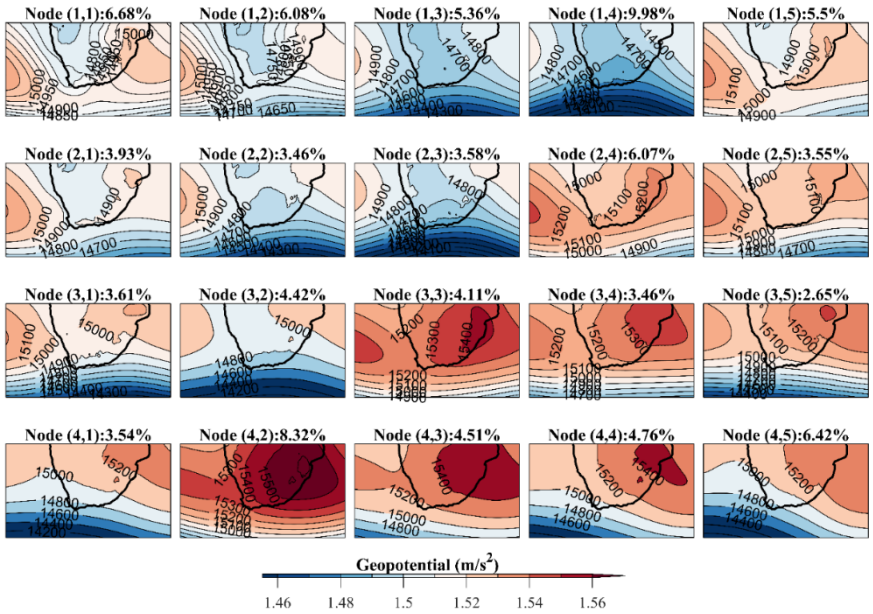

Figure 9: SOM geospatial heights together with frequency of SOM node occurrence over South Africa.

Table 2: Conditional return level for each SOM node at different return periods for both clusters.

Node	Cluster 1			Cluster 2		
	48	168	744	48	168	744
(1,1)	0.61	0.72	0.80	0.44	0.57	0.76
(1,2)	0.61	0.76	0.87	0.46	0.62	0.85
(1,3)	0.62	0.76	0.88	0.45	0.57	0.71
(1,4)	0.59	0.72	0.81	0.45	0.55	0.65
(1,5)	0.51	0.64	0.75	0.40	0.51	0.65
(2,1)	0.41	0.55	0.64	0.51	0.64	0.79
(2,2)	0.43	0.55	0.65	0.44	0.50	0.52
(2,3)	0.59	0.69	0.77	0.49	0.64	0.78
(2,4)	0.49	0.60	0.69	0.42	0.49	0.53
(2,5)	0.34	0.45	0.55	0.45	0.54	0.64
(3,1)	0.49	0.62	0.72	0.43	0.51	0.60
(3,2)	0.58	0.74	0.89	0.46	0.57	0.66
(3,3)	0.44	0.56	0.67	0.48	0.54	0.57
(3,4)	0.36	0.46	0.61	0.50	0.64	0.80
(3,5)	0.55	0.70	0.82	0.47	0.57	0.68
(4,1)	0.49	0.66	0.85	0.49	0.64	0.77
(4,2)	0.34	0.45	0.55	0.45	0.55	0.66
(4,3)	0.43	0.56	0.66	0.47	0.55	0.60
(4,4)	0.51	0.67	0.82	0.45	0.56	0.70
(4,5)	0.56	0.72	0.89	0.46	0.58	0.74

3.4.Copulas application

As seen in Section 3.3, the results from different clusters can be contradictory and it can be challenging for system operators to make system-wide decisions based on the univariate analysis. This paper uses copula functions to model the bivariate joint distribution from the univariate distributions obtained in Section 3.2.

To obtain a joint distribution using copulas, the first step is to select the appropriate copula function. The Gaussian copula is widely used due to its simplicity [21], [48]. However, the Gaussian copula lacks the flexibility to model the tail dependence. As a result, this paper uses the t-Student copula, which is a realistic function for modeling tail dependence [21], [48].

Once obtaining the bivariate joint distribution, we can conduct a wide range of probabilistic analyses on system-wide forecast error without losing spatial-temporal correlations between clusters. For example, we can analyze the probability that both clusters simultaneously exceed certain thresholds (s and d) using (9). If $d = s = 0.44$, then $F_D(d)$, $F_S(s)$ and $C\left(F_D(d), F_S(s)\right)$ are equal to 0.96, 0.98 and 0.94, respectively. Therefore, the probability that the forecast error of both clusters will exceed 0.44 is 0.0035.

With copulas, it is also easy to derive the conditional forecast error distribution of Cluster 1 given that the forecast error of Cluster 2 exceeds a certain threshold, and vice versa. Figure 10 illustrates the conditional forecast error distribution of clusters 1 and 2, given that clusters 2 and 1 exceed various forecast error thresholds ($s'$and d'), respectively. From Figure 10 we can deduce, for example, that the probability that the forecast error of Cluster 1 is less than 0.37 given that the forecast error of Cluster 2 exceeds 0.64 is equal to 0.83.

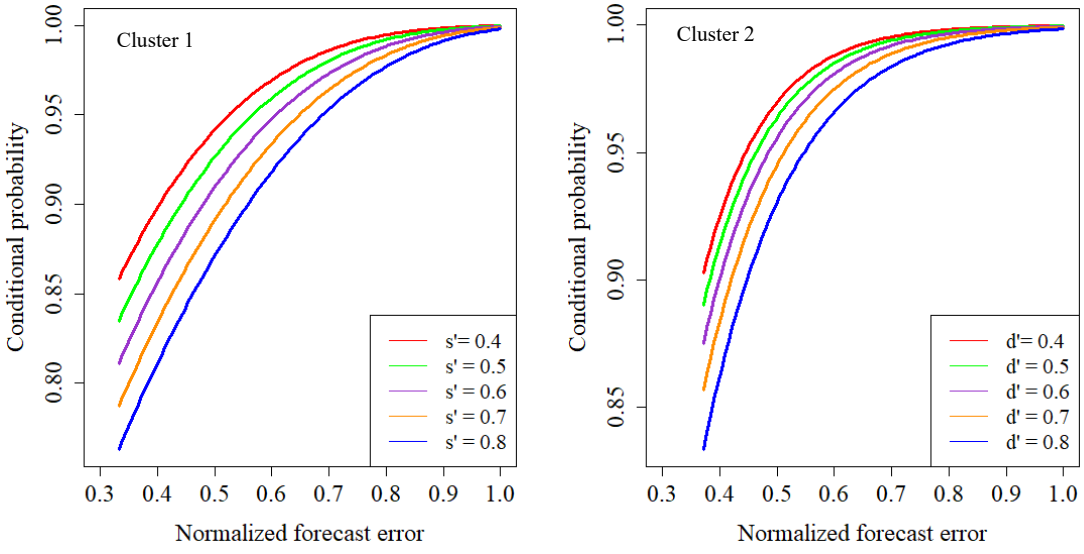

Figure 10: Conditional forecast error distribution of clusters 1 and 2, given that the forecast error of clusters 2 and 1 exceeds $\boldsymbol{s}'$ and $\boldsymbol{d}'$, respectively.

3.5.Running time

To assess the computational cost, the average running times of the models that are part of the proposed methodology are listed in Table III. All models were tested on a Windows PC with 2 GHz and 8 GB RAM. The creation of the SOM-map can be a slow process especially when working with large datasets and depends on the SOM set-up, initialization and training parameters (i.e. number of training iterations, number of SOM nodes, size of neighborhood function, training algorithm etc.). It took approximately 48 hours to create the SOM map used in this study. It should however be noted that, in the implementation of the methodology described in this paper, the creation of the initial SOM is a once off procedure. The operational application of the proposed methodology will be in classifying each atmospheric state based on the set of SOM nodes already created the average running time of which is described in Table 3.

Table 3: Average running time of the proposed models.

Model	**Running time (s)**
Parameter estimation of GPD	0.11
Classification of atmospheric states per time step	0.23
Copula application	61.14

4. Conclusion

This paper has demonstrated that some of the common distributions (normal, hyperbolic, Weibull, and beta) currently used for modeling wind power forecast errors can be inappropriate in representing extreme forecast errors. The paper then modeled the extreme forecast errors using the EVT by fitting the GPD. The GPD showed a superior representation of extreme forecast errors as compared to the commonly used distributions. The paper also estimated the conditional GPDs associated with each hour of day, month of year, and SOM node. It was found that extreme forecast errors can have strong diurnal and seasonal components depending on the location of wind farms under consideration. Therefore, diurnal and seasonal cycles play an important role in the occurrence of extreme forecast errors and can improve estimation thereof. In addition, extreme forecast errors can also change significantly from one SOM node to the other. The dominant high-pressure circulation, particularly the ridging of the Indian Ocean

High-Pressure System is associated with reduced extreme forecast errors. This not only improves the estimation of extreme forecast errors but also allows for the estimation of extreme forecast errors based on physical meteorological phenomena. This paper then used the copula functions to estimate the bivariate joint forecast error distribution of different wind generation clusters. With numerical examples, this paper showed that copulas could be effective in providing a wide range of probabilistic analyses, giving more insight into the characteristics of region-wide extreme forecast errors.

The most significant contribution made by this paper is in improving the estimation and understanding of extreme forecast errors. This is an important step toward better allocation of operating reserves to account for wind power uncertainty. In future, one can test the proposed methodology using individual wind farms' data and not as clusters. This will ensure more spatial-temporal information is extracted from the data, which could further improve the estimation of extreme forecast errors in a region. Furthermore, because the power grid is often made up of a mix of variable renewable sources, it may be valuable to evaluate the applicability of the proposed methodology to other variable renewable sources.

Acknowledgements

This work was supported by the Centre for Renewable and Sustainable Energy Studies (CRSES) at Stellenbosch University, and the Eskom Power Plant Engineering Institute (EPPEI).

References

[1] B. Hodge, D. Lew, M. Milligan, E. Gómez-lázaro, D. Flynn, and J. Dobschinski, "Wind power forecasting error distributions: An international comparison," in *The 11th Annual International Workshop on Large-Scale Integration of Wind Power into Power Systems as well as on Transmission Networks for Offshore Wind Power Plants Conference*, 2012, pp. 1–8.

[2] Z. S. Zhang, Y. Z. Sun, D. W. Gao, J. Lin, and L. Cheng, "A versatile probability distribution model for wind power forecast errors and its application in economic dispatch," *IEEE Trans. Power Syst.*, vol. 28, no. 3, pp. 3114–3125, 2013.

[3] T. Ouyang, X. Zha, and L. Qin, "A Survey of Wind Power Ramp Forecasting," *Energy Power Eng.*, vol. 05, no. 04, pp. 368–372, 2013.

[4] M. A. Ortega-Vazquez and D. S. Kirschen, "Estimating the spinning reserve requirements

in systems with significant wind power generation penetration," *IEEE Trans. Power Syst.*, vol. 24, no. 1, pp. 114–124, 2009.

[5] R. Doherty and M. O'Malley, "A new approach to quantify reserve demand in systems with significant installed wind capacity," *IEEE Trans. Power Syst.*, vol. 20, no. 2, pp. 587–595, May 2005.

[6] P. V. Swaroop, I. Erlich, K. Rohrig, and J. Dobschinski, "A stochastic model for the optimal operation of a wind-thermal power system," *IEEE Trans. Power Syst.*, vol. 24, no. 2, pp. 940–950, 2009.

[7] F. Bouffard and F. D. Galiana, "Stochastic security for operations planning with significant wind power generation," in *2008 IEEE Power and Energy Society General Meeting - Conversion and Delivery of Electrical Energy in the 21st Century*, 2008, pp. 1–11.

[8] K. Methaprayoon, C. Yingvivatanapong, W.-J. Lee, and J. R. Liao, "An integration of ANN wind power estimation into unit commitment considering the forecasting uncertainty," *IEEE Trans. Ind. Appl.*, vol. 43, no. 6, pp. 1441–1448, 2007.

[9] E. D. Castronuovo and J. A. P. Lopes, "On the optimization of the daily operation of a wind-hydro power plant," *IEEE Trans. Power Syst.*, vol. 19, no. 3, pp. 1599–1606, Aug. 2004.

[10] J. Wu, B. Zhang, H. Li, Z. Li, Y. Chen, and X. Miao, "Electrical power and energy systems statistical distribution for wind power forecast error and its application to determine optimal size of energy storage system," *Int. J. Electr. Power Energy Syst.*, vol. 55, pp. 100–107, 2014.

[11] S. Tewari, C. J. Geyer, and N. Mohan, "A statistical model for wind power forecast error and its application to the estimation of penalties in liberalized markets," *IEEE Trans. Power Syst.*, vol. 26, no. 4, pp. 2031–2039, Nov. 2011.

[12] H. Bludszuweit, J. A. Dominguez-Navarro, and A. Llombart, "Statistical analysis of wind power forecast error," *IEEE Trans. Power Syst.*, vol. 23, no. 3, pp. 983–991, Aug. 2008.

[13] J. M. Lujano-Rojas, G. J. Osorio, J. C. O. Matias, and J. P. S. Catalao, "Wind power forecasting error distributions and probabilistic load dispatch," in *2016 IEEE Power and Energy Society General Meeting (PESGM)*, 2016, pp. 1–5.

[14] B. Hodge and M. Milligan, "Wind power forecasting error distributions over multiple

timescales," in *2011 IEEE Power and Energy Society General Meeting*, 2011, pp. 1–8.

[15] B. S. Hodge, E. G. Ela, and M. Milligan, "Characterizing and modeling wind power forecast errors from operational systems for use in wind integration planning studies," *Wind Eng.*, vol. 36, no. 5, pp. 509–524, Oct. 2012.

[16] B. M. Hodge, D. Lew, and M. Milligan, "Short-Term Load Forecast Error Distributions and Implications for Renewable Integration Studies," in *2013 IEEE Green Technologies Conference (GreenTech)*, 2013, pp. 435–442.

[17] D. D. Tung and T. Le, "A statistical analysis of short-term wind power forecasting error distribution," *Int. J. Appl. Eng. Res.*, vol. 12, no. 10, pp. 2306–2311, 2017.

[18] P. Pinson, "Estimation of the uncertainty in wind power forecasting," Ph.D dissertation, Mines ParisTech, Paris, France, 2006.

[19] G. Liao *et al.*, "Wind power prediction errors model and algorithm based on non-parametric kernel density estimation," in *2015 5th International Conference on Electric Utility Deregulation and Restructuring and Power Technologies (DRPT)*, 2015, pp. 1864–1868.

[20] A. Z. Zambom and R. Dias, "A review of kernel density estimation with applications to econometrics," *Int. Econom. Rev.*, pp. 20–42, 2012.

[21] G. D'Amico, F. Petroni, and F. Prattico, "Wind speed prediction for wind farm applications by Extreme Value Theory and Copulas," *J. Wind Eng. Ind. Aerodyn.*, vol. 145, pp. 229–236, 2015.

[22] E. C. Morgan, M. Lackner, R. M. Vogel, and L. G. Baise, "Probability distributions for offshore wind speeds," *Energy Convers. Manag.*, vol. 52, pp. 15–26, Jan. 2011.

[23] D. Ganger, "Enhanced power system operation performance with anticipatory control under increased penetration of wind energy," Ph.D dissertation, School of Electrical, Computer and Energy Engineering, Arizona State University, Tempe, AZ, 2016.

[24] M. Fripp and R. H. Wiser, "Effects of Temporal Wind Patterns on the Value of Wind-Generated Electricity in California and the Northwest," *IEEE Trans. Power Syst.*, vol. 23, no. 2, pp. 477–485, May 2008.

[25] S. Rehman, "Wind energy resources assessment for Yanbo, Saudi Arabia," *Energy Convers. Manag.*, vol. 45, no. 13–14, pp. 2019–2032, Aug. 2004.

[26] B. Karki and R. Billinton, “Effects of seasonality and locality on the operating capacity benefits of wind power,” in *2009 IEEE Electrical Power & Energy Conference (EPEC)*, 2009, pp. 1–6.

[27] K. Knorr, B. Zimmermann, S. Bofinger, A. Gerlach, T. Bischof-Niemz, and C. Mushwana, “Wind and solar PV resource aggregation study for South Africa,” Council for Scientific and Industrial Research, Pretoria, South Africa, RFP No. 542-23-02-2015, 2016.

[28] F. M. Mulder, “Implications of diurnal and seasonal variations in renewable energy generation for large scale energy storage,” *J. Renew. Sustain. Energy*, vol. 6, no. 3, p. 033105, May 2014.

[29] R. Carapellucci and L. Giordano, “The effect of diurnal profile and seasonal wind regime on sizing grid-connected and off-grid wind power plants,” *Appl. Energy*, vol. 107, pp. 364–376, 2013.

[30] L. Zhou, Y. Tian, S. Baidya Roy, Y. Dai, and H. Chen, “Diurnal and seasonal variations of wind farm impacts on land surface temperature over western Texas,” *Clim. Dyn.*, vol. 41, no. 2, pp. 307–326, Jul. 2013.

[31] A. Dalton, B. Bekker, and M. J. Koivisto, “Simulation and detection of wind power ramps and identification of their causative atmospheric circulation patterns,” *Electr. Power Syst. Res.*, vol. 192, pp. 1–13, Mar. 2021.

[32] A. Dalton, B. Bekker, and M. J. Koivisto, “Classified atmospheric states as operating scenarios in probabilistic power flow analysis for networks with high levels of wind power,” *Energy Reports*, vol. 7, pp. 3775–3784, 2021.

[33] A. Dalton, B. Bekker, and M. J. Koivisto, “Atmospheric circulation archetypes as clustering criteria for wind power inputs into probabilistic power flow analysis,” in *2020 International Conference on Probabilistic Methods Applied to Power Systems (PMAPS)*, 2020, pp. 1–6.

[34] Y. Zhang and J. Wang, “K-nearest neighbors and a kernel density estimator for GEFCom2014 probabilistic wind power forecasting,” *Int. J. Forecast.*, vol. 32, no. 3, pp. 1074–1080, 2016.

[35] W. Hu, Y. Min, Y. Zhou, and Q. Lu, “Wind power forecasting errors modelling approach considering temporal and spatial dependence,” *J. Mod. Power Syst. Clean Energy*, vol. 5,

no. 3, pp. 489–498, May 2017.

[36] G. Papaefthymiou and D. Kurowicka, "Using Copulas for Modeling Stochastic Dependence in Power System Uncertainty Analysis," *IEEE Trans. Power Syst.*, vol. 24, no. 1, pp. 40–49, Feb. 2009.

[37] M. Yang, Y. Lin, S. Zhu, X. Han, and H. Wang, "Multi-dimensional scenario forecast for generation of multiple wind farms," *J. Mod. Power Syst. Clean Energy*, vol. 3, no. 3, pp. 361–370, Sep. 2015.

[38] N. Zhang, C. Kang, Q. Xia, and J. Liang, "Modeling Conditional Forecast Error for Wind Power in Generation Scheduling," *IEEE Trans. Power Syst.*, vol. 29, no. 3, pp. 1316–1324, May 2014.

[39] R. Huth *et al.*, "Classifications of atmospheric circulation patterns," *Ann. N. Y. Acad. Sci.*, vol. 1146, no. 1, pp. 105–152, Dec. 2008.

[40] T. Kohonen, "The self-organizing map," *Proc. IEEE*, vol. 78, no. 9, pp. 1464–1480, 1990.

[41] Copernicus Climate Change Service, "ERA5: Fifth generation of ECMWF atmospheric reanalyses of the global climate." Copernicus Climate Change Service Climate Data Store (CDS), 2017.

[42] R. J. Davy, M. J. Woods, C. J. Russell, and P. A. Coppin, "Statistical downscaling of wind variability from meteorological fields," *Boundary-Layer Meteorol.*, vol. 135, no. 1, pp. 161–175, 2010.

[43] J. Chen, X. Lei, L. Zhang, and B. Peng, "Using extreme value theory approaches to forecast the probability of outbreak of highly pathogenic influenza in Zhejiang, China," *PLoS ONE*, vol. 10, no. 2. 2015.

[44] K. Sharma, V. Chavez-Demoulin, and P. Dillenbourg, "An application of extreme value theory to learning analytics: predicting collaboration outcome from eye-tracking data," *J. Learn. Anal.*, vol. 4, no. 3, pp. 140–164, 2017.

[45] Y. Liu, R. H. Weisberg, and C. N. K. Mooers, "Performance evaluation of the self-organizing map for feature extraction," *J. Geophys. Res.*, vol. 111, no. C05018, pp. 1–14, 2006.

[46] L. Bhangwandin, "Multivariate extreme value theory with an application to climate data in the Western Cape," M.S. thesis, Department of Statistical Science, University of Cape

Town, Cape Town, South Africa, 2017.

[47] M. Rydman, “Application of the peaks-over-threshold method on insurance data,” Uppsala, Sweden, U.D.D.M. Project Report 2018:32, 2018.

[48] A. AghaKouchak, S. Sellers, and S. Sorooshian, “Methods of tail dependence estimation,” in *Extremes in a Changing Climate*, 1st ed., Dordrecht: Springer, 2013, ch. 6, pp. 163–179.

Paper 4

N. Mararakanye and B. Bekker, "Estimating wind power uncertainty using quantile smoothing splines regression," *Accepted for publication in 57th International Universities Power Engineering Conference (Conference content will be submitted for inclusion into the IEEE Xplore)*, September 2022.

To comply with the copyright requirements, the final pre-print version of the article is presented here, formatted in dissertation style.

The final published paper will be available at IEEE Xplore once presented in the conference.

Estimating wind power uncertainty using quantile smoothing splines regression

Ndamulelo Mararakanye [a] and Bernard Bekker [a]

[a] *Department of Electrical and Electronic Engineering, Stellenbosch University, Private Bag X1, Matieland, 7602, South Africa*

Abstract

Forecast errors in wind power forecasting are unavoidable due to the complex nature of weather systems and other influences. As a result, quantifying wind power uncertainty is essential for optimally operating grids with a high share of wind energy. This paper uses the quantile smoothing splines (QSS) regression to estimate conditional quantiles of wind power forecast error for a given wind power forecast. This approach is tested using data from eight wind farms in South Africa and evaluated using reliability, sharpness, resolution, and skill score. The results are compared to that of two commonly used approaches: linear regression and fitting beta distributions in different bins. Despite the slight superiority of QSS regression, this paper finds that the results of QSS regression and fitting beta distributions in different bins are comparable. The benefit of using QSS regression, however, is that it is a nonparametric approach that produces smooth results with no discontinuities, and no need for parameter estimations for each bin, making it easily applicable. System operators can use the estimated quantiles to allocate operating reserves and hence ensure the efficient integration of wind farms into the power grid.

Keywords: Forecast error, power forecast, quantile smoothing splines, wind energy

1. Introduction

The global wind generation capacity has grown drastically over the past decade as regions continue to switch to cleaner electricity generation sources. However, wind power varies over time, posing challenges for system operators who must always maintain a balance between demand and supply [1]. Accurate short-term wind power forecasts are important in reducing operational costs and reliability risks that accompany inherent wind power variability. Despite advances made in forecasting accuracy over the years, wind power forecast errors remain unavoidable due to the complex nature of weather systems and other influences [2]–[4]. The day-ahead forecast errors can be as high as 60-80% of total wind capacity [5], [6]. It is, therefore, crucial to also understand and quantify the uncertainty of wind power forecasts.

The normal distribution is a typical parametric distribution assumed for modeling wind power forecast errors [7]–[12]. Owing to the Central Limit Theorem, the normal distribution tends to

work relatively well for geographically distributed wind farms [5], [13], [14]. However, the forecast error distribution of individual sites or wind farms clustered in one location is often skewed and heavy-tailed, which cannot be accurately described by the normal distribution [5], [13], [15]–[19]. In addition, the forecast error distribution can change significantly with the length of the forecasting horizon [5], [14]. The kurtosis and skewness of forecast error distribution tend to decrease with the increase in the forecast horizon, and the normal distribution may struggle to represent these changes [5], [14].

The forecast error distribution also changes with the wind power forecast [17], [20]–[23]. The variance of forecast error varies with the wind power forecast (heteroscedasticity) [20], [24]–[28]. The variance is often small at low and high power forecasts but large at mid-range power forecasts. This is commonly linked to the slope of wind to power conversion curves – the steeper the slope, the larger the variance [28]. The forecast error is also bounded at each wind power forecast. For example, if the wind power forecast is 10% of installed wind capacity, the forecast error will range between -10% and 90% of installed wind capacity. This often implies skewness in forecast error distribution at different power forecasts - skewed right at low power forecasts, symmetric at mid-range power forecasts, and skewed left at high power forecasts [21]–[23]. As a result, the commonly used normal distribution may lack the flexibility required to represent conditional forecast error distributions at different wind power forecasts.

In [17], [23], and [29], the beta distribution is used to model forecast errors at different wind power forecast bins. This methodology is extended in [30] to include additional distribution for modeling extreme forecast errors. In [21], the gamma-like (gamma plus flipped gamma) distributions are used to estimate forecast error distributions at different forecast bins. While the parametric models above have the required flexibility, they require separate distribution parameters for each bin, which can be challenging during practical application. To mitigate against this challenge, [20] proposes using logit transformation to ensure that the wind forecast and actual data are jointly close to normally distributed. The confidence intervals of forecast errors are estimated using this close to normally distributed data and are then compared with the intervals achieved by fitting beta distributions in different forecast bins. While some computed intervals are close to those from beta distributions, others are far apart, demonstrating a lack of flexibility in the logit transformation-based approach.

This work was supported by the Centre for Renewable and Sustainable Energy Studies (CRSES) at Stellenbosch University and by Eskom.

This paper uses the quantile smoothing splines (QSS) regression to derive the conditional quantiles of wind power forecast error for a given wind power forecast. The quantile smoothing splines regression was first introduced in [31] and has been used for various applications (e.g. [32], [33]). The benefit of this approach is that it is nonparametric and flexible for modeling data with heterogeneous conditional distributions [32], [33], as is the case with forecast errors at various wind power forecasts. In addition, quantile smoothing splines regression is robust to outliers [32], [33], which is important in representing the well-known heavy tails of conditional forecast error distributions. Furthermore, this approach is easily applicable and generates smooth results without discontinuities and no need for parameter estimations that arise between bins. The proposed approach is tested using the day-ahead aggregated wind power data from eight wind farms in South Africa. The performance of the proposed approach is compared to that of a linear regression model (assuming normality), and fitting beta distributions in different forecast bins. This paper uses four common metrics for evaluating quantile estimations: reliability, sharpness, resolution, and skill score [34], [35].

The remainder of this paper is outlined as follows: Section 2 provides the theoretical framework of the quantile smoothing splines regression and defines the evaluation framework for conditional quantiles. Section 3 introduces the case study used for testing the proposed approach, and Section 4 presents results and discussion. Section 5 summarizes the findings and concludes the paper.

2. Methodology

2.1.Quantile smoothing splines regression

In a nonparametric regression model, the relationship between X and Y (in this case wind power forecast and forecast error, respectively) is given by [32]:

$$y_i = f(x_i) + \varepsilon_i \tag{1}$$

where the regression function $f(.)$ is unknown and ε_i is the random error term that is assumed to be normally and identically distributed with mean 0, and variance σ^2 [33]. Several approaches have been developed to model nonparametric regression [33]. One of the most commonly used approaches that have been extended to quantile regression is smoothing splines [33]. The approach was developed in [31] and computes the conditional quantile function of Y given the covariate vector X_i by minimizing the following objective function:

$$\sum_{i=1}^{n} \rho_\tau(y_i - f(x_i)) + \lambda \int |f''(x)| dx \tag{2}$$

where $\rho_\tau(u) = [\tau - 1(u < 0)]u$ is a check function, $\tau \in (0,1)$ is the quantile of interest, $\int |f''(x)| dx$ is the roughness penalty, and $\lambda \in \mathbb{R}^+$ is a smoothing parameter that controls the amount of penalty. The penalty can also be expressed based on the total variation penalty, given by [31]:

$$V(f') = \sum_{i=1}^{n-1} |f'(x_{i+1}) - f'(x_i)| \tag{3}$$

The objective function in (2) can thus be written as:

$$\sum_{i=1}^{n} \rho_\tau(y_i - f(x_i)) + \lambda V(f') \tag{4}$$

The function $f(.)$ minimizing (4) is a linear spline with knots corresponding to the observations $x_1, x_2, \dots, x_n$. This means that $\hat{f}(x) = \alpha_i + \beta_i(x - x_{i+1})$ for $x \in [x_i, x_{i+1})$ and $i = 0, \dots, n$. Thus,

$$\beta_i = \frac{f(x_{i+1}) - f(x_i)}{x_{i+1} - x_i} = \frac{\alpha_{i+1} - \alpha_i}{h_i} \tag{5}$$

where $h_i = x_{i+1} - x_i$. Therefore, the penalty can also be written as:

$$V(f') = \sum_{i=1}^{n-1} |(\alpha_{i+2} - \alpha_{i+1})/h_{i+1} - (\alpha_{i+1} - \alpha_i)/h_i| \tag{6}$$

and the objective function in (4) can be written as:

$$\sum_{i=1}^{n} \rho_\tau(y_i - f(x_i)) + \lambda \sum_{i=1}^{n-1} |d_j^T \alpha| \tag{7}$$

where $d_j^T = \left(0, \dots, 0, h_j^{-1}, -(h_{j+1}^{-1} - h_j^{-1}), h_{j+1}^{-1}, 0, \dots, 0\right)$ and $\alpha = (\alpha_1, \alpha_2, \dots, \alpha_n)$. The Schwarz information criterion (SIC) is proposed in [31] to find the optimal value of the smoothing parameter λ. The SIC is given by:

$$SIC(\lambda) = \log\left[\frac{1}{n}\sum_{i=1}^{n} \rho_\tau\{y_i - \hat{q}_\tau(y_i|x_i)\}\right] + \frac{logn}{2n} p(\lambda) \tag{8}$$

The optimal λ is found by minimizing the SIC.

2.2.Evaluation framework

The conditional quantiles of wind power forecast errors for a given wind power forecast are evaluated using four metrics: reliability, sharpness, resolution, and skill score. This evaluation

framework is defined in [34], [35] and has been widely used to evaluate quantile and interval forecasts in recent literature (e.g. [2], [3]).

a) Reliability: This metric measures the statistical consistency between quantile estimates and observations. For example, 90% of the forecast error observations should be less than or equal to a quantile estimate with a nominal level of 0.9. Given a quantile estimate $\hat{q}_t^{(\tau)}$ at time t with nominal level τ, and the corresponding forecast error observation e_t, the indicator variable $\xi_t^{(\tau)}$ is given by:

$$\xi_t^{(\tau)} = \begin{cases} 1, & if\ e_t < \hat{q}_t^{(\tau)} \\ 0, & otherwise \end{cases} \tag{9}$$

By taking the mean of $\xi_t^{(\tau)}$across a set of T quantile estimates, the empirical level a^τ can be calculated:

$$a^\tau = \frac{1}{T}\sum_{t=1}^{T} \xi_t^{(\tau)} \tag{10}$$

The quantile estimates are reliable if the empirical level a^τ is equal to the nominal level τ.

b) Sharpness and resolution: This metric assesses the tightness of the prediction intervals. If $\delta_t^{(\beta)} = \hat{q}_t^{(1-\tau/2)} - \hat{q}_t^{\tau/2}$ is the width of a given prediction interval estimated at time t, then the sharpness $\bar{\delta}_t^{(\beta)}$ is calculated by taking the mean of $\delta_t^{(\beta)}$ across a set of T quantile estimates:

$$\bar{\delta}_t^{(\beta)} = \frac{1}{T}\sum_{t=1}^{T} \delta_t^{(\beta)} \tag{12}$$

Lower values of sharpness (subject to reliability) are preferred because they suggest that the estimation has more information content.

c) Resolution: This metric evaluates the ability of a quantile estimate to provide information on uncertainty given specific conditions. When the sharpness of the two approaches is comparable (subject to reliability), a higher resolution means that the related quantile estimates are of higher quality. The resolution can be calculated by considering the standard deviation of the prediction interval width. A high standard deviation means a high variation in interval width, and thus a better ability to provide a situation-specific assessment of uncertainty.

d) Skill score: This metric attempts to condense the metrics discussed above into a single score, making it easier to compare different quantile estimation methods. This paper calculates the skill score S_c for a set of M quantiles as [34]:

$$S_c = \frac{1}{T}\sum_{t=1}^{T}\sum_{i=1}^{M}(\xi_t^{\tau_i} - \alpha_i).(e_t - \hat{q}_t^{\tau_i}) \tag{13}$$

A higher score denotes a more skilled quantile estimation approach, whereas a score of zero denotes a perfect quantile estimation approach.

3. Description of case study

The proposed methodology is validated using day-ahead aggregated wind power point forecast error data (from 01 January 2018 to 31 March 2021) obtained from eight wind farms in South Africa (see their geographical locations in Figure 1). These wind farms have installed capacities ranging from 22 MW to 138 MW, with an average of 70 MW. The aggregated forecast errors (expressed as a ratio of installed capacity) range from -0.64 to 0.67, with an average of 0.02. Figure 2 shows the probability density function (PDF) and box plot of forecast error data. As seen from this figure, the forecast error distribution is positively skewed, with a significant number of errors outside the whiskers of the boxplots, indicating that the distribution is also heavy-tailed.

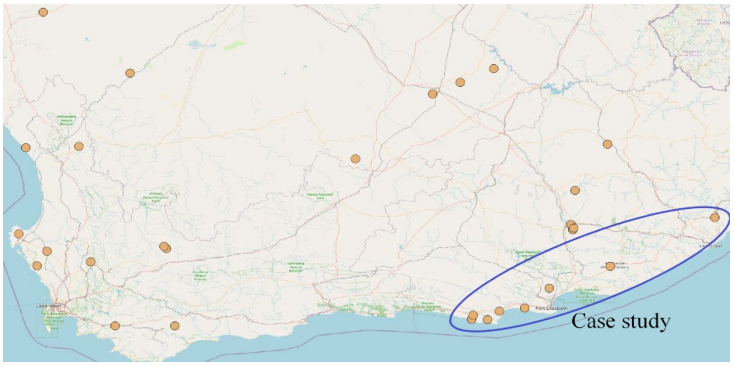

Figure 1: Geographical locations of wind farms in South Africa and the eight wind farms used for testing the proposed approach.

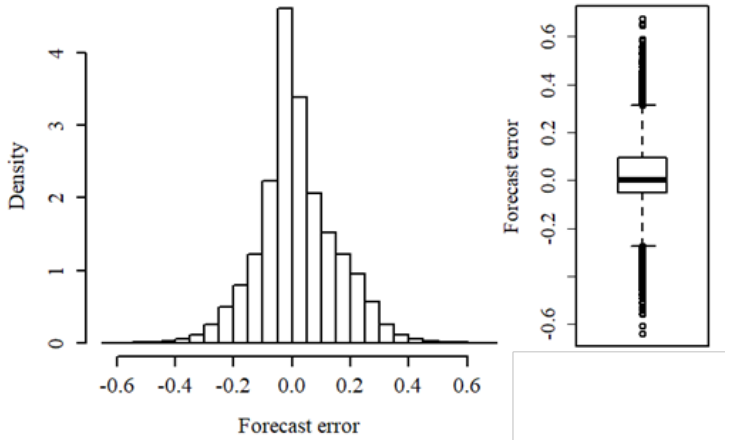

Figure 2: PDF and boxplot of forecast error.

Figure 3 shows a scatter plot of forecast error versus wind power forecast. As seen from this plot, the forecast error is heteroscedastic across different wind power forecasts. The variance appears to be small at low and high power forecasts, but large at mid-range power forecasts (which is similar to the findings in the literature). In addition, the upper and lower edges of the scatter plot appear to be two straight lines (that are nearly parallel), indicating the boundedness of forecast errors across different power forecasts.

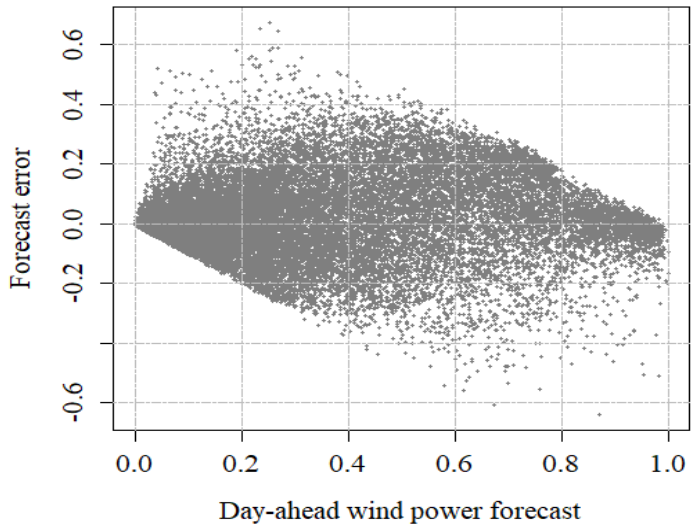

Figure 3: Wind power forecast errors plotted against wind power forecast.

Figure 4 shows the forecast error PDFs across three different power forecasts. As seen from the PDFs, the forecast error is skewed right at low power forecasts, relatively symmetric at mid-power forecasts, and skewed left at high power forecasts. The forecast error characteristics observed in this case study are similar to those found in the literature studies discussed in Section 1.

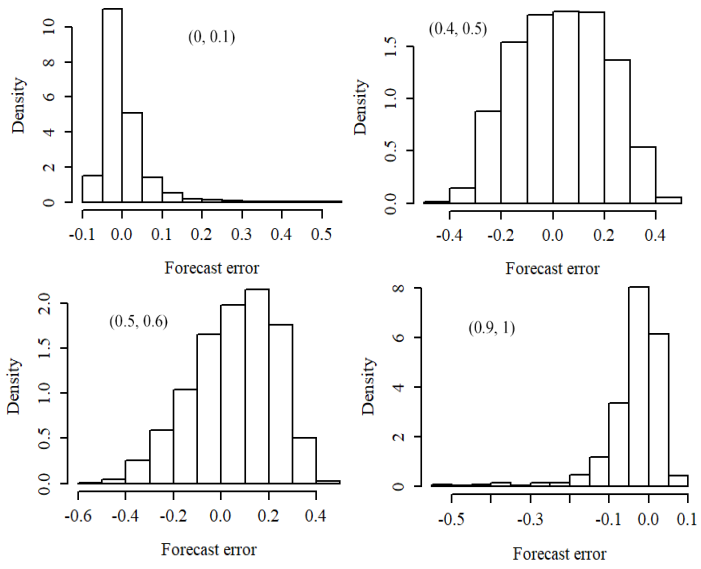

Figure 4: PDFs of forecast errors corresponding to the four bins of power forecast.

The full dataset (shown in Figure 2) was divided into a training set (by randomly selecting 90% rows from the full dataset) and a testing set (the remaining 10% from the full dataset). This is to ensure that the performance of the proposed model is tested on data that was not used to train it.

4. Results and discussion

Figure 5 shows the scatter plot in Figure 3 together with 0.05 and 0.95 quantiles estimated from the QSS regression discussed in Section 2.1. For comparison purposes, Figure 5 also shows the 0.05 and 0.95 quantiles estimated from linear regression and by fitting beta distribution in 20 bins of wind power forecasts as was done in [17], [23], [29]. Note that the choice of bins was based on the minimum bins after which the outcome did not change significantly. It is also worth noting that an excessive number of bins can lead to a small sample size per bin, making it difficult to make accurate statistical inferences.

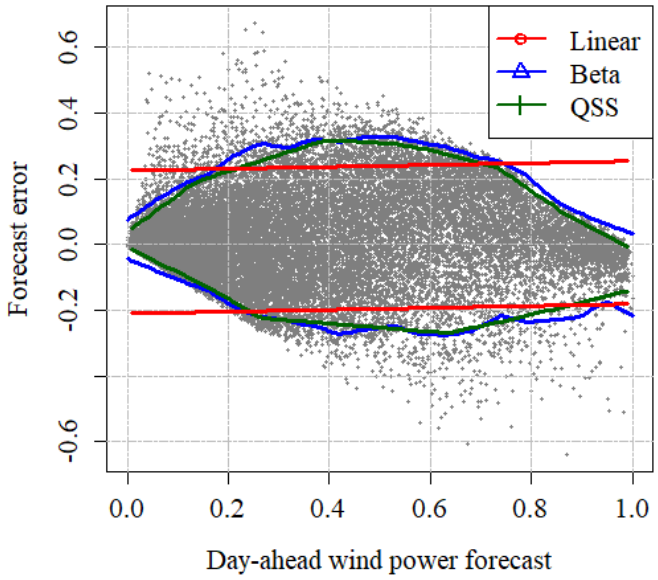

Figure 5: The 0.05 and 0.95 quantiles estimated from QSS, linear and fitting beta distribution in different bins.

Figure 6 shows the reliability diagrams (empirical level vs nominal level) of estimated quantiles from linear, QSS, and beta distribution in different bins. As seen from these plots, the results obtained from all these models align well with the desired diagonal line (indicating the reliability of estimated quantiles). For better comparison, Figure 7 plots the error between empirical and nominal levels versus the nominal level. A general finding from this plot is that the QSS model produces better reliability results compared to linear and beta distribution at different bins. In addition, the QSS model slightly underestimates the forecast errors as seen by negative errors across different nominal levels.

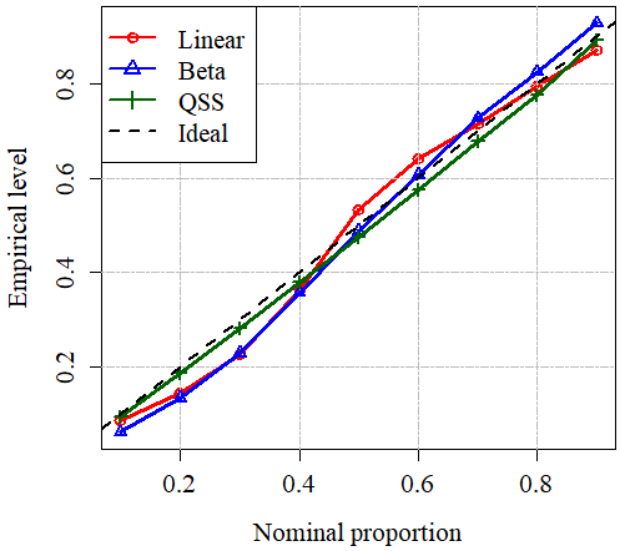

Figure 6: Reliability diagrams of estimated quantiles from QSS, linear and fitting beta distribution in different bins.

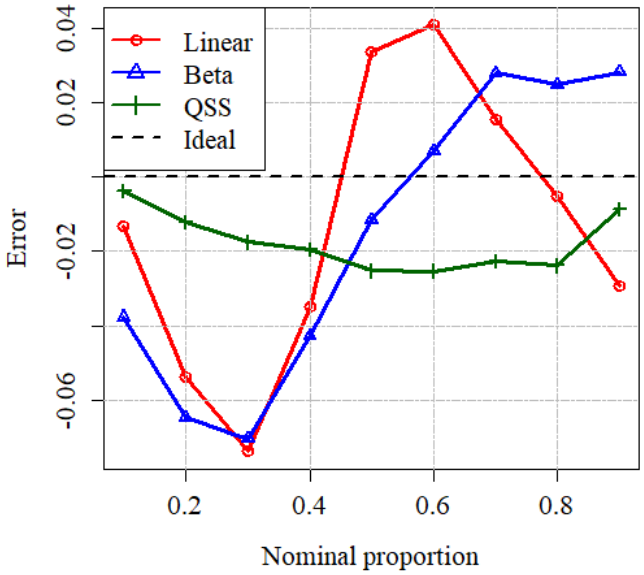

Figure 7: The error between empirical and nominal levels against nominal level.

Figure 8 shows the sharpness results of estimated quantiles from linear, QSS, and beta distribution at different bins. As seen from this plot, the QSS regression achieved better sharpness results compared to linear regression and fitting beta distribution in different bins. Judging just by sharpness, it is tempting to select linear regression for estimating quantiles given its simplicity and little improvement coming from the QSS and fitting beta distribution in different bins. In this case, the models under consideration are as reliable and similarly sharp, and therefore, it is important to also consider the resolution as discussed in Section 2.2.

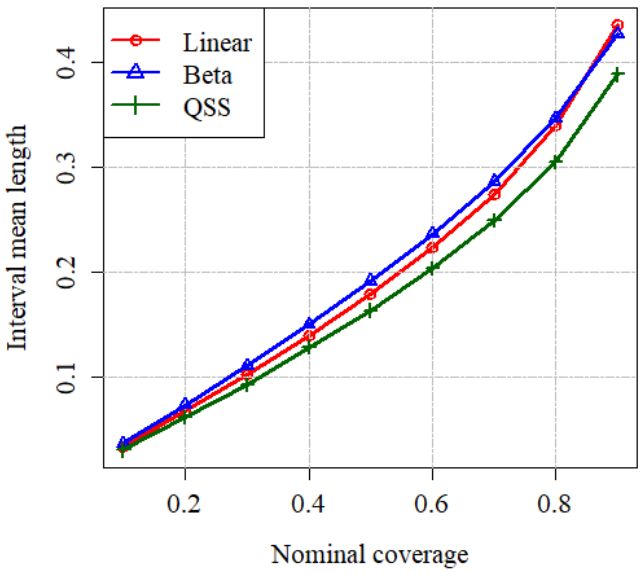

Figure 8: Sharpness results of estimated quantiles from QSS, linear and fitting beta distribution in different bins.

Figure 9 shows the standard deviation of the interval width at different nominal coverages. From this plot, one can notice that the prediction intervals from linear regression have very low variation in width across all nominal coverages, i.e., they have no resolution. The QSS regression achieves higher resolution throughout all considered nominal coverages, while fitting beta distribution at different bins also yields good resolution results. This is what we expect from these models – the linear regression model assumes homoscedasticity across all power forecasts, changing beta parameters across different bins ensures the change in variation across different power forecasts, and QSS is a nonparametric model that is flexible for modeling data with heterogeneous conditional distributions.

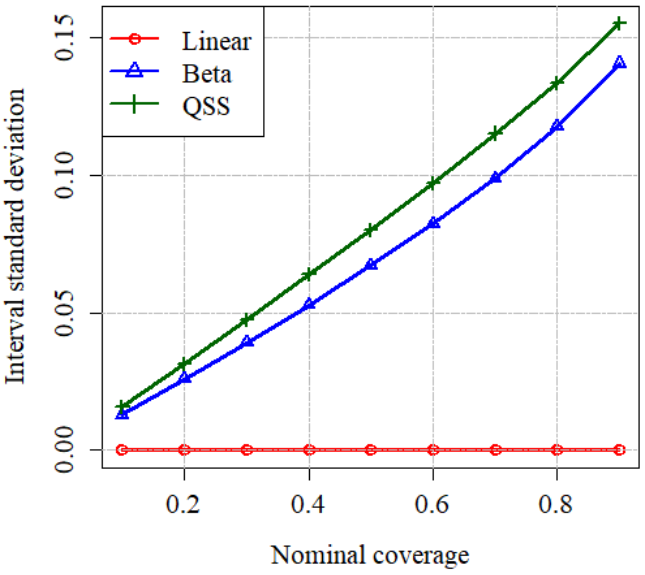

Figure 9: Resolution evaluation - standard deviation of the interval width at different nominal coverages.

Table 1 shows the skill score results for the three considered models. It can be seen from this table that QSS regression achieved the best skill score followed by fitting beta distributions at different bins. The linear regression achieved the worst skill score, emphasizing the above results.

Table 1: Skill score results of estimated quantiles from QSS, linear and fitting beta distribution in different bins.

Model	Skill score
Linear	-0.36
Fitting beta distribution in different bins	-0.33
QSS	-0.32

Note that all models are tested on a Windows PC with 2.3 GHz and 32 GB RAM. For the considered case study, the running times for estimating conditional quantiles are 0.05 seconds for the linear regression model, 2.3 seconds for beta distributions in different bins, and 12.9 seconds for the QSS model.

5. Conclusion

This paper uses QSS regression to estimate the conditional quantiles of wind power forecast error given the wind power forecast. This approach is tested using the day-ahead aggregated wind power data from eight wind farms in South Africa. The results are compared to that of two commonly used approaches (linear regression (assuming normality) and fitting beta distributions in different bins) using reliability, sharpness, resolution, and skill score.

Despite the slight superiority of the QSS regression, the reliability and sharpness results of the three considered approaches are comparable. However, the prediction intervals' resolution reveals that both QSS regression and fitting beta distributions in different bins can provide a wind power forecast-dependent assessment of uncertainty, whereas linear regression intervals, as expected, has no resolution. Similarly, the QSS regression and fitting beta distributions in different bins show superior skill scores as compared to linear regression. Although the results from QSS regression and fitting beta distributions in different bins are similar, QSS regression is a nonparametric approach that generates smooth results without discontinuities and parameter estimations for each bin, and thus is easily applicable. Note that the proposed model is tested with hourly data, but there is no reason why it would not work with other time resolutions as well. In addition, because the proposed model is nonparametric, it can be easily applied to other renewable energy sources.

The estimation of wind power uncertainty for a given wind power forecast can be used by system operators to allocate operating reserves and hence ensure the efficient integration of wind farms into the power grid.

References

[1] N. Mararakanye and B. Bekker, "Renewable energy integration impacts within the context of generator type, penetration level and grid characteristics," *Renewable and Sustainable Energy Reviews*, vol. 108, no. March, pp. 441–451, 2019, doi: 10.1016/j.rser.2019.03.045.

[2] P. Li, X. Guan, and J. Wu, "Aggregated wind power generation probabilistic forecasting based on particle filter," *Energy Convers. Manag.*, vol. 96, pp. 579–587, 2015.

[3] A. Lenzi, I. Steinsland, and P. Pinson, "Benefits of spatiotemporal modeling for short-term wind power forecasting at both individual and aggregated levels," *Environmetrics*, vol. 29, no. 3, pp. 1–17, 2018.

[4] C. Wan, Z. Xu, P. Pinson, Z. Y. Dong, and K. P. Wong, "Probabilistic forecasting of wind power generation using extreme learning machine," *IEEE Trans. Power Syst.*, vol. 29, no. 3, pp. 1033–1044, May 2014.

[5] B. Hodge, D. Lew, M. Milligan, E. Gómez-lázaro, D. Flynn, and J. Dobschinski, "Wind power forecasting error distributions: An international comparison," in *The 11th Annual International Workshop on Large-Scale Integration of Wind Power into Power Systems as well as on Transmission Networks for Offshore Wind Power Plants Conference*, 2012, pp. 1–8.

[6] Z. S. Zhang, Y. Z. Sun, D. W. Gao, J. Lin, and L. Cheng, "A versatile probability distribution model for wind power forecast errors and its application in economic dispatch," *IEEE Trans. Power Syst.*, vol. 28, no. 3, pp. 3114–3125, 2013.

[7] M. A. Ortega-Vazquez and D. S. Kirschen, "Estimating the spinning reserve requirements in systems with significant wind power generation penetration," *IEEE Trans. Power Syst.*, vol. 24, no. 1, pp. 114–124, 2009.

[8] R. Doherty and M. O'Malley, "A new approach to quantify reserve demand in systems with significant installed wind capacity," *IEEE Trans. Power Syst.*, vol. 20, no. 2, pp. 587–595, May 2005.

[9] P. V. Swaroop, I. Erlich, K. Rohrig, and J. Dobschinski, "A stochastic model for the optimal operation of a wind-thermal power system," *IEEE Trans. Power Syst.*, vol. 24, no. 2, pp. 940–950, 2009.

[10] F. Bouffard and F. D. Galiana, "Stochastic security for operations planning with significant wind power generation," in *2008 IEEE Power and Energy Society General Meeting - Conversion and Delivery of Electrical Energy in the 21st Century*, 2008, pp. 1–11.

[11] K. Methaprayoon, C. Yingvivatanapong, W.-J. Lee, and J. R. Liao, "An integration of ANN wind power estimation into unit commitment considering the forecasting uncertainty," *IEEE Trans. Ind. Appl.*, vol. 43, no. 6, pp. 1441–1448, 2007.

[12] E. D. Castronuovo and J. A. P. Lopes, "On the optimization of the daily operation of a wind-hydro power plant," *IEEE Trans. Power Syst.*, vol. 19, no. 3, pp. 1599–1606, Aug. 2004.

[13] Y. Huang, Q. Xu, X. Jiang, T. Zhang, and J. Liu, "A comprehensive model for wind power forecast error and its application in economic analysis of energy storage systems," *J. Electr. Eng. Technol.*, vol. 13, no. 6, pp. 2168–2177, 2018.

[14] B. Hodge and M. Milligan, "Wind power forecasting error distributions over multiple timescales," in *2011 IEEE Power and Energy Society General Meeting*, 2011, pp. 1–8.

[15] J. Wu, B. Zhang, H. Li, Z. Li, Y. Chen, and X. Miao, "Electrical power and energy systems statistical distribution for wind power forecast error and its application to determine optimal size of energy storage system," *Int. J. Electr. Power Energy Syst.*, vol. 55, pp. 100–107, 2014.

[16] S. Tewari, C. J. Geyer, and N. Mohan, "A statistical model for wind power forecast error and its application to the estimation of penalties in liberalized markets," *IEEE Trans. Power Syst.*, vol. 26, no. 4, pp. 2031–2039, Nov. 2011.

[17] H. Bludszuweit, J. A. Dominguez-Navarro, and A. Llombart, "Statistical analysis of wind power forecast error," *IEEE Trans. Power Syst.*, vol. 23, no. 3, pp. 983–991, Aug. 2008.

[18] D. D. Tung and T. Le, "A statistical analysis of short-term wind power forecasting error distribution," *Int. J. Appl. Eng. Res.*, vol. 12, no. 10, pp. 2306–2311, 2017.

[19] N. Mararakanye, A. Dalton, and B. Bekker, "Characterizing Wind Power Forecast Error Using Extreme Value Theory and Copulas," *IEEE Access*, vol. 10, pp. 58547–58557, Jun. 2022, doi: 10.1109/access.2022.3179697.

[20] B. Mauch, J. Apt, P. M. S. Carvalho, and M. J. Small, "An effective method for modeling wind power forecast uncertainty," *Energy Syst.*, vol. 4, no. 4, pp. 393-417, 2013.

[21] N. Menemenlis, M. Huneault, and A. Robitaille, "Computation of dynamic operating balancing reserve for wind power integration for the time-horizon 1–48 Hours," *IEEE Trans. Sustain. Energy*, vol. 3, no. 4, pp. 692–702, Oct. 2012.

[22] W. Ko, D. Hur, and J.-K. Park, "Correction of wind power forecasting by considering wind speed forecast error," *J. Int. Counc. Electr. Eng.*, vol. 5, no. 1, pp. 47–50, Jan. 2015.

[23] A. Fabbri, T. GomezSanRoman, J. RivierAbbad, and V. H. Mendez Quezada, "Assessment of the cost associated with wind generation prediction errors in a liberalized electricity market," *IEEE Trans. Power Syst.*, vol. 20, no. 3, pp. 1440–1446, Aug. 2005.

[24] J. Zhang, B.-M. Hodge, J. Mierttinen, H. Holttinen, E. Gomez-Lazaro, and N. Cutulis, "Analysis of variability and uncertainty in wind power forecasting: An international comparison," in *12th International Workshop on Large-Scale Integration of Wind Power into Power Systems*, 2013, pp. 1–16.

[25] M. Marquis *et al.*, "Forecasting the wind to reach significant penetration levels of wind energy," *Bull. Am. Meteorol. Soc.*, vol. 92, no. 9, pp. 1159–1171, Sep. 2011.

[26] I. González-Aparicio and A. Zucker, "Impact of wind power uncertainty forecasting on the market integration of wind energy in Spain," *Appl. Energy*, vol. 159, pp. 334–349, Dec. 2015.

[27] B. Mauch, J. Apt, P. M. S. Carvalho, and P. Jaramillo, "What day-ahead reserves are needed in electric grids with high levels of wind power?," *Environ. Res. Lett.*, vol. 8, no. 3, p. 034013, Sep. 2013.

[28] J. J. Miettinen and H. Holttinen, "Characteristics of day-ahead wind power forecast errors in Nordic countries and benefits of aggregation," *Wind Energy*, vol. 20, no. 6, pp. 959–972, Jun. 2017.

[29] S. Bofinger, A. Luig, and H. G. Beyer, “Qualification of wind power forecasts,” in *Proc. Global Wind Power Conf.*, 2002.

[30] A. T. Al-Awami and M. A. El-Sharkawi, “Statistical characterization of wind power output for a given wind power forecast,” in *41st North American Power Symposium*, 2009, vol. 0, no. 1, pp. 1–4.

[31] R. Koenker, P. Ng, and S. Portnoy, “Quantile smoothing splines,” *Biometrika*, vol. 81, no. 4, pp. 673–680, 1994.

[32] S. Mulyani, Y. Andriyana, and Sudartianto, “Modeling the human development index and the percentage of poor people using quantile smoothing splines,” in *AIP Conference Proceedings 1827*, 2017.

[33] A. A. Yirga, S. F. Melesse, H. G. Mwambi, and D. G. Ayele, “Additive quantile mixed effects modelling with application to longitudinal CD4 count data,” *Sci. Rep.*, vol. 11, no. 1, p. 17945, Dec. 2021.

[34] P. Pinson, H. A. Nielsen, J. K. Møller, H. Madsen, and G. N. Kariniotakis, “Non-parametric probabilistic forecasts of wind power: required properties and evaluation,” *Wind Energy*, vol. 10, no. 6, pp. 497–516, Nov. 2007.

[35] P. Pinson, G. Kariniotakis, H. A. Nielsen, T. S. Nielsen, and H. Madsen, “Properties of quantile and interval forecasts of wind generation and their evaluation,” in *European Wind Energy Conference and Exhibition*, 2006, pp. 1647–1656.